# FORMATION OF ELLIPTICALLY POLARIZED BEAM FROM H-PLANE SECTORAL HORNS USING CORRUGATED FLANGES

A THESIS SUBMITTED BY

**MOHANAN P.**

IN PARTIAL FULFILMENT OF
THE REQUIREMENTS
FOR THE DEGREE OF
DOCTOR OF PHILOSOPHY
TO
**THE UNIVERSITY OF COCHIN**

Dedicated

To my loving **mother** and to the memory of my beloved **father**

CERTIFICATE

This is to certify that this thesis is a report of the original work carried out by Mr. P. Mohanan, under my supervision and guidance in the Microwave laboratory, Department of Physics, University of Cochin,Cochin- 22 and that no part thereof has been presented for any other degree.

Dr. K.G. Nair
(Supervising teacher)
Cochin- 682 022
27 th March 1985.
Professor and Head of the
Department of Electronics
University of Cochin.

DECLARATION

I hereby declare that the work presented in this thesis is based on the original work done by me under the supervision of Dr. K.G. Nair, in the Department of Physics, University of Cochin, and that no part thereof has been presented for any other degree.

Cochin- 682 022
27 th March 1985.

Mohanan.P

CONTENTS

## ACKNOWLEDGEMENTS

# Formation of elliptically polarized beam from H-plane sectoral horns using corrugated flanges

CHAPTER : 1

INTRODUCTION

Chapter 1

## INTRODUCTION

In 1865 James Clark Maxwell, the talented
genius of 19th century, formulated electromagnetic field
equations and predicted that electric oscillations in
a circuit can produce electromagnetic waves in the
surrounding space travelling with very high velocity of
$3 \times 10^8$ m/sec. This stimulated the scientists to peep into
the world of electromagnetic waves and conduct experiments
to detect the presence of such waves. In 1882 Prof.Amos
Dolbar of Tufts college constructed an induction coil,
with one secondary terminal connected to the ground and
the other to a condenser. A microphone and battery were
connected to the primary of the induction coil. He
constructed a receiver also in a similar manner. Even
though the transmission was entirely due to induction,
he could receive the transmitted "signal".

In 1887 Henrich Hertz started experimental
investigation on the properties of these "newly discovered
form of energy". He, with deep scientific enthusiasm,
tried to generate, transmit and receive electromagnetic

form of energy. The first connecting link between free space and the transmitter or receiver, the "Antenna", was used by Hertz in his classical experiments at Karlsruhe in 1887. The transmitter was a spark coil. The receiver was a single loop of wire, broken at one point by an adjustable spark gap. It was possible to produce signal spikes in the receiver, whenever there was a spark at the transmitter. He also proved that, like ordinary optical beams, these waves can also be reflected by plane metallic plates. He also conducted experiments showing reflection, refraction, and polarization of electromagnetic waves.

In 1897, J.C.Bose, the famous Indian scientist, used hollow pipes of circular and rectangular cross-section as waveguides and open ended radiators on wave lengths from 5 mm to 2.5 cm. In his "microwave spectrometer" the receiver was a pyramidal horn called "the collecting funnel". All these classical works inspired Signar Gugbemo Marconi to erect a large cone-type antenna at Poldhu in Cornwell. In 1901, he succeeded in transmitting a wireless signal across the Atlantic. This triggered the scientists to develop efficient radiators of electromagnetic energy.

1.2  Different types of electromagnetic Antennas

The simplest type of antenna is the centre fed

dipole. The antenna is symmetrically fed at the centre by a balanced two wire transmission line. When the antenna diameter is less than 0.01 $\lambda$ the current distribution is assumed to be sinusoidal with zero current ac the ends. For very short dipoles, the amplitude of the current decreases uniformly from a maximum at the centre to zero at the ends. One type of such antenna is a half wave dipole and is commonly taken as a reference antenna. Folded dipoles are also used in certain applications.

Any simple wire, connected to a source, acts as a monopole antenna, which is a modification of the dipole. The wire is insulated from the ground. One type of monopole antenna is a vertical whip antenna used for portable communication set. It is vertically polarized with omnidirectional radiation pattern. Vertical quarter-wave grounded antennas commonly called Marconi Antennas, are used in broadcast. Other long wave radiating elements are rhombic antennas, loop antennas, biconical antennas, helical antennas, etc.

There is another class of antennas called aperture antennas. In these antennas electromagnetic energy is emanating from a physical aperture or opening. Compared to linear antennas, these antennas have higher gain and more directivity.

Electromagnetic horns, lens, reflectors and some surface-wave antennas come under this class.

Reflectors are commonly used in radar, radio astronomy and communication systems in which large gain is needed. Paraboloidal reflectors are usually used in radar. A small feed like a dipole or horn is placed at the focus of the paraboloid. The working of the system is based on the geometrical ray concept. Due to large aperture area, the gain of this antenna is quite large. Very narrow pencil beams can be obtained from such reflectors. To avoid aperture blocking due to the feed, special type of reflectors called offset paraboloids are used. Cassegrain antennas are also employed in certain applications.

Open waveguides and small horns are often used when simple structure having modest gain is required. They are commonly used as feed for illuminating primary antennas like reflectors and lenses. A small horn is essentially a waveguide with one end flared·to increase the aperture area and hence the gain. Due to this flaring, the transmission between the guide and free space is made smooth and this eventually results in better matching. They exhibit good directivity, high gain and broad band-width. A detailed discussion of electromagnetic horn antennas is given in the next section.

Several other reflectors like corner reflectors, pill box, parabolic torus, hog horn etc. are used for specific applications. Dielectric lens antennas employ low loss dielectric material to focus the electromagnetic energy and to produce a pencil beam.

Surface-wave and leaky-wave antennas are part of a larger class called "travelling wave antennas". They radiate energy because of the discontinuity of the guiding surface. Longitudinal slots made on the guide-walls will radiate energy. By varying the parameters of the slots, the pattern can be conveniently controlled. Surface-wave and leaky-wave antennas can be designed to obtain omni-directional coverage or a beam of desired pattern shape and polarization.

Today, microwave integrated circuits (MIC) are receiving increasing attention in view of their low cost, low weight, simple structure and ease of fabrication. Commonly used MIC antennas are patches and slots. The microstrip antenna consists of a highly conducting radiating planar structure of any shape like circular, rectangular or elliptical over a conducting ground plane separated by a thin layer of dielectric. These can be used in conjunction with other microstrip circuits, such as feed networks,

matching networks etc, all on the same substrate. Hence, such antennas form compact array modules. These types of antennas are used in missiles and rockets.

## 1.3 Electromagnetic horns

Electromagnetic horn is essentially a waveguide with one end flared to increase the aperture area. Since the directivity is proportional to the aperture size, any desired directivity can be obtained from a waveguide by the suitable choice of dimensions. According to Southworth[6] "In the case of hollow conducting pipe, radiation issues from the open end much the same as sound waves from a hollow tube. It has been possible to expand the ends of these pipes into horns, thereby obtaining effects very much similar to those common in acoustics".

If the aperture dimensions are much increased, higher order modes will be generated. Single mode field, with large aperture-size can be achieved by the gradual transition produced by flaring terminal section of the waveguide to form an electromagnetic horn. Large number of modes are excited at the throat of the horn. If all these modes propagate, the radiation pattern will be distorted. The attenuation for each mode is large at the

throat and relatively small at the mouth. According to Chu and Barrow[7] "The radial distance to which the region of relatively high attenuation extend is greater for waves of higher order than the waves of lower order". Thus, for a fixed flare angle, particular value of cut off length of throat permits the dominant mode to propagate and all the other modes will be attenuated to negligible amplitude in the throat region before the free propagation into free space. Thus, the throat of the horn will act as a mode filter.

There are different types of horns suitable for different applications. Pyramidal horns, sectoral horns, conical horns, etc. are commonly used.

Pyramidal horn is frequently used as a gain standard of known gain in making gain measurements of other antennas. It is an aperture antenna with flaring in both principal planes of a waveguide. The gain of a pyramidal horn can be calculated within a tenth of a decibel from the aperture dimensions. It is commonly used to obtain desired independent beam width in the two principal planes.

Sectoral horns are actually derivatives of pyramidal horns with flaring only along one of the principal planes.

If the E-plane of the waveguide is flared, then it is called an E-plane sectoral horn. Similarly if the H-plane is flared, an H-plane horn is formed. They are usually used to obtain specified sharpness in the plane containing the flare. The pattern is broad and same as that of an open-ended waveguide in the other plane.

Conical horns derived from a circular waveguide are also used as a primary standard. Due to axial symmetry, it can handle any polarization. Biconical horn finds application when an omnidirectional horizontal radiation pattern is necessary in broadcasting purpose. Vertical radiation pattern of such antenna can be controlled by choosing suitable flare angle and length.

Besides this Box horns, with good H-plane pencil beam than H-plane sectoral horns, compound horns with long H-plane flare and short E-plane flare with broad band matching to free space and Hog-horns etc. are commonly used for certain specific applications.

1.4 Circularly polarized radiators

Polarization is defined by the direction of the orientation of the electric vector during the passage of the

wave, at least for one full cycle. But in general, both magnitude and direction of the electric vector will vary during each cycle and the electric vector will map an ellipse in a plane normal to the direction of propagation. Then the wave is said to be elliptically polarized. The ratio of major to minor axis of the ellipse is called the axial ratio[120]. An elliptical polarization is produced by the superposition of the two orthogonal waves. If these two orthogonal waves are of equal amplitude and phase-quadrature .the net result is circular polarization. Here the tip of the electric field vector, in a plane perpendicular to the direction of propagation will trace a circle. For circular polarization the axial ratio is 0 dB. When the axial ratio is in between zero to infinity, the wave is said to be elliptically polarized. The direction of the major axis is called the tilt angle or the polarization orientation. For a plane polarized wave the axial ratio is equal to infinity. In this case the electric vector always lies along a fixed line. Diagrammatic illustration of different polarization is shown in fig.1(1).

Circularly polarized waves are broadly divided into left-hand circularly polarized (LHCP) and right-hand circularly polarized (RHCP) waves. According to IEEE[120] standard, RHCP and LHCP are defined as follows. "When the

Point of observation

Electric vector

Direction of propagation
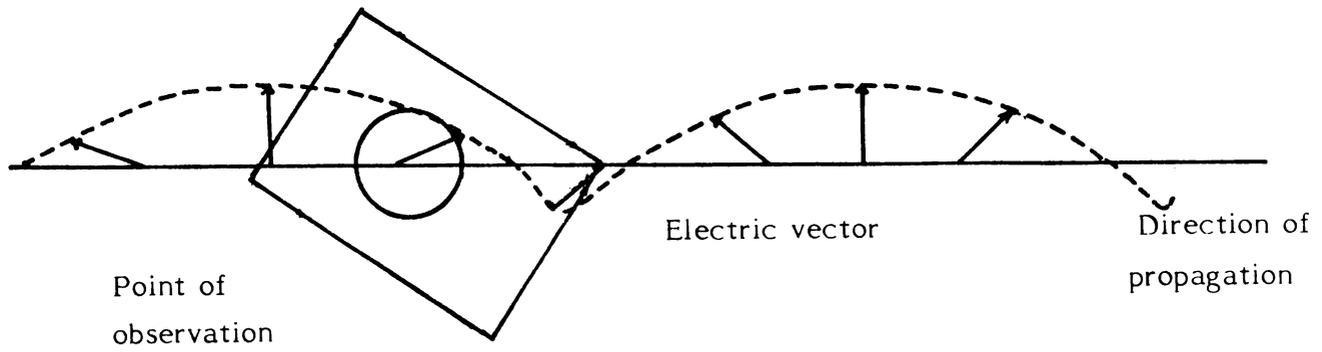
(a)
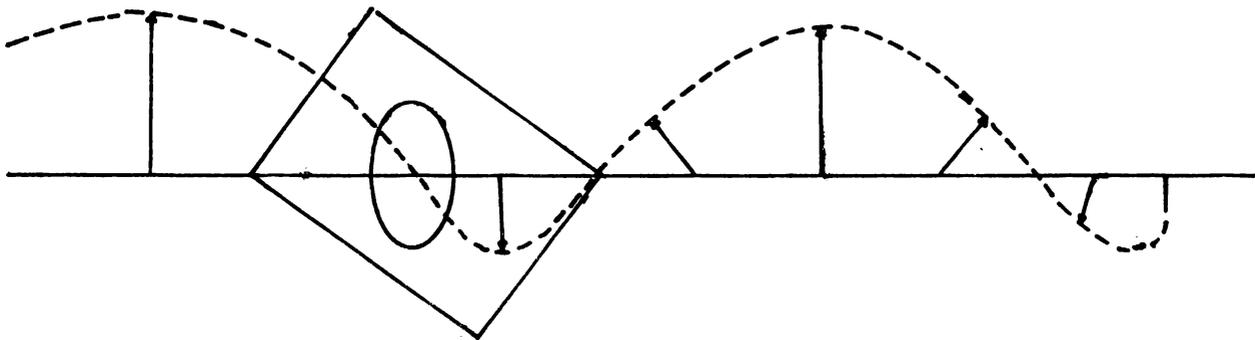
(b)
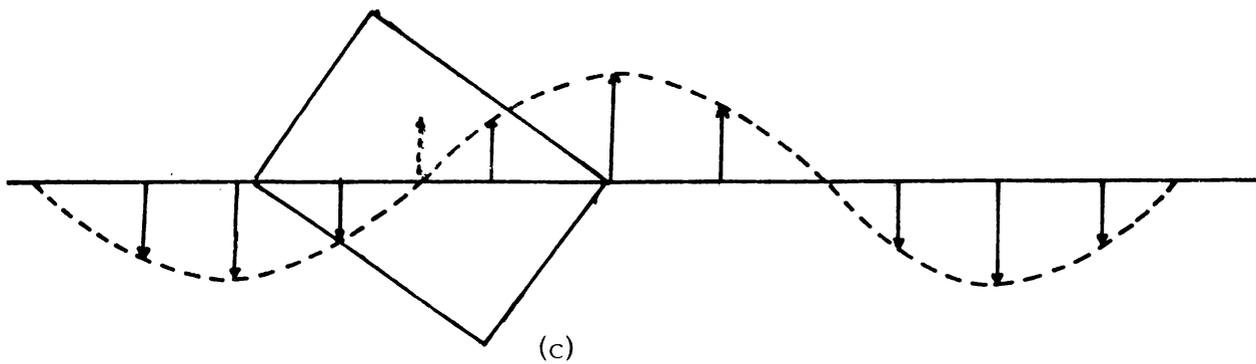
(c)

Fig.1-1: Diagrammatic illustration of different polarizations
(a) circular, (b) elliptical and (c) linear polarizations.

plane of polarization is viewed from a specified side, if
the extremity of the field vector rotates clockwise (counter
clockwise) the sense is right-handed (left-handed)". For a
plane wave the plane of polarization shall be viewed looking
in the direction of propagation.

In an alternate approach, an elliptically polarized
wave is considered to be the resultant of two circularly
polarized waves of opposite rotation direction of unequal
amplitude[110]. When their amplitudes are equal, the result-
ant is a linearly polarized wave. If they are unequal in
amplitude, the resultant is said to be elliptically polarized
with rotation of polarization same as for the larger
component wave. If one of the component goes to zero then
the net result is the original circularly polarized wave.
Fig.1(2) shows the different combination of two circularly
polarized waves and their resultant polarization.

Circularly polarized radiators are frequently
used in communication satellite antenna to provide response
to a linearly polarized wave of arbitrary orientation. In
communication systems rotation of electric vector may occur
due to Faraday rotation when it passes through the ionosphere.
To detect such signals, circularly polarized antennas are

12



Fig.1-2: Different combinations of two circularly polarized waves and their resultant polarizations

used. In radar, it is used for the suppression of preci-
pitation of clutter. When a circularly polarized wave is
reflected from a smooth surface, its horizontal component
is altered by 180° and hence the sense of rotation is
reversed. Therefore when it is reflected from a spherically
symmetric obstacles like rain drops etc. the sense of
rotation is changed and it will not respond the reflected
wave (LHCP is changed to RHCP or vice-versa). Hence these
antennas are blind to its image from a spherically symmetric
surface. This property is utilized to avoid unwanted
echoes from rain drops, hail etc. It is also used in
biology for studying the specific absorption rate (SAR)[121].
Wide variety in absorption due to constant changes in the
animal orientation and posture are eliminated. This tries
the energy coupled to the animal load fairly a constant value
and hence the errors in the experiment can be reduced.


1.5  Production of circular polarization

A combination of electric and magnetic antennas
with equal amplitude and time-phase quadrature can produce
circular polarization. One of the simplest example is the
combination of a loop and a dipole. To obtain time-phase
quadrature their currents must be in phase.

A pair of crossed half-wave dipoles will give a circularly polarized wave by having equal currents in the dipoles with phase quadrature. In this case the radiation in one direction is RHCP and in the other direction is LHCP. If the crossed dipoles are separated by a distance equal to $\lambda/4$ where $\lambda$ is the free space wavelength, and fed in phase, will also produce circular polarization. The beam is circularly polarized only along the on-axis. Narrow slots at right angles to each other on the broad side of a waveguide will produce circular polarization if they are properly located.

The simplest way to produce circular polarization is by using Helical antennas introduced by J.D.Karus. By adjusting the helical antenna parameters, RHCP or LHCP can be produced. It is simple in structure and easy to fabricate. Helical antennas are used as feeds in satellite communications. The axial and omnidirectional modes of helical antennas are obtained by trimming different parameters.

When a horn is fed through a square waveguide with equal amplitudes of vertically and horizontally polarized modes in phase quadrature, circular polarization is obtained at the peak of the radiation. At other points in the azimuth it is not circularly polarized, because the beam widths of the vertical

and horizontal radiation patterns are different. Production of circular polarization in horns are reviewed in detail in the next chapter.

Other commonly used circularly polarized antennas are equiangular spiral, biconical horns, circularly polarized yagi etc.

1.6   Beam shaping of sectoral horns

In certain applications like point to point communication, illuminating parabolic reflectors etc. axially symmetric radiation pattern is necessary. Hence it is necessary to modify the radiation pattern in the unflared plane of a sectoral horn. Several methods have been developed to modify the radiation characteristics of sectoral horn antennas.

Pao[9] suggested the possibility of beam shaping by putting small pins and other obstacles at the mouth of the horn. He found that these obstacles are useful in narrowing the E-plane pattern of a E-plane sectoral horn. The 'Gril technique' developed by K.G.Nair and Hariharan[74] is effective in controlling the E-plane radiation pattern of E-plane sectoral horns. Grooved walls on the inner surface

of the sectoral horn is another efficient method to obtain
axially symmetric radiation pattern with broad band-width.
Using metallic and dielectric lens the pattern can be
controlled by adjusting different parameters. If low loss
dielectric is used to load a horn, directivity can be
increased. Different methods are reviewed in the next
chapter.

The flange technique, suggested by Reynolds[72]
is another simple technique to improve antenna characteri-
stics. Using flange technique we can trim the antenna
characteristic by suitably adjusting the flange parameters[75].
Later corrugated flanges[87] are used for beam shaping. The
important parameters of the corrugated flanges are (a) flange
angle, (b) flange width, (c) flange position, (d) conductivity
of the flange, (e) amplitude excitation of the flange
elements, (f) period of corrugation etc. Compared to a
compound horn the flange technique offers great convenience
in trimming antenna characteristics.

Horns are commonly used as a feed in radar and
satellite communications. A large number of work had been
done to improve the characteristics of horn antennas. It is
an established fact that grooved walls on the inner surface

of a horn can improve the antenna characteristics[44].
Corrugated comb surface can be used for the circular
polarization[98], tilt of polarization[99] etc. This suggests
the possibility to combine these two phenomena and to
obtain a resultant beam. This thesis presents the result
of an investigation to study the possibility of controlling
different antenna characteristics like polarization, beam
shaping, matching etc, using corrugated flange techniques.

## 1.7   Scheme of the present work

The following parameters of the system were
studied in detail.

1. Variation of copolar and cross-polar on-axis
   power density

2. Polarization pattern

3. Radiation pattern

4. Gain

5. Half power beam width (HPBW)

6. Voltage standing wave ratio (VSWR)

Theoretical analysis of axial ratio is attempted
on the basis of line source theory and method of images.

Using certain simple approximations experimental results, could be explored on the basis of this theory.

The scheme of work presented in this thesis is as follows:-

An elaborate review of the past work done in the field of electromagnetic horns are presented in the first part of the second chapter. The second section of the chapter reviews important work carried out on corrugated horns and surfaces. The effect of plane and corrugated metal flanges on beam shaping is reviewed in the third section and the circularly polarized horns and its importance are summarised in the last part of the chapter.

A concise description of the experimental set-up used for this investigation is presented in the third chapter. Experimental arrangement for automatic plotting of polarization pattern is described. This chapter ends with the description of the measurement techniques adopted for axial ratio, tilt angle, sense of rotation, VSWR, gain and HPBW.

The fourth chapter highlights the experimental results of the investigations. Certain experimental results

of elliptically polarized antennas are presented using various established methods.

Theoretical explanation  of the experimental results are presented in the fifth chapter of the thesis. A comparison between experimental and theoretical results is  also given in this chapter.

In chapter six, final conclusion drawn from this study are discussed.  The advantage of the present system over other existing systems is examined in this chapter.  Scope for further investigation  in continuation of the present work is also included in this chapter.

The results of a few investigation  in related fields done by the author during his research period are given in appendices A, B and C.  Axially symmetric radiation from E- and H-plane sectoral horns using corrugated flanges is presented in appendix A.  Appendix B presents some aspects of flanged feed for illuminating secondary reflectors. Phase modulation of microwave signal using point contact Ge signal diode is presented in appendix C.

CHAPTRE : 2

**Review of past work**

Chapter 2

## REVIEW OF PAST WORK

An elaborate review of past work in the field of electromagnetic horn antennas, circularly polarized horns, beam shaping of sectoral horns etc. are presented in this chapter.

### 2.1 Electromagnetic horns

In 1894, Sir Oliver Lodge in his memorial lecture on "The work of Hertz and some of his successors" demonstrated a hollow pipe radiator for radiating and receiving microwaves. Later in 1897, Prof.J.C.Bose in his microwave spectrometer used a pyramidal horn as a receiver and referred as "Collecting funnel". An interesting review of these past work before 1900 has been given by Ramsay[1].

After the suggestion of Southworth[2] and Barrow[3] about waveguide radiator, the first experimental and theoretical analysis of waveguide radiator was reported by Barrow and Greene[4] in 1938.

In 1939, Barrow and Chu[5] presented theoretically the function of sectoral horn antennas. Quantitative curves for the design of sectoral and pyramidal horns were presented.

Experimental results of directive properties of metal pipes and conical horns were described by Southworth and King[6]. The variation of on-axis power with aperture size was discussed and the effects of different horn parameters like flare angle, aperture size, horn length etc. on radiation patterns were reported. According to them, this system can provide 20 dB power gain with respect to a half wave antenna.

At the same time Chu and Barrow[7] reported the principle of designing horn antennas to obtain desired power gain and beam width. They found that for a horn of given length there is an optimum flare angle to provide maximum power gain. Optimum design data of sectoral horns having shortest radial length and flare angle of desired power gain are discussed.

Radiation properties of hollow pipes and horns using Vector Kirchhoff's formula are given by Chu[8] in his theoretical paper in 1940. Power gain of a horn compared to

dipole is given and formulae for the radiation fields of
$TE_{01}$ and $TE_{10}$ waves in a sectoral horn were derived.

H-plane and E-plane radiation patterns of rectangu-
lar horns as a function of flare angle for different lengths
have been discussed by Rhodes[10]. He found sidelobes in the
E-plane and total absence of sidelobe in the H-plane. A
qualitative explanation of the results in terms of field
distribution was given. He noticed that the interference
from nearby objects becomes more and more objectionable as
the frequency of operation takes higher values.

Watson and Mckinney[11] described two different
methods for determining gain and effective area of an
electromagnetic horn. One method was using the reciprocal
properties and the other was using the measured radiation
patterns.

In 1949, Woonton et al[12] made an extensive experi-
mental study on the radiation patterns of horns. The results
were compared with Kirchhoff's formula and with corrected
formula by Stratten and Chu. They proved that principles in
physical optics can be applied to predict the magnitude of
E-plane field with good accuracy of roughly 1 dB upto an

angle of 20° and that of H-plane field with fairly good accuracy.

A simple integral method for computing the radiation pattern of rectangular and circular horns is given by Horton[13]. According to him, when the flare angle goes to zero, the modes of vibration in sectoral and conical horns approach that of rectangular and circular waveguide. A fairly good agreement between theory and experiment was achieved by him.

Herbert S.Bennett[14] analysed a sectoral horn considering it as a non-uniform transmission line and called "Sectoral radial transmission line". The results of his investigation were presented through various curves which were very useful for designing sectoral horns. Physical significance of the normalized functions de ived was discussed by him in detail.

Reflection coefficient at the junction of a straight waveguide and a sectoral horn using WKB approximation is given by Rice[15]. Some numerical data for a 60° H-plane horn is presented.

Later, Southworth[16] published a paper dealing with the principle and application of a waveguide transmission,

starting with early history of the waveguide. Electrical transmission and radiation from the flared end of a trans- mission line and the effect of aperture size on directivity were described in detail, in this paper.

Measured radiation characteristics of conical horns having linear rate of flare were presented by King[17]. Graphs for absolute gain of a conical horn as a function of aperture diameter for a number of axial lengths were shown and dimensional data in terms of wavelength for the design of optimum horns were presented.

In the same year, Schorr and Beck[18] solved Maxwell's equations in a conducting conical horn and cal- culated the propagation coefficient. He calculated the field at the mouth of the horn and computed the radiation pattern in an integral form. According to him the same field equations with slight modification can be used for a pyramidal horn. Physical explanation of mode filtering in horn with small flare angle was given by him.

Jakes[19] conducted experimental investigations to calculate the error in the calculated gain of pyramidal horns. He pointed out that the error due to the edge

effect can be ignored and can be calculated from the physical dimension and Schelkunoff's curve.

Braun[20] discussed the error in the measurement of gain due to two horns separated by short distance. From his experimental curves the error in gain could be directly calculated. In another paper[21] he published the details of design of electromagnetic horns. He has published a table connecting gain and aperture size of a horn   The design procedure of a horn with equal E and H-plane patterns was elaborately given by him.

Epis[22] put metallic nails radially on the rim of conical horns. This reduced the fringes of E-field in the E-plane and hence narrowed the E-plane beam-width. The design and development of an axially symmetric radiation pattern for all polarization is also presented in this paper.

Walton and Sundberg[23] corrected the phase-error at the mouth of a horn using dielectric lens. With this method, they were able to increase the band width of the system.

Russo et al[24] applied geometrical theory of diffraction to pyramidal horn and computed the E-plane pattern. It has been shown that the radiation of the horn is due to diffraction by the E-plane edges and by direct radiation from the source at the apex of the horn. Theoretical and experimental patterns were in excellent agreement.

Tingye and Turrin[25] computed the nearfield of a conical horn by numerical integration method. They assumed that the field at the mouth of the horn is the same as that exists at the mouth of an infinite horn having the same cross section.

Later Yu et al[26] made a more accurate calculation of E-plane radiation pattern of a pyramidal horn considering higher order diffraction at the edges and reflection inside the horn. A corner reflector with a magnetic line source located at the vertex is proposed as a model for the E-plane radiation of the horns. Considerable reduction in farfield side and backlobes were obtained.

Hamid[27] applied geometrical theory of diffraction to investigate gain and radiation pattern of a conical horn excited by circular waveguide with $TE_{11}$ mode. The farfield

at a point is the sum of fields excited by the geometrical optical rays and edge rays passing through that point. The edge rays excited at the aperture plane of the horn were also taken into account.

Using the nearfield transmission formula Chu and Semplak[28] computed the ratio between farfield and nearfield gain of pyramidal horns as a function of dimension and separation distance. This calculated correction is applied for the absolute gain and achieved an accuracy of $\pm$ 0.035 dB.

Jull[29] made accurate gain measurement with revised correction. He considered mismatch of the horn and aperture edge diffraction to the gain formula. Later, he incorporated[30] the finate-range effect in the Fresnel zone. Using this modified formula the gain can be obtained from two single-line curves.

Phase centre of different horn antennas was treated as a vector problem by Muchldorf[31]. Expressions are derived for the phase centres of E and H-planes. The dependence of horn dimension on phase center is given graphically.

Narasimhan and Rao[32] formulated a simpler solution for horn modes in conical horns. They used an asymptotic

solution to find the modes in conical horns. Vector
diffraction formula is used to find radiation pattern and
gain of a conical horn with $TE_{11}$ mode. Radiation patterns
of conical horns with large flare angle, excited with $TE_{11}$
mode using vector diffraction formula were given by the
above authors[33] in 1971. They also corrected[34] the available
formula for the radiation patterns of an E-plane sectoral
horn.

Kerr[35] reported a short axial length horn with
broad band-width. Using grid type H-plane walls, Half
Power Beam Width (HPBW) was reduced.

Using GTD, the on-axis power gain of a two
dimensional E-plane sectoral horn was analysed by Jull[36]
in 1973. Taking into consideration the reflection of
diffracted field from the horn and double diffraction at
the aperture, the gain equation was modified.

Potter[37,38] developed a new method using $TE_{11}$
and $TM_{11}$ mode excitation at the throat. By adjusting the
relative amplitude and phase of these two modes, sidelobe
suppression and beam width equilisation were achieved. He
computed the radiation pattern of this "Dual-mode" conical
horn theoretically.

Iskander and Hamid[39] analysed the higher order interaction between two H-plane sectoral horns. The field distribution at the aperture of the horn was calculated and a correction for the gain was reported.

Jull and Allen[40] reported an accurate gain measurement of E-plane sectoral horns. They made a new proposal against Kirchhoff's theory incorporating the exact $TE_{10}$ mode field of an open ended waveguide.

Mentzer et al[41] used slope diffraction function to correct the errors around the shadow boundary region. The fields of E-plane edge diffracted rays are also included in the H-plane pattern analysis.

In 1981, Mather[42] developed a broad band, low sidelobe horn. A circular horn flared as a trumpet was used as the radiator. Radiation pattern calculated using GTD was in accordance with the experimental patterns in which the sidelobe level was 75 dB down from the main lobe.

Menendez[43] gave analytical expression for the far-field radiation pattern and reflection coefficient of horn antennas based upon multiple image model. The calculated radiation pattern and reflection coefficient are in good agreement with the experiments.

## 2.2  Corrugated horns and surfaces

In 1966, Simmon and Kay[44] reported an ideal feed for paraboloidal reflectors. They came to the realization that metallic surface with closely spaced transverse groove would present same boundary condition for TM and TE waves at grazing incidence and create a tapered aperture field distribution in all planes. They termed such horns as "scalar feeds". Since the radiated energy is confined to the angular sector determined by the horn flare angle rather than aperture size in wavelength, the band width is nearly 2:1. A comparison between standard horn and scalar horn is also given.

At the same time, Lawrie and Peters[45] modified horn antenna for low sidelobe levels. Use of choke slots or corrugated surfaces in the walls provided an effective method for reducing the side and backlobes. Corrugated surfaces are proved to be superior to choke slots. They proved that by proper adjustments, an axially symmetric radiation pattern can be produced from a horn antenna.

A linearly polarized horn with axially symmetric radiation pattern is reported by Rumsay[46]. A theoretical analysis for obtaining such pattern from a circular waveguide is given. Minnett and Thomas[47] studied the radiation from

a cylindrical hybrid-mode guide which results in equal
E- and H-plane patterns.

Clarricoats and Saha[48] studied the propagation
behaviour of a corrugated horn by analysing hybrid modes.
A procedure for achieving a balanced hybrid condition in
the horn aperture is discussed by them. In another paper[49],
they have analysed the fields in a corrugated horn using
spherical hybrid modes. Their computed radiation patterns
show excellent agreement with those computed by Kay et al[44].
Later they calculated[50] the radiation patterns by model
expansion technique and Kirchhoff's Huygens method. These
two methods show good agreement over a wide range of obser-
vation angles.

Mac A.Thomas[51] studied the band-width properties
of corrugated conical horns. The aperture fields of
corrugated conical horns remain virtually unchanged over a
wide range of frequency. The band-width is increased by
increasing the length of the horn.

Jeuken[52,53] carried out experimental studies on
corrugated conical horns of small flare angles, with symmetric
radiation patterns in the frequency range of 1:1.3. Using
Kirchhoff's-Huygens integration method he calculated the

radiation patterns of small conical horns having wide
flare angle.

The performance of one and two hybrid mode feeds
designed to illuminate Parkes 210 ft radio telescope has
been discussed by Mac A Thomas[54]. The two hybrid mode feed
gave increased aperture efficiency for paraboloids and
allowed more efficient illumination of spherical reflectors
by proper adjustments of amplitude and phase. An increased
efficiency of 12% was obtained by the two-hybrid mode feed.

A simpler solution of spherical hybrid modes
in a corrugated conical horns has been reported by Narasimhan
and Rao[55]. Their formula for radiation pattern and gain
yielded accurate results when the flare angle was less than
20°. Later, they[56] analysed the radiation pattern from wide
flared corrugated conical horns. Here the phase variation
of the aperture field was also taken into account. Using
vector diffraction formula the farfield radiation patterns
of these horns were computed.

A detailed study of the propagation and radiation
characteristics of corrugated waveguide has been described
using cylindrical mode analogy by Clarricoats and Saha[57].
The band-width of such a system is reported to be 1:1.5.

In another paper[58] they used Kirchhoff's-Huygens integration over a constant phase surface at the mouth of the horn to calculate the radiation pattern. It is also obtained by expanding aperture field in terms of TE and TM spherical modes.

Baldwin and Mcinnes[59] discussed the radiation characteristics of a corrugated conical horn. The experimental pattern and theoretical ones computed by them showed good agreement.

A method for mode conversion in a corrugated cylindrical guide is given by Mac A.Thomas[60] using $TE_{1n}$ and $TM_{1n}$ modes. $TM_{1n}$ modes can be produced from $TE_{11}$ excited mode by proper adjustments of corrugation parameters.

Jensen et al[61] derived expression for the radiation patterns of corrugated conical horns, in which dominant mode within the grooves was transverse magnetic (TM). An axially symmetric radiation pattern was obtained when the groove depth is $\lambda/4$.

Knop and Wiesenfrath[62] showed that $HE_{11}$ mode in a corrugated pipe with large diameter and $\lambda/4$ teeth width radiate as a "scalar feed". This model revealed that

the E-plane pattern approaches H-plane pattern and is
linearly polarized only if the aperture is sufficiently
large. The beam efficiency is higher than that of the
same size uncorrugated pipe.

Narasimhan[63] studied the field inside a horn
with arbitrary corrugation depths $\lambda/4 < h < \lambda/2$. When
the depth is equal to $\lambda/2$ the hybrid mode solution
degenerated to the solution of $TE_{11}$ mode. Later, he
studied[64] the problem of conical horns for illuminating
phased arrays. He has given the design formula for the
optimum flared corrugated conical horns.

Mentzer and Peters[65,66] reported the properties
of square corrugations. Their analysis included surface
current flowing on the corrugations, losses in corrugations
and scattering from them. When the ratio of width to
period is 0.9 the loss is minimum. The properties of
corrugated horn as an antenna standard are also reported.

Narasimhan and Rao[67] gave an analytical and
experimental investigations of E-plane corrugated horns.
The farfield radiation patterns are calculated by two
methods: (a) vector diffraction formula over a constant
phase surface at the aperture, (b) expansion of aperture

field in terms of free space cylindrical TE and TM wave function.

Baldwin and McInnes[68,69] discussed the radiation characteristics of a corrugated rectangular horn with moderate flare angle. Considering the hybrid modes inside the horn they calculated the radiation pattern using Krichhoff's-Huygens integration. Experimental results were presented for square corrugated horn and small horn with rectangular aperture, producing an elliptical beam for either of the two orthogonally polarized signals.

Bielli et al[70] gave a detailed characteristics of conical horns radiating balanced hybrid $HE_{11}$ mode. With the aid of their curves, a corrugated horn with specified amplitude radiation pattern could be designed.

Moriss[71] recently published a broad band constant beam width corrugated rectangular horn. Using aperture field, he had designed a horn with constant E and H plane beam width to operate over a band width of 2.4:1. The broad band nature of this antenna is due to the end loaded T-slots whose capacitive admittance is nearly constant in the band. A large separation between E and H-plane phase centre is also obtained.

## 2.3 Flange technique

Owen and Reynolds[72] first established the effect of metal flanges on the radiation patterns of small horns. They found the flanges are effective in controlling the E-plane radiation pattern of a H-plane horn. They also studied the effect of length and included angle on the radiation patterns.

Later Butson and Thomson[73] have conducted an elaborate study on the effect of flanges on the radiation patterns of waveguides and sectoral horns. The effects of such flanges are explained on the basis of secondary sources at the free ends of the flanges. The amplitude of the secondary source is attributed to be 0.077 times that of primary source. With an overall obliquity factor, the theoretical calculations and experimental results showed good agreement.

Nair and Srivastava[75] found that the radiation pattern from a flanged horn depends sufficiently on the position of the flange from the aperture of the horn. At certain positions of the flange with respect to the aperture of the horn pencil beam with maximum on-axis power density is obtained. This position is called "optimum position"

(O-position). Similarly at another position the on-axis
power is found to be minimum and this position is called
"minimum position" (M-position).

Contrary to earlier observations, Nair et al[76,77]
observed that H-plane pattern of an E-plane sectoral horn
can also be controlled by flange technique. But for an
E-plane horn, flange technique is effective only to some
optimum value of flange angle below 90°.

Nair et al[78] reported the effect of symmetric
and asymmetric flanges on the radiation patterns of H-plane
sectoral horn. With the aid of secondary sources a probable
theory is presented. At certain positions of the flange
H-plane patterns of the horn is found to be completely cut
off and this phenomena is called "beam elimination".

Koshy et al[79] considered the effect of asymmetry
in amplitude excitation of the secondary sources due to
their heterogeneous condition. Using this they obtained a
general expression for the E-plane radiation pattern of
H-plane sectoral horns.

Later Singh et al[80] conducted experimental studies
on the effect of asymmetric flanges. They found that beam
tilt is possible due to flange length asymmetry.

Nair[81] in 1970, modified the expression for the
E-plane radiation pattern of a flanged horn taking primary
horn as a linear aperture and considering its radiation
pattern than approximating it as a line source.

The effects of flange angle on the radiation pattern
of flanged H-plane sectoral horns are reported by Koshy et al[82].
Beam focusing and broadening can be achieved by adjusting
the flange angle alone.

Effect of slotted flange on a square waveguide is
studied by Sreevastava et al[83]. An optimum feed for deep
reflectors producing square radiation pattern have been
reported by them.

Nair et al[84] reported that dielectric flanges are
also effective in modifying the radiation patterns of
sectoral horn antennas. Beam tilting with asymmetric flanges,
one metallic and other dielectric, is also presented.

Jazi and Jull[85] adopted parabolic flanges to a
small pyramidal horn. The flanges decreased both HPBW and
back radiation. Theoretical analysis is given using geometrical
theory of diffraction (GTD).

Comparison between flanged sectoral horn and corner reflector system in beam shaping and tilting is analysed by Mathew and Nair[86]. They suggested that corner reflector analogy can be given to flanged sectoral horns, for theoretical interpretation of radiation patterns.

In 1979 Zachariah et al[87,88] studied the effect of corrugated flanges on the radiation pattern of H-plane sectoral horns. Tips of the corrugations are orthogonal to the E-vector. They found that corrugated flanges are more effective than plane flanges for improving radiation characteristics. Theoretical analysis of the radiation pattern is given on the basis of line sources and ray-optic principle.

Vasudevan and Nair[89,90] analysed the radiation characteristics of corrugated corner reflectors. It is found that at the optimum position of the feed, sharp radiation pattern is obtained with improved matching. Theoretical analysis of the corner reflector system on the basis of line source theory and method of image is given by them. Theoretical computations were compared with experimental results.

## 2.4  Circularly polarized horns

Ordinary waveguide horn can be used to produce circul rly polarized radiations[110].  A circularly polarized wave with good axial ratio along the axis can be obtained from a square horn fed with equal amplitude of vertically and horizontally polarized modes with space quadrature.  The radiated field is not circularly polarized at other points of radiation pattern due to the different beam width of vertical and horizontal polarization.  Methods for compensating the beam width are also given.

In 1962, A.W.Love[91] studied in detail the performance of diagonal horn antennas.  Here the E-vector is adjusted to be parallel to one of the diagonals.  He achieved perfect circular symmetry.  He also proposed a method to obtain circular polarization using this antenna. A diagonal horn can be easily converted into a circularly polarized one by inserting a differential phase shifter in the guide where the cross section is circular.  It will result in circular polarization over a considerable portion of the waveguide band width.

Han and Wickert[92] developed a multimode rectangular horn for generating a circularly polarized elliptical beam. This antenna operates in two orthogonal mode sets, namely

$TE_{10} + TE/TM_{12}$ and $TE_{10} + TE/TM_{21}$. A portion of $TE_{10}$ mode energy is converted into $TE/TM_{12}$ and $TE/TM_{21}$ modes called beam shaping modes with proper amplitudes and phase. Due to this, the far field beam width is equal to H-plane and resulting axial ratio is less than 2 dB over an earth coverage angle of 9°x16°.

R.W.Gurner in 1974[93] considered a circularly polarized feed horn with circular symmetry, over the 4 and 6 GHz satellite communication bands. In the 4 GHz band a corrugated section is added to the waveguide. At 6 GHz a step discontinuity is introduced inside the waveguide to launch $TM_{11}$ mode. A broad band polarizer in conjunction with the orthogonal mode transducer provided circularly polarized signals of opposing sense in the respective transmit and receive bands with an isolation of 55 dB.

In 1977, Ebisui et al[94,95] described the design theory of a flare iris type dual mode horn antenna. The variation of axial ratio with relative amplitude and phase of $TM_{11}$ and $TE_{11}$ mode has been described. $TM_{11}$ mode is excited by an iris in between the horn and circular wave-guide. According to them, the worst axial ratio is of 0.3 dB over the 18° earth coverage area.

Design description of 4 and 6 GHz earth coverage antennas has been given by Takeichi et al[96] in 1978. They used a flare-iris type dual mode horn. Summary of the performance is given as a table.

Dewey[97] in his invited paper in 1982 presented some aspects of design data of circularly polarized elliptical beam-shape horn antennas. He has thrown some light on circular polarizers, rectangular corrugated polarizers etc. Extension of his technique to compensate differential phase shift in non-symmetrical horns has been discussed by him.

Jull[98] proposed a method to produce circular polarization using metallic corrugated surface. The normally incident plane-polarized wave is oriented with its planeo of polarization at 45° to the grooves. The waves on the reflecting surface can be resolved into transverse electric (TE) and transverse magnetic (TM), components in which the tips of corrugations are parallel to the electric and magnetic fields respectively. During reflection, the TM component travels a quarter wavelength further than the TE component (If the corrugation depth is $\lambda/8$) which is totally reflected at the top of the corrugations. So a differential phase shift of $\lambda/2$ radian is obtained between

two orthogonal components. This caused circular polarization of the beam.

Rotation of plane of polarization of a beam of microwaves by corrugated reflecting surface is reported by Paul and Nair[99]. Orientation of the corrugations with plane of polarization of the incident radiation determines the tilt of polarization. It is reported that when the corrugation depth is $\lambda/4$, $90^{\circ}$ rotation of electric field is obtained.

An excellent review of circular p larization for CW radar has been presented by J.F.Ramsey[100]. The elliptical polarization can be conveniently represented in wave polarization chart[106]. It is a rectangular chart with ratio of electric fields and phase angle between them as coordinates. Using this technique

Rumsey and Tice[101,106] have devised a convenient method for representing the wave polarization. This technique employs a chart similar to a Carter charteand called the p-plane representation where p is j times the polarization ratio. Here the axial ratio is equivalent to SWR and tilt angle of the polarization ellipse takes the place of the line length in smith chart.

Rumsey employed[101] a Smith impedance chart with altered co-ordinate for representing elliptical polarization. The axial ratio is equivalent to SWR and the tilt angle is just one half of the polar angle. Elliptical polarizations are represented by points inside the unit circle. Any point on the unit circle represents the linear polarization with proper tilt angle.

Deshamps[102] used a map projection of Poincare's spherical representation into a plane diagram. Here the outside scale marked 0 to 180° gives the tilt angle of the polarization ellipse. The vertical scale is the ratio of vertical to horizontal polarization. Horizontal scale represents the phase difference in degrees between them. Axial ratio is given by circles of radius equal to the lower half of the vertical scale.

A detailed discussion about elliptically polarized waves and antennas is given by Kales[103] in the same issue.

From the review of past work given above, it can be seen that circularly polarized antennas are of great importance. Circular polarization is important in radar since it can reduce clutter. It is also important in communication systems

in which rotation of electric vector can occur. It may be noted that no attempt has been made to study the effect of tilted corrugated flanges on H-plane sectoral horns. This thesis presents the results of an investigation on exploring the possibility of producing circular polarization by flanges with tilted corrugations on the beams from H-plane sectoral horns.

CHAPTER : 3

**Methodology and experimental set up**

Chapter 3

## METHODOLOGY AND EXPERIMENTAL SET UP

This chapter is devoted to the description of the equipment and measurement techniques used for the experimental study.

3.1  Microwave source and waveguide components

A Gunn diode oscillator is used as a microwave source in the present investigation. The oscillator can be tuned over a broad band of frequencies at X-band (8.2 to 12 GHz). The dimensions of the waveguide are such that the waveguide can support $TE_{10}$ mode. A sweep oscillator (HP model 8620C) is also used as a source for certain observations. Variable attenuator, isolator, frequency meter, slotted-line section, crystal detector etc. are the important waveguide components used in the experimental set up. A direct reading frequency meter having sensitivity 0.002 GHz is employed for frequency measurements. A standard pyramidal horn is used as receiver f microwave signals. The aperture of the pyramidal horn is 9.5x7.5 sq.cm and the flare angle in H-plane and E-plane are 35° each.

As far as this work is concerned, H-plane sectoral horns are the major component used for investigation. All these horns are made locally with thin brass sheets. For better conductivity, inner surfaces are silvered. Care is taken to avoid any non-uniformity in construction. Parameters of different horns used in this study are shown in table 3(1).

3.2 Corrugated flanges

As stated earlier, the aim of the thesis is to study the effect of corrugated flanges on H-plane sectoral horns. Therefore corrugated flanges are the prime part of the experimental set up. A corrugated flange is a thick metal plate with a comb surface. It is made locally by machining grooves on aluminium, brass or copper sheets using circular saws. Most of the flanges used in this study are made of aluminium as it is of good conductivity with less weight and cost. Parameters of different flanges used in this study are shown in table 3(2).

Three types of flanges are used in this work.

Circular flanges: Here the shape of the flange is a circular flanges having 12.5cm diameter. Using this circular flanges the corrugations can be adjusted to any convenient respect to the E-vector without causing any

As far as this work is concerned, H-plane sectoral horns are the major component used for investigation. All these horns are made locally with thin brass sheets. For better conductivity, inner surfaces are silvered. Care is taken to avoid any non-uniformity in construction. Parameters of different horns used in this study are shown in table 3(1).

## 3.2 Corrugated flanges

As stated earlier, the aim of the thesis is to study the effect of corrugated flanges on H-plane sectoral horns. Therefore corrugated flanges are the prime part of the experimental set up. A corrugated flange is a thick metal plate with a comb surface. It is made locally by machining grooves on aluminium, brass or copper sheets using circular saws. Most of the flanges used in this study are made of aluminium as it is of good conductivity with less weight and cost. Parameters of different flanges used in this study are shown in table 3(2).

Three types of flanges are used in this work. (a) Circular flanges: Here the shape of the flange is a circle having 12.5cm diameter. Using this circular flanges the tilt of the corrugations can be adjusted to any convenient angle with respect to the E-vector without causing any

Table 3(1)

Parameters of the horns used in this study

| Horn number | Horn length cms | Aperture in H-plane | Aperture in E-plane | Flare angle |
|---|---|---|---|---|
| $H_1$ | 23.5 | 10 | 1 | 24 |
| $H_2$ | 12.5 | 6.8 | 1 | 21 |
| $H_3$ | 9.5 | 5.7 | 1 | 20 |
| $H_4$ | 9 | 7.5 | 1 | 30 |

Table 3.2

Parameters of the flanges used in this study

| Flange Number | Corrugation height h (mm) | Corrugation width w (mm) | Thickness of the element | Material |
|---|---|---|---|---|
| $F_1$ | 4 | 5 | 1 | Aluminium |
| $F_2$ | 5 | 5.5 | 2.5 | ,, |
| $F_3$ | 3.2 | 5 | 1 | Brass |
| $F_4$ | 3.2 | 5 | 1 | Aluminium |
| $F_5$ | 11 | 7 | 4 | ,, |
| $F_6$ | 4 | 3 | 1 | ,, |
| $F_7$ | 4 | 8 | 1 | ,, |
| $F_8$ | 4 | 5 | 1 | Perspex |
| $F_9$ | 4 | 6 | 1 | Aluminium |
| $F_{10}$ | 4 | 7 | 1 | ,, |
| $F_{11}$ | 4 | 11 | 1 | ,, |
| $F_{12}$ | 4 | 5 | 1 | Aluminium coated |
| $F_{13}$ | 4.5 | 4 | | Aluminium |
| $F_{14}$ | 4.5 | 4 | 2 | ,, |
| $F_{15}$ | 4.5 | 14 | 6 | ,, |

asymmetry. (b) Rectangular flanges with tilt of corrugations inclined 45° to the E-vector. From the study using circular flanges, it was found that circular polarization could be obtained only when the tilt of corrugation is 45° with respect to E-vector. Fig.3(1) presents photographs of the different types of flanges used. These types of flanges were utilised for further investigations. (c) Rectangular flanges with tilt of corrugation 90° to the E-vector. These types of flanges are exclusively used for obtaining axially symmetric radiation patterns. When the tilt of corrugation is 90°, cross-polar component is negligibly small. Hence there is no scope for the beam to have circular polarization. These flanges are used to obtain axially symmetric radiation patterns from feeds for illuminating paraboloidal reflectors. Work carried out in this field is described in the appendix.

The flanges are mounted on a metallic mount called the base-frame. An aluminium sheet is bent to form the base frame so that the two edges subtend the desired flange angle. Separate base frames are used for flanges of different flange-angles. The flanges are fitted on the base-frame and clamped to a movable metallic frame which can be moved over the horn by a rack and pinion arrangement. For fixing circular flanges, the above system is slightly modified.
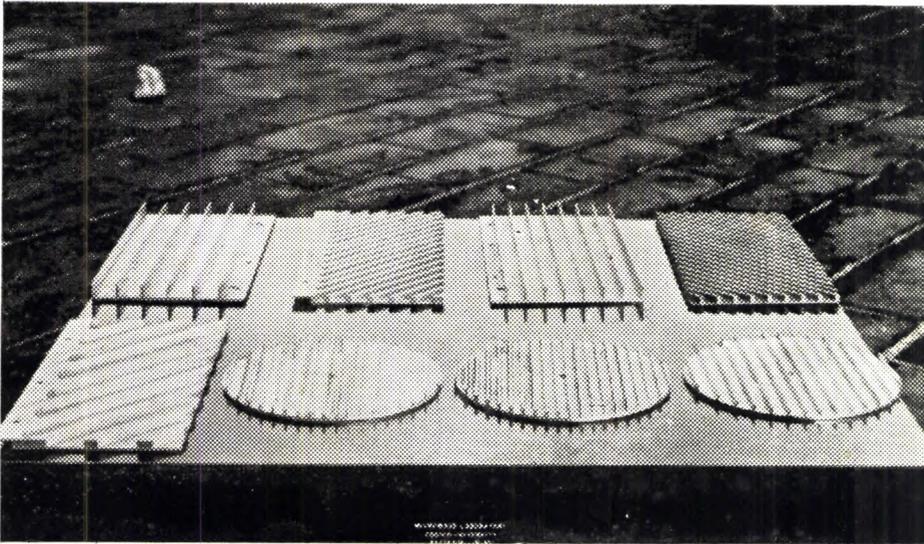
Fig 3.1 Some of the corrugated flanges used in this study.
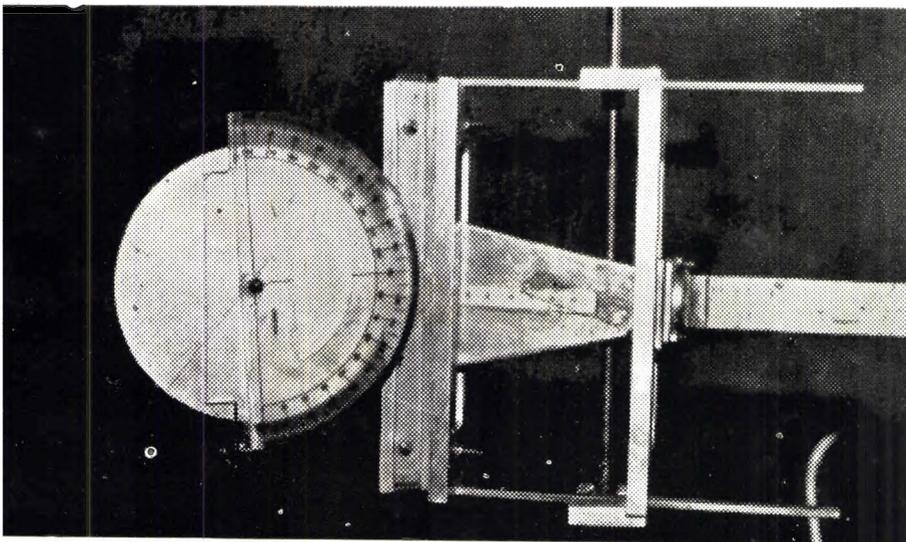


Fig 3.2 (a) Sectoral horn with flange moving mechanism.

A perspex sheet with circular scale is mounted on the metallic frame. A circular flange is mounted on the above system through a hole on the perspex sheet so that it can be rotated about an axis perpendicular to the plane of the flange. The tilt of corrugation can be directly noted from the circular scale on the perspex sheet. Photograph of flanged sectoral horn feed is shown in fig.3(2)(a),(b) and (c).

3.3 Antenna positioner

Usually, in antenna measurements, the test antenna will be used as a receiver. However, this method is not convenient in the present system since the corrugated flanges fitted to the horn may cause asymmetries as it rotates about an axis. Hence, the flanged sectoral horn under investigation is used as a transmitter of microwave energy in most of the experiments. The flanged sectoral horns as the transmitter of microwaves is shown in fig.3.3. To take the radiation patterns of a flanged horn, a pick-up horn will be moved on a circle of constant radius, with the transmitter as the centre. The pick-up horn (a pyramidal horn) is mounted on a platform fitted with smooth wheels of which one is coupled to the shaft of a highly shielded 6V DC motor through reduction gears. The system is designed to move freely, with minimum friction along the circumference of a circle about a vertical axis passing
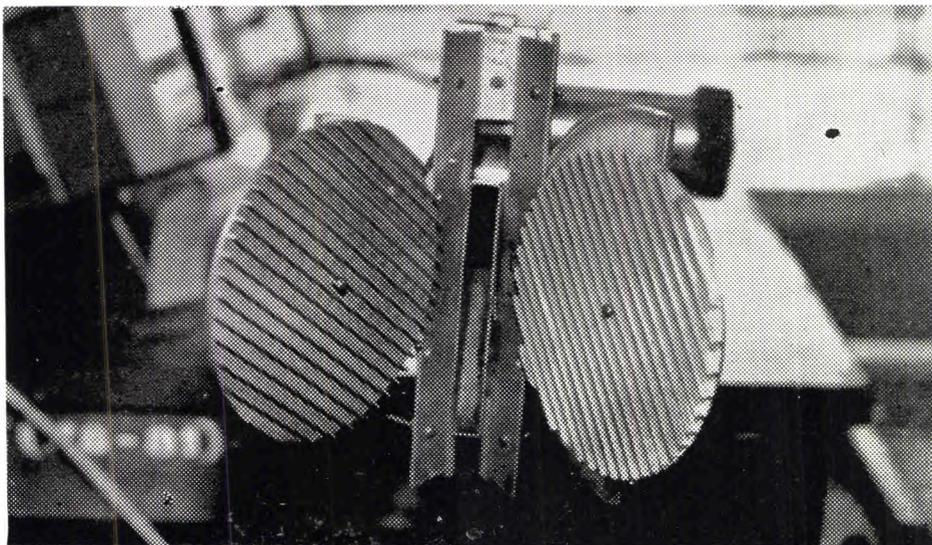
*Fig 3.2 (b)* Flanged sectoral horn feed (Front view)
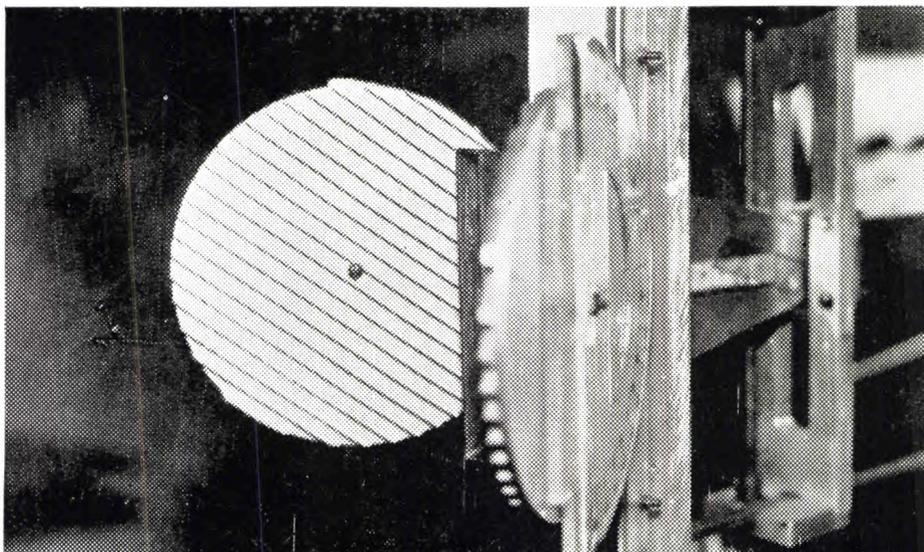


*Fig 3.2 (c)* Flanged sectoral horn feed (Angular view)
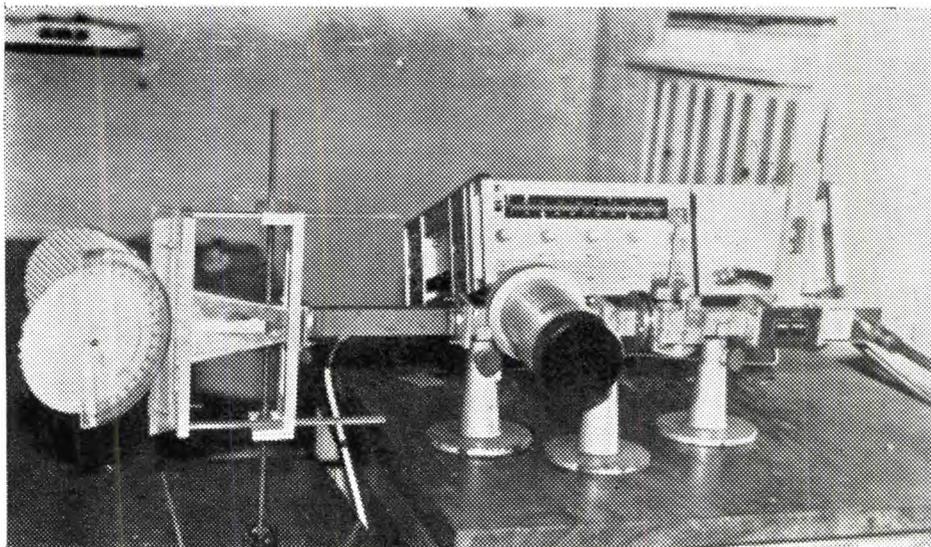
*Fig 3.3* Flanged sectoral horn as the transmitter.
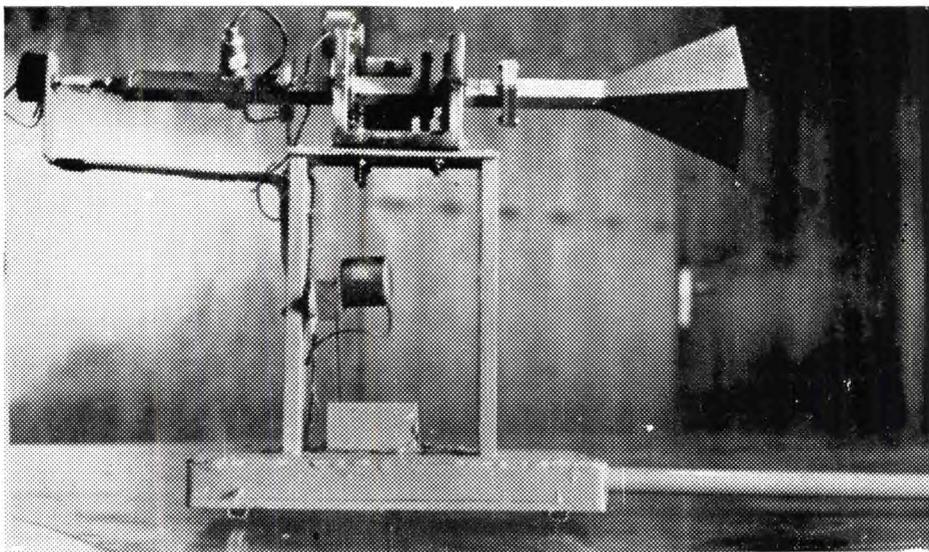


*Fig 3.4* Pyramidal horn used as the receiver.

through the apex of the test antenna system. A long PVC
pipe having length 2m is used as the arm of the rotating
system. The whole system is moving on a horizontal levelled
platform. The system can be rotated through -90° to 90°, with
a uniform speed of 1 rpm. A wire wound potentiometer, the
shaft of which rotates in synchronization with the turn
table, is employed for obtaining the angular position at
any instant. The voltage at the centre tap of the potentio-
meter is proportional to the angle through which it is
rotated. This voltage is fed to one input of an X-Y
recorder. The received signal after rectification is fed
to the other input. Using this arrangement, the radiation
pattern through -90° to 90° is automatically plotted. The
pyramidal horn as the receiver is shown in fig.3.4.

3.4 Antenna polarization positioner

For polarization measurements it is necessary to
rotate the transmitter about a horizontal axis. A motorized
remote control facility is used for polarization measurements.
A waveguide piece is passed through two bearings A and B
fitted on a metallic frame. One end of the waveguide is
connected to a pyramidal horn and the other end to a crystal
detector with an adjustable short. C is a circular tooth
wheel coupled to another gear box D, which is connected to

a 6V DC motor through a pulley and belt. Diagrammatic
representation of the antenna polarization positioner is shown
fig.3.5. A wire wound linear potentiometer rotating
in synchronization with the horn gives the angular position
of the horn in a vertical plane. The photograph of the
antenna polarization positioner is shown in fig.3.6.


3.5 Circularly polarized standard receiver

To test the sense of circular polarization two
symmetrical helical antennas are employed. One is left
handed circularly polarized and the other is right handed
circularly polarized. The parameters of the helical antennas
used are given in table 3(3). The helical antenna is used
as a receiver. The variation of received on axis power
density with flange position and tilt of corrugation are
noted. Using this circularly polarized helical antenna as
a receiver the radiation pattern is also plotted, with flanged
horn as transmitter of microwaves.


3.6 Measurement of on-axis, co-polar and cross-polar
    power density

The power density radiated by the antenna along
the axis is termed the "on-axis power". It is an important
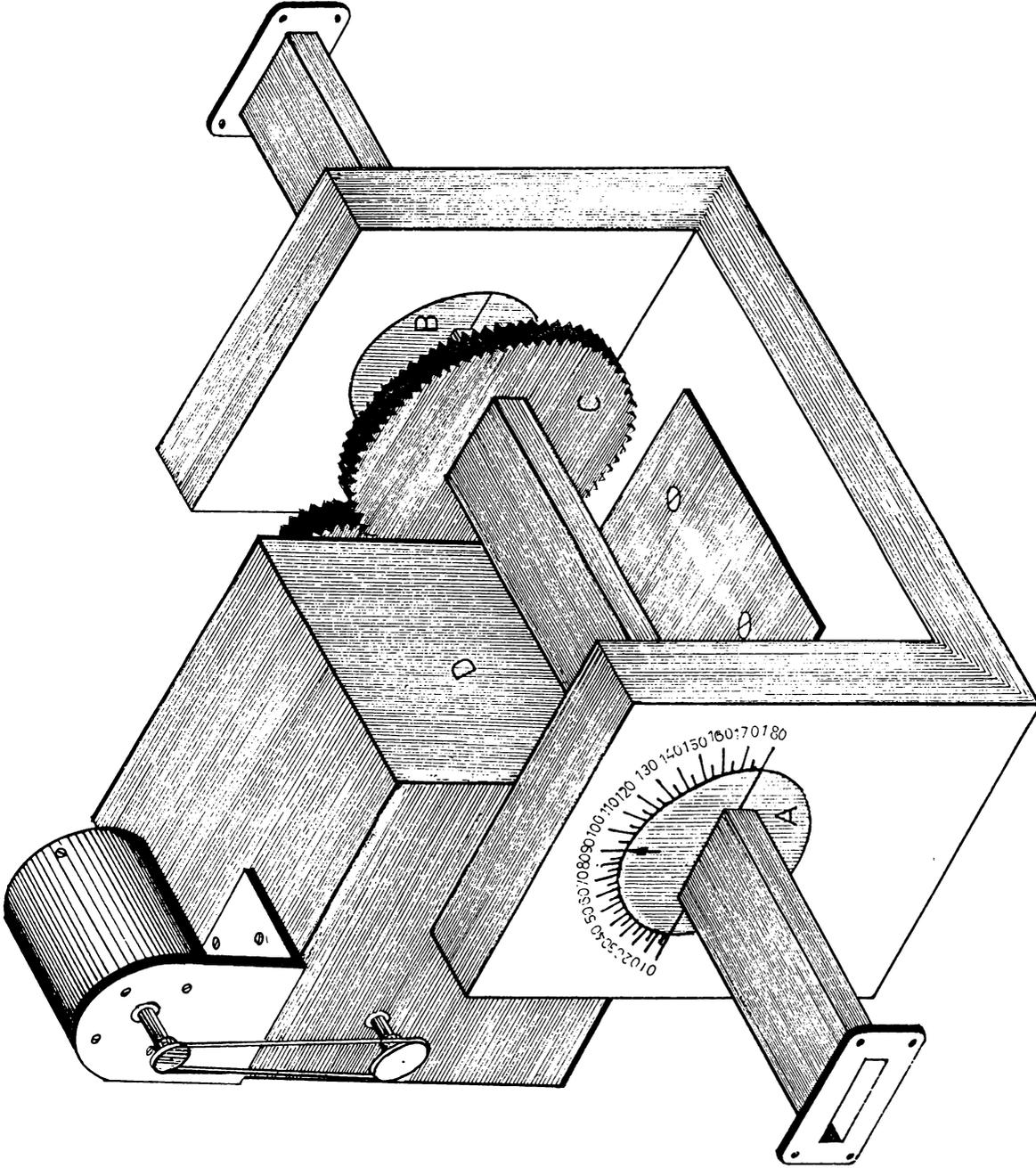
Fig. 3·5 : Dia gramatic representation of the antenna polarization positioner.

58
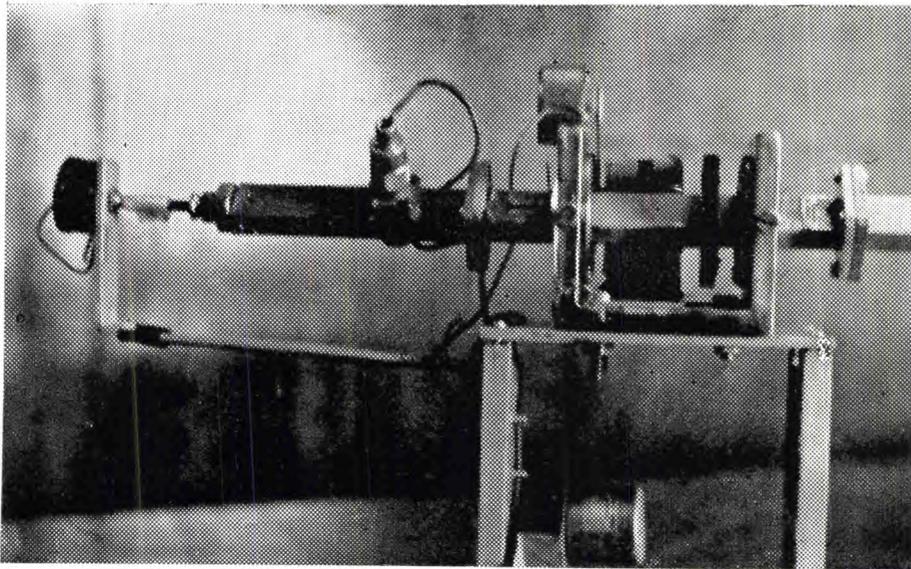


Fig 3.6  Receiving antenna rotating mechanism used for plotting
polarization pattern.
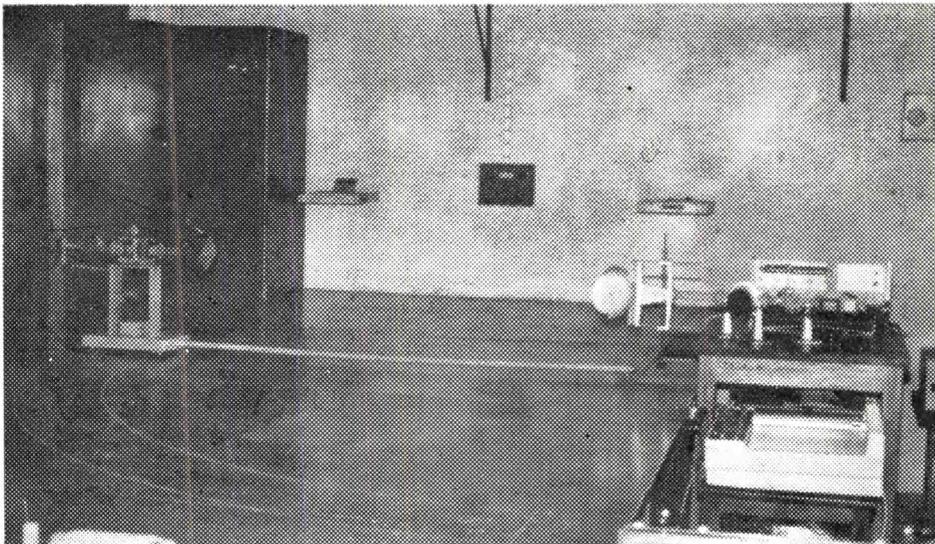


Fig 3.7  Experimental setup for plotting the radiation pattern.

Table 3(2)

Parameters of the helical antenna

------------------------------------------------------------

       Diameter of the helix D     =  1 cm

       Spacing between turns S     =  0.7 cm

       Conductor diameter d       =  0.064 cm

       Spacing from the ground ᛁ$_g$ =  0.4 cm
       plane to the first turn ᛁ

       Pitch angle              =  12°

       Ground plane           =  6x6 sq.cm

------------------------------------------------------------

factor because it gives a qualitative idea of the sharpness
of the beam. A flanged H-plane sectoral horn is used as the
transmitter of microwaves. A standard pyramidal horn whose
polarization is parallel to that of the transmitter is used
as the receiver. The receiver is kept at a distance greater
than $\dfrac{D_1^2 + D_2^2}{\lambda}$ , where $D_1$ and $D_2$ are the largest dimension of
the receiver and transmitter and $\lambda$ is the free space wave-
length, to ensure plane electromagnetic waves at the receiver.
The received power is rectified and fed to one axis of the
X-Y recorder and the DC signal from a linear potentiometer,
whose wiper moving in synchronization with the position of
the flange from the aperture is given to the other axis.
The flange is moved at a uniform slow speed along the length
of the horn from its aperture and the variation of an-axis
power density is automatically traced. To find the cross
polar power density the receiver is rotated through 90° and
the experiment is repeated.

## 3.7 Measurement of VSWR

When the antenna is not matched to free space,
reflection is produced at the boundary. Due to the interaction
of the incident and reflected wave, a standing wave pattern
is formed inside the waveguide. Using a slotted section,

VSWR of the system is monitored[104,107]. Since a crystal
obeying square law is used, the output current from the
crystal is proportional to the power.

$$\text{VSWR} = S = \frac{V_{max}}{V_{min}} = \frac{\sqrt{P_{max}}}{\sqrt{P_{min}}} = \sqrt{\frac{I_{max}}{I_{min}}}$$

VSWR of the system is found at the desired position
of the flange for different flange parameters and frequency.
From the measured VSWR, the amount of matching and efficiency
of radiation to or from the horn can be determined.

## 3.8  Polarization pattern

Polarization of an electromagnetic wave, whether
linear, elliptical or circular can be considered to be some
form of elliptical polarization.  Following methods are
commonly employed for measuring the polarization characteristic
of electromagnetic waves.

a)  Polarization pattern method[106,110]

A linearly polarized antenna with a crystal detector
is used as a receiver and it is rotated through 360° about a
horizontal axis.  A graph between the received signal and the

angle of rotation will give the polarization pattern.
Typical polarization ellipse and polarization pattern
for different cases are shown in fig.3.8. The polariza-
·tion ellipse of the antenna in a given direction is similar
to one which can be inscribed in the polarization pattern
with points of tangency at the maxima and minima. The
ratio of major axis to minor axis is called the "axial-
ratio". The direction of maximum electric field is the
tilt angle. The direction of rotation of the E-vector
can be obtained by comparing the received signal by two
circularly polarized antennas with opposite sense of
polarization. The antenna with largest response would
be the one with proper polarization rotation.

$$\text{Axial ratio} = 20 \log \frac{E_{max}}{E_{min}}$$

b) Linear component method

In this case two identical linearly polarized
antennas with polarization orthogonal to each other are
employed as the receiver. The received signal by these
two antennas are noted. The phase difference between these
two signals are measured using a Magic Tee. If the phase
difference is positive the sense of rotation is clockwise

TEST ANTENNA                    DIPOLE

(a)

LINEAR            ELLIPTICAL            CIRCULAR

(b)
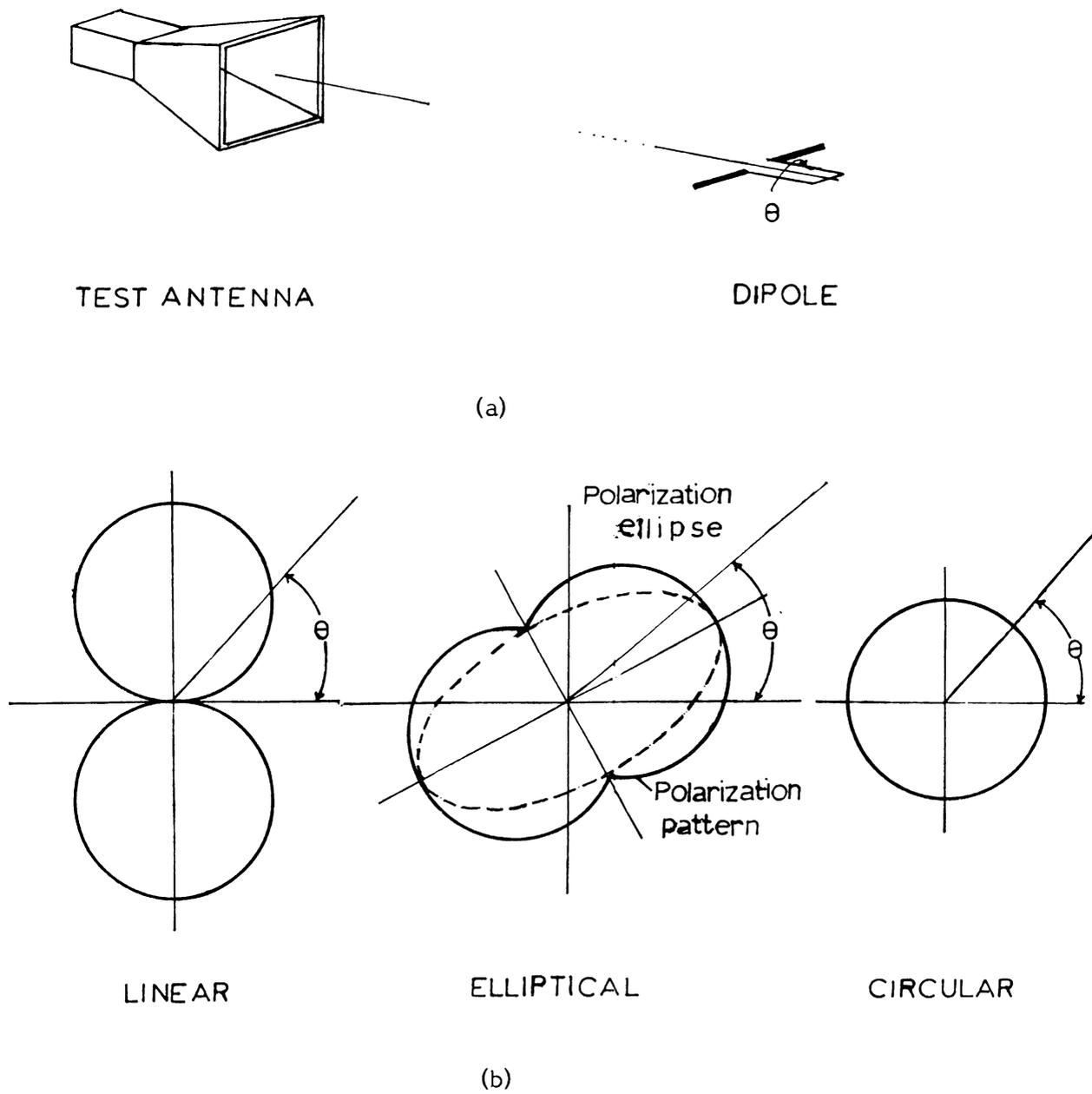
Fig.3-8: a) Basic experimental arrangement for polarization studies.

b) Typical polarization ellipse and polarization pattern for different cases.

and vice-versa. The tilt angle is given by the formula

$$\tau = \tfrac{1}{2}\tan^{-1}\frac{2E_1 E_2 \cos\delta}{E_1^2 - E_2^2}$$

where $E_1$ and $E_2$ are the received signals by two antennas and $\delta$ is the phase difference between them.

c) Circular component method

Two circularly polarized antennas of opposing sense are employed as receiver. The two antennas must be identical. The received power by the LHCP and RHCP antennas are monitored and axial ratio is calculated using the formula

$$A.R = \frac{E_R + E_L}{E_R - E_L}$$

where $E_R$ is the signal received by RHCP and $E_L$ that by the LHCP antenna. The tilt of polarization can be found by rotating a linearly polarized antenna. Since the polarization pattern measurement is simpler, this method is used throughout this work.

A linearly polarized pyramidal horn kept at the
far field with remote control facility is employed as a
receiver. Polarization isolation of the horn is 30 dB.
The received rectified signal is given to one channel of
the X-Y recorder. The voltage across one terminal and
centre tap of a linear potentiometer is fed to the other
channel. Polarization pattern is automatically plotted
for different parameters.

## 3.9 Axial ratio and tilt angle

Axial ratio is the ratio of the two extreema
of the polarization ellipse taken along the axis of the
beam. Axial ratio $= 20 \log\dfrac{E_{max}}{E_{min}}$ . For a circularly polarized
wave axial ratio is unity or 0 dB. For all other cases it
is greater than this value. Another quantity which is
commonly used in broad-beam work is the "polarization ratio".
It is defined as the ratio of the major axis to minor axis
of the polarization pattern at any angle in the beam of the
antenna. Axial ratio and polarization ratio are calculated
from the polarization pattern. Since a square law crystal
is used axial ratio is equal to

$$20 \log \left( \frac{I_{max}}{I_{min}} \right)^{0.5} = 10 \log\left(\frac{I_{max}}{I_{min}}\right).$$

Another quantity of great interest in dealing with elliptical polarization, is the tilt angle. Polarization ellipse is usually tilted in space with respect to the co-ordinate axis. The angle of tilt of the major axis of the polarization ellipse with the horizontal is the "tilt angle". Tilt angle is measured from the polarization pattern.

## 3.10 Sense of rotation

In elliptical polarization, the electric vector makes one complete revolution per cycle at a uniform rate. For a RHCP wave the electric vector in a transverse plane is clockwise to an observer looking in the direction of propagation. For LHCP the reverse is true. To detect the direction of rotation, the received signals by two circularly polarized helical antennas with identical characteristics except the sense of polarization are compared. The proper direction of rotation of the electric vector is given by the sense of rotation of the helical antenna with largest response. From the measurements of axial ratio, tilt angle and sense of polarization, complete information about elliptical polarization can be obtained.

## 3.11 Radiation pattern

The radiation pattern of an antenna determines the spatial distribution of radiated energy from that antenna. Usually it is a three dimensional field-intensity variation over all angles of space. Radiation pattern is commonly taken along the H and E-planes on $\gamma$. H-plane pattern shows the angular distribution of field intensity along the direction of magnetic vector. According to the reciprocity theorem, radiation pattern can be measured by two methods: (a) Test antenna as receiver, and (b) test antenna as transmitter. As mentioned earlier, second method is followed in this work. A standard pyramidal horn is used as a receiver and is rotated along a circular path with radius greater than $\dfrac{D_1^2 + D_2^2}{\lambda}$ where $D_1$ and $D_2$ are the maximum aperture dimensions of the receiving and transmitting antennas. Radiation pattern is automatically traced using a HP 7007 A model X-Y recorder having a voltage sensitivity of 0.02 mv/cm. Fig.3.7 in page 58 shows the photograph of the set up for plotting the radiation pattern. To take the cross polar pattern the receiver is rotated through 90° and the experiment is repeated. Final experiments are conducted in an anechoic chamber to simulate free space environments.

3.12  Half power beam width and gain

Antenna half power beam width is an important
parameter because it shows the sharpness of the beam.  Beam
width of the radiation pattern is the width of the pattern
at the specified power level.  Half power beam width is
the angular width of the radiation pattern when the power
is reduced to half.  It is also called 3 dB beam width. In
certain cases 10 dB, 20 dB or beam width between the nulls
are also specified.  In this work attention is given only
to half power beam width (HPBW).

Gain in this thesis refers to the directive gain.
It is the ratio of the maximum radiation intensity to the
average radiation density.  It is also obtained from the
radiation pattern by the method of pattern integration[105].
Directive gain

$$G = \frac{2\pi I_{max}}{\int_{o}^{2\pi} I_\theta d\theta}$$

where $I_{max}$ is the maximum radiation intensity and $I_\theta$ is
the radiation intensity an angle $\theta$.  $\int_{o}^{2\pi} I_\theta d\theta$ is given by
the area enclosed by the radiation pattern and $\theta$ axis

within the limits 0 to 360°. Other quantity which is of great interest is the sidelobe level. It is the level of any lobe of the radiation pattern except the main lobe. It is also calculated from the radiation pattern. Sidelobe level is given by $10 \log \frac{P_1}{P_2}$ where $P_1$ is the peak power of the main lobe and $P_2$ is the peak power of the sidelobe.

CHAPTER : 4

**Experimental results**

Chapter 4

EXPERIMENTAL RESULTS


This chapter highlights the outcome of the experimental results carried out on H-plane sectoral horns fitted with tilted corrugated flanges. The experimental investigations have been conducted at X-band for the dominant $TE_{10}$ mode. The following important antenna characteristics were studied in detail during the course of investigation:

1) Co-polar and cross-polar on-axis power density

2) Polarization pattern

3) Axial ratio

4) Tilt angle

5) Sense of rotation

6) Radiation pattern

7) Voltage standing wave ratio (VSWR)

8) Half power beam width (HPBW)

9) Directive gain

Variation of all these antenna characteristics with various flange parameters like the position of the flange from the aperture, tilt of corrugation, flange angle and frequency are studied and summarised below.

## 4.1 Co-polar and cross-polar power density

On-axis co-polar and cross-polar power densities are the power radiated by a flanged sectoral horn parallel and orthogonal to the E-vector respectively along the axis. A circularly polarized antenna will behave identically to both polarizations. So, the on-axis co-polar and cross-polar power density must be equal for a circularly polarized radiator. The present attempt is to explore the possibility of equalising these two power densities by varying the flange parameters. As a preliminary observation, the effects of flange parameters on the on-axis co-polar and cross-polar power densities are studied. The possibility of achieving circular polarization by equalising these two fields is also investigated.

## 4.1(i)  Variation of co-polar and cross-polar power density with flange position (Z):

As described earlier the flanges are attached to the flange mounting mechanism. On-axis co-polar power

density is monitored by using a small standard pyramidal
horn at the far field of the flanged horn. By rotating
the receiver through 90°, the cross-polar power density
is monitored. The experiments are repeated with different
flange positions at an increment of 2 mm from the mouth of
the horn.

It is found that the on-axis co-polar and cross-
polar power densities are very much dependent on the
position (Z) of the flange from the aperture. On axis
power density fluctuates between a maximum and minimum
values. For a particular position of a 45° tilted corru-
gated flange, there is an appreciable amount of cross-polar
component which is nearly equal in amplitude to that of
co-polar one.

Fig.4.1 presents the typical curves showing the
variation of co-polar and cross-polar power density with
position Z of the flange with respect to the aperture
for different tilt of corrugations. From the observations
it is obvious that there is an optimum value of Z, and tilt
of corrugations for which the co-polar and cross-polar
components have nearly equal values. It is observed that
the optimum corrugation tilt angle is 45° with respect to
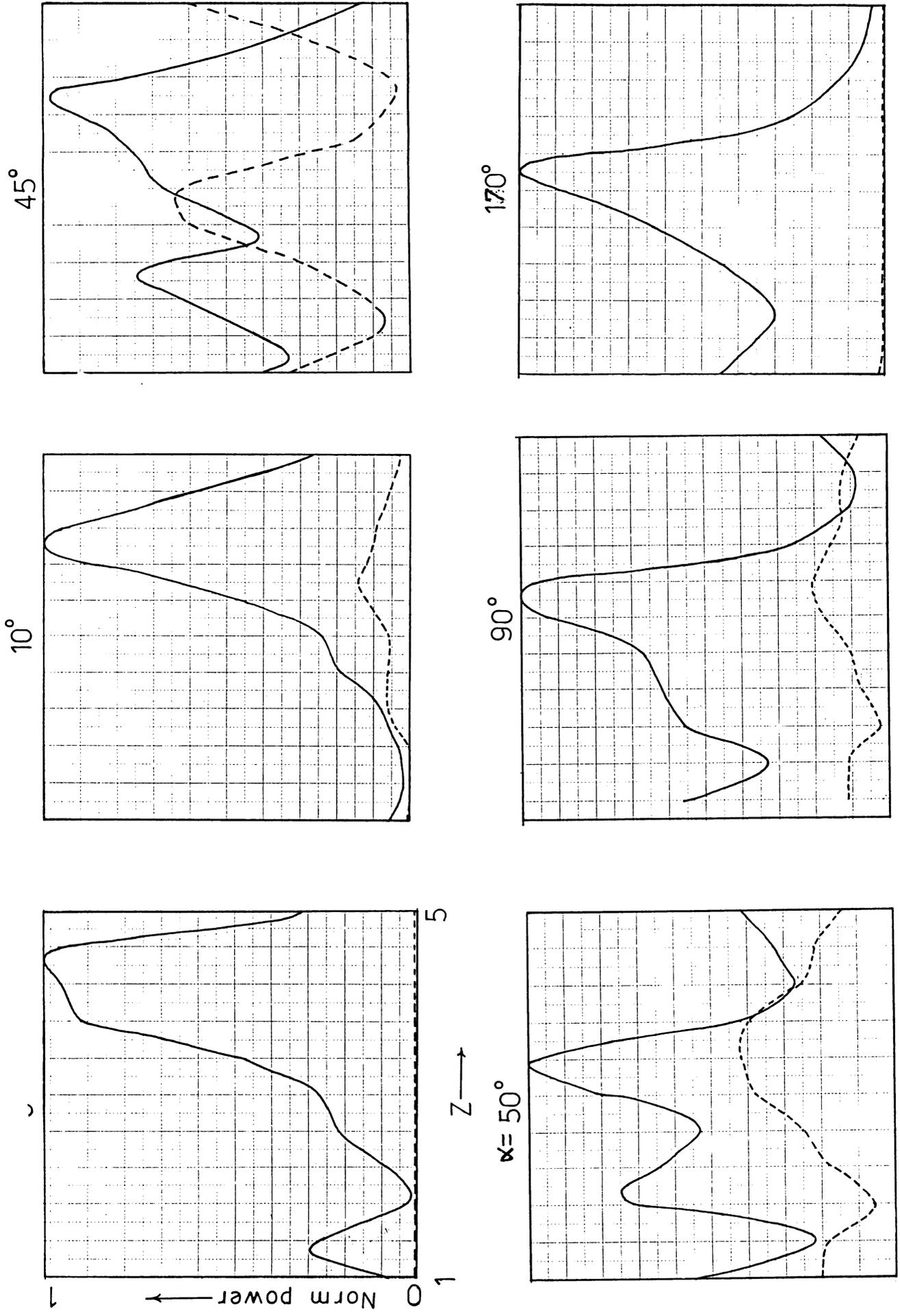
Fig. 4.1: Variation of Co-polar & Cross-polar power density with Z . —— Co-polar, – – – –Cross-polar.
Horn H2, Flange F1, Freq. 9.375 GHz, 2β=45°.

a line orthogonal to the on-axis. If this angle is greater
than or less than 45°, the cross-polar component is very
small. These results are true with all flanges, flange
angles and frequency of operation. These observations
show that circular polarization can be obtained from H-plane
sectoral horns fitted with a tilted corrugated flange.

4.1(ii)   Variation of co-polar and cross-polar power
          density with tilt of corrugations ($\alpha$)

It is found that on-axis co-polar and cross-polar
power density varies with tilt of corrugations. Keeping one
flange at a constant corrugation tilt, the tilt of corrugation
of the other flange is varied. The corresponding co-polar
and cross-polar power densities are noted. It is again
observed that when corrugations on both the flange  elements
are tilted through 45° to the H-vector, co-polar and cross-
polar components are equal. Typical experimental results are
shown in fig.4(2). Again, from the above data, the optimum
tilt of corrugation for circular polarization is observed
to be 45°. These results are found to be true for other
flanges fitted to other horns also.

4.2   Axial ratio

For an elliptically polarized wave, an important
antenna characteristic to be studied in detail, is the
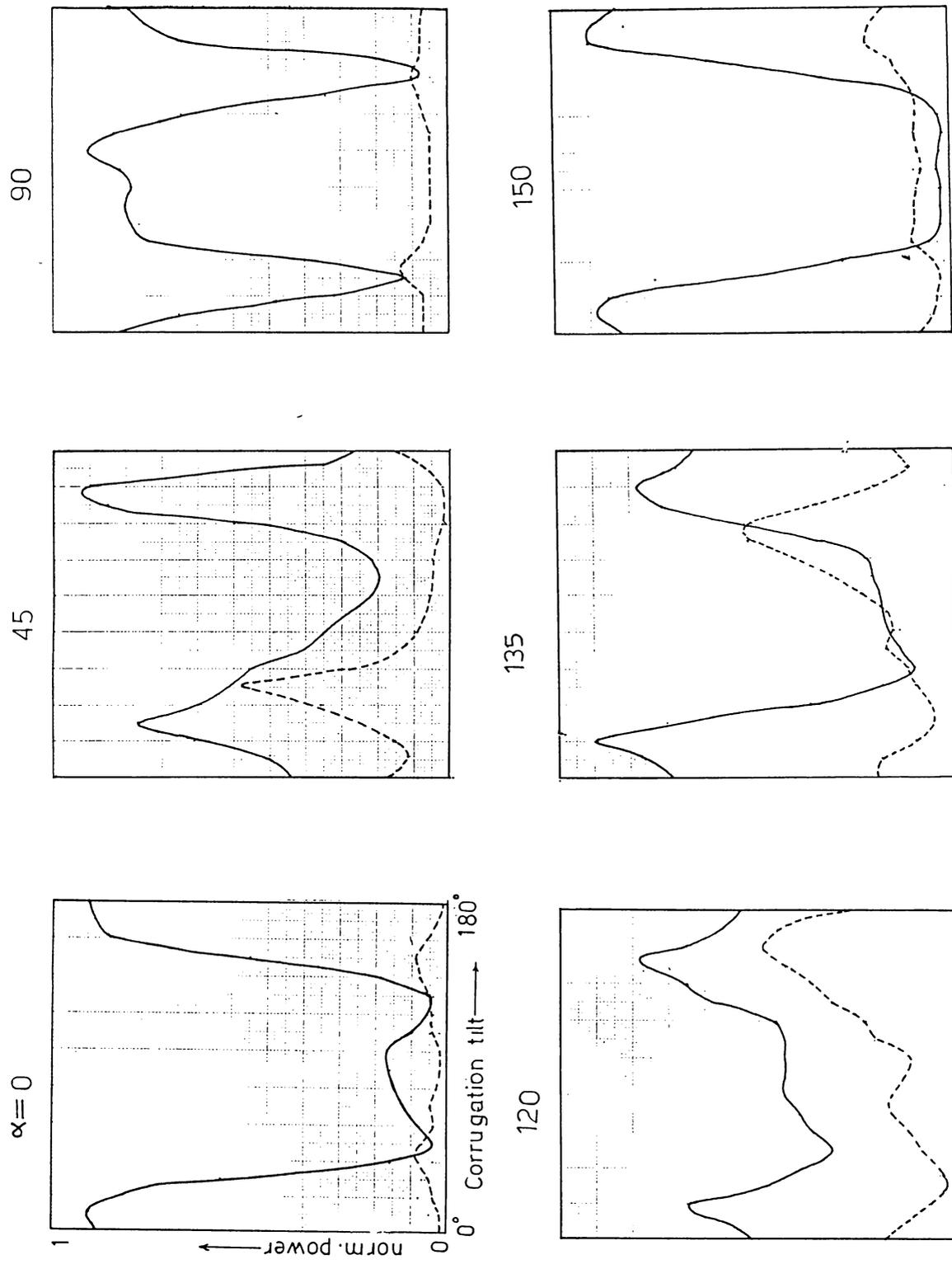
Fig. 4.2: Variation of Co-polar & Cross-polar power density with corrugation tilt ——— Co,——— Cross.
Horn H2, Flange F1, Freq. 9·375 GHz, 2β=45, Z=2·5.

"axial-ratio". "Axial-ratio" is defined as the ratio of the major to minor axis of the polarization-ellipse along the peak of the radiation pattern. This being an important antenna characteristic of an elliptically polarized antenna, as pointed in chapter 3, its dependence on the various flange parameters are studied in detail. Axial ratio is calculated from the polarization pattern which is obtained by rotating a small pyramidal horn at the far field, about the incident beam.

4.2(i)  Dependence of axial ratio on flange position (Z)

It is found that axial ratio is strongly influenced by the position of the flange from the aperture of the horn. Axial ratio fluctuate from a maximum to minimum as the flanges are moved back from the aperture of the horn. At certain position  the axial ratio approaches 0.5 dB, and the radiation is almost circularly polarized.  If the axial ratio is high,the polarization is elliptical.  It is found that depending upon the position of the flange a linearly polarized co-polar and cross-polar radiation can be produced. The variation of axial ratio in dB with Z for different flange angles and horns are shown in fig.4.3(a,b&c). Typical variation of polarization ellipse with Z is presented in fig.4(4) for better clarity.  It can be seen that the radiation is found to be circularly polarized only for a
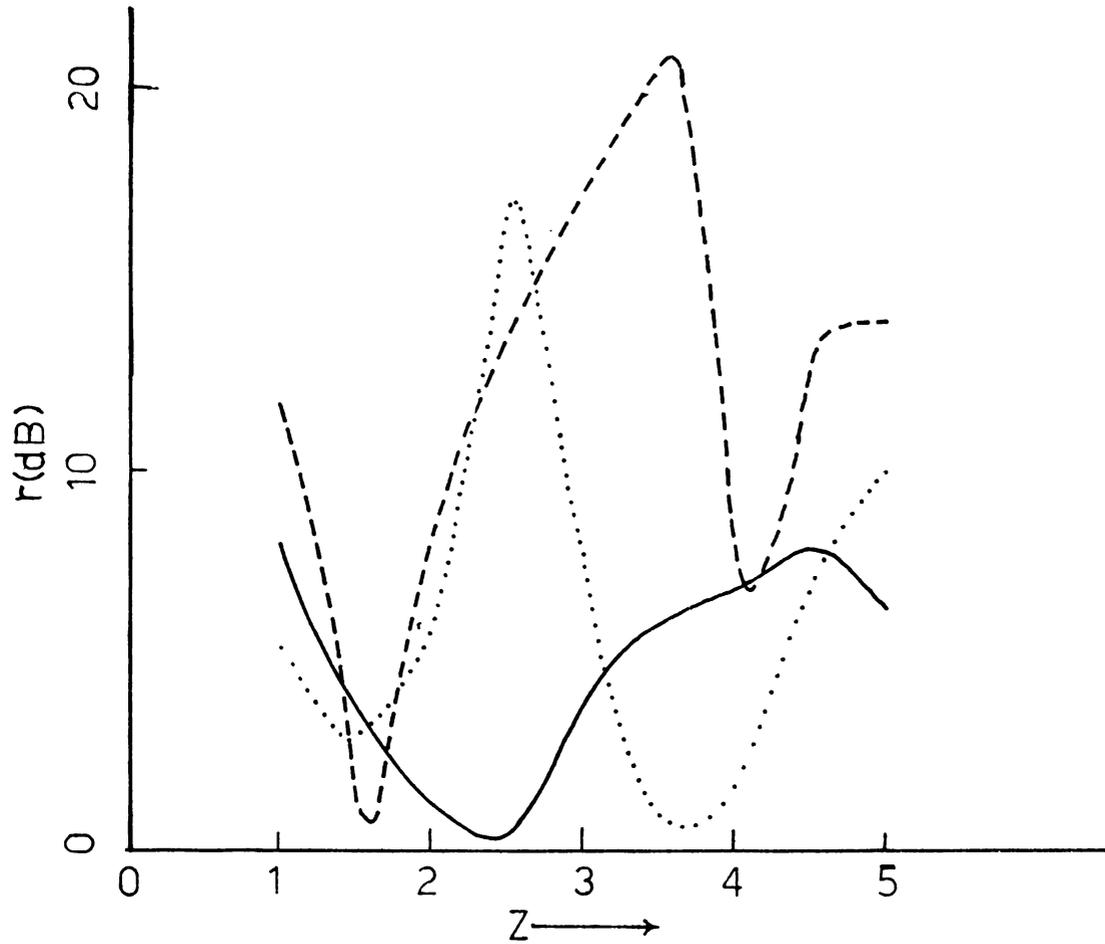
Fig.4.3(a): variation of axial ratio with flange position Z.Horn H2
Fla. F1,Freq. 9.375 GHz._____2β=45,---- 2β=90,...... 2β=60
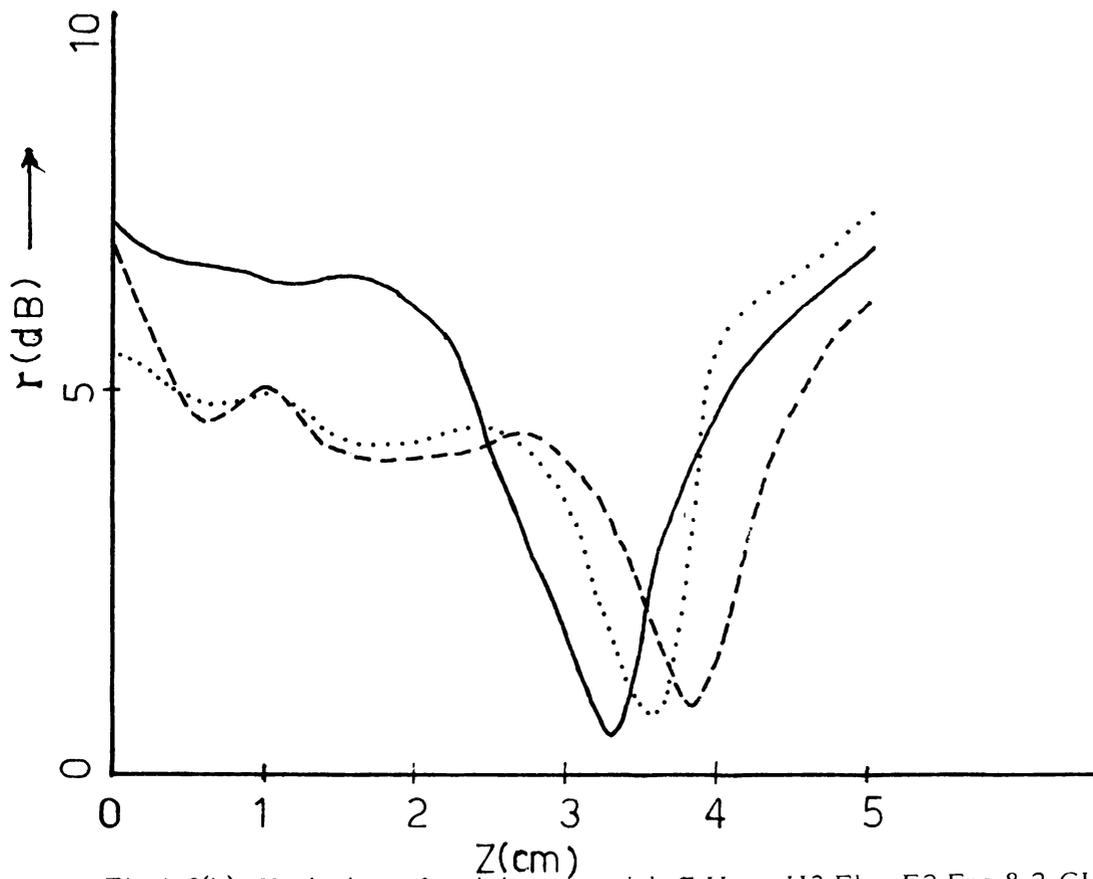


Fig.4.3(b): Variation of axial ratio with Z,Horn H3,Fla. F2,Fre.8.2 GHz.
_____ 2β =60,------- 2β=45,....... 2β= 30.
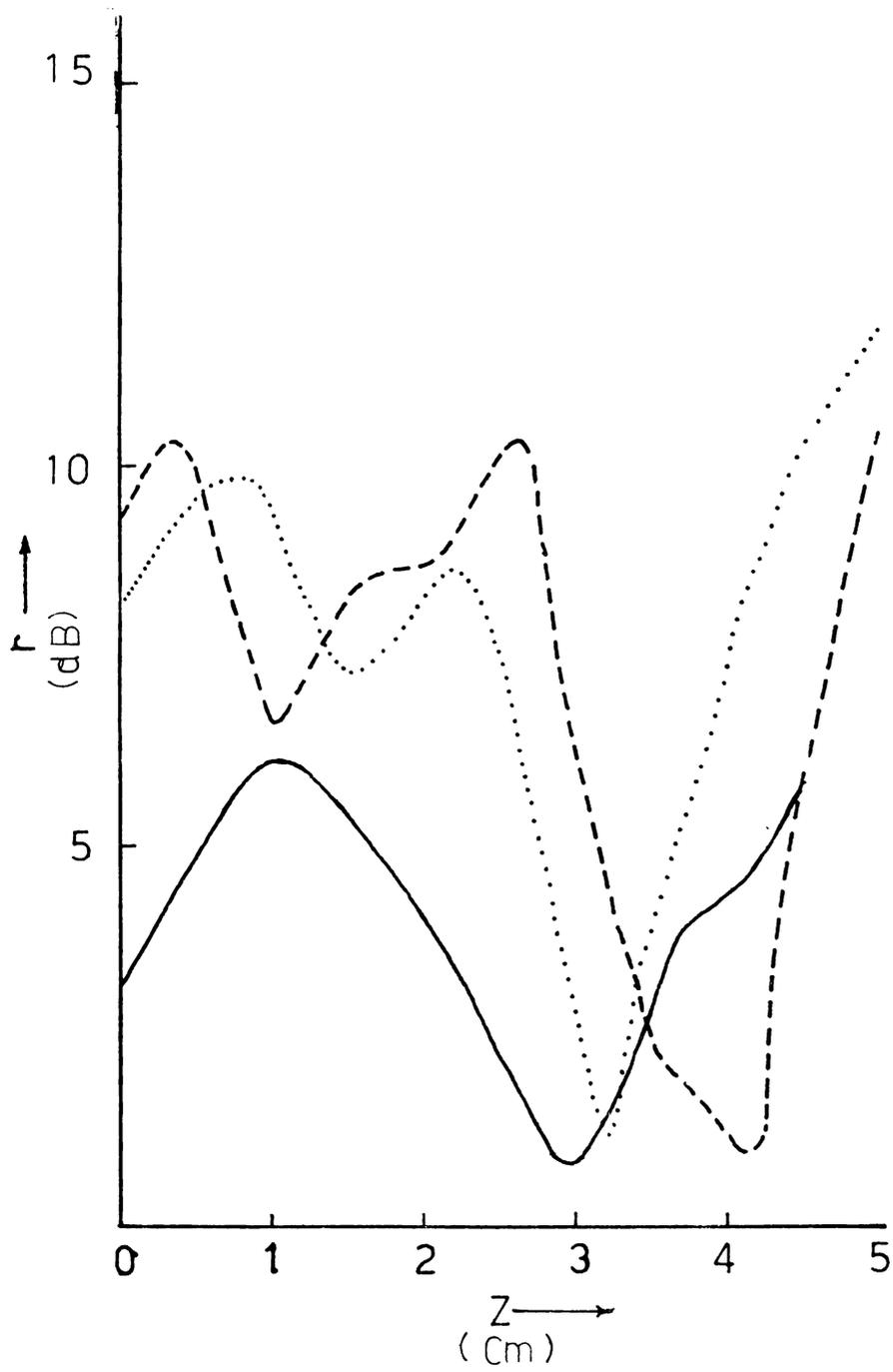
Fig.4.3(c): Variation of axial ratio with flange position (Z).

Horn H2, flange F7 and frequency 8.2 GHz.

_____ $2\beta = 10^{\circ}$, ----- $2\beta = 60^{\circ}$, ..... $2\beta = 30^{\circ}$
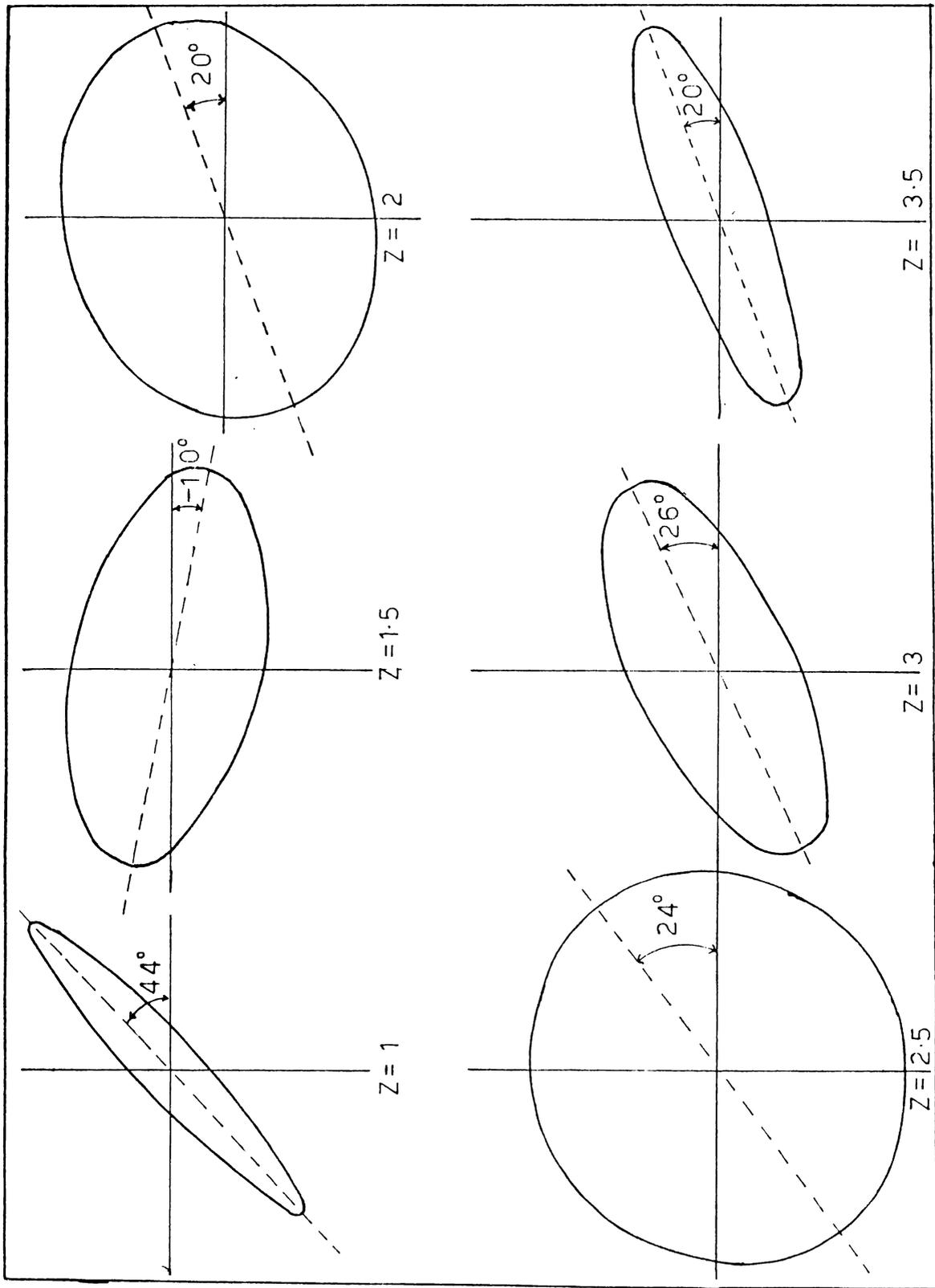
Fig.4.4: Typical variation of polarization ellipse with z.Horn h2. flange F1. 2β = 45 and frequency 9.375 GHz.

particular position. For convenience, let us call this position as "Circular polarization position" or 'C' position.

## 4.2(ii) Variation of axial ratio with tilt of corrugation ($\alpha$)

It is found that axial ratio, strongly depends upon the tilt of corrugations. When the tilt of corrugation is zero degree i.e., parallel to the magnetic field vector, a very high axial ratio is obtained. Similarly axial ratio is found to be high when the corrugation tilt is 90°. But for a corrugation tilt of 45°, the axial ratio is found to be minimum at 'C' position. Typical variation of axial ratio with tilt of corrugations are presented in fig.4(5). As seen earlier, it is found that the optimum corrugation tilt-angle is 45°.

## 4.2(iii) Variation of axial ratio with flange angle ($2\beta$)

As far as flanged horns are considered flange angle is an important parameter. Again, axial ratio of radiation from a flanged horn varies from a maximum to minimum when the flange angle is varied. Thus we can see that flange-angle is also an effective parameter to trim the antenna-characteristics. Variation of axial ratio with
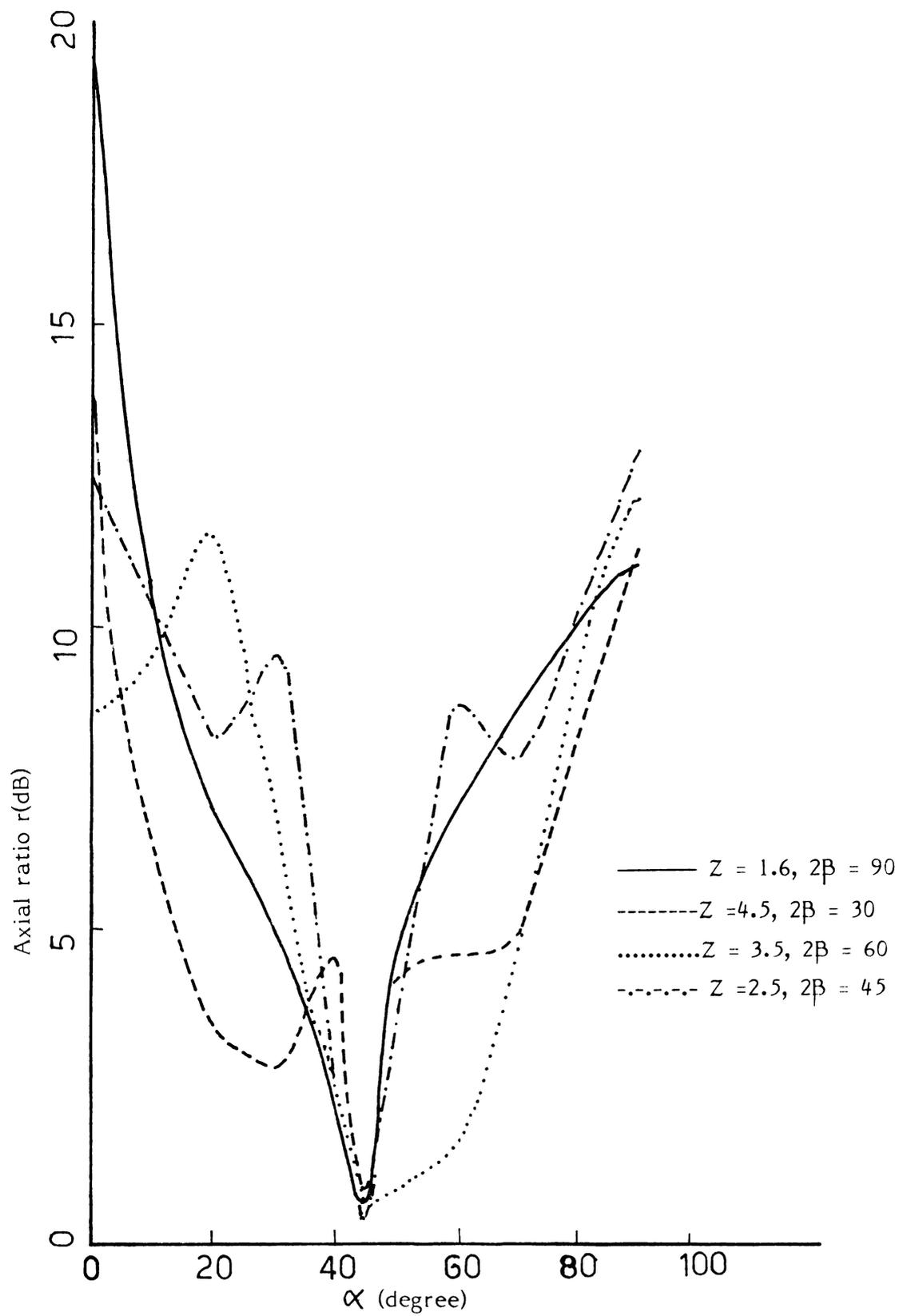
Fig.4.5: Variation of axial ratio with corrugation tilt
Horn H2, flange F1, frequency 9.375 GHz.

flange angle (2$\beta$) is shown in fig.4(6). It is obvious from
the figure that for a particular flange, there is an optimum
flange angle for which the polarization is nearly circular.
The variations are more or less in the same manner for all
flanges fitted on various horns. However the positions
of maxima and minima are varied.

4.2(iv) Variation of axial ratio with frequency (f)

The effect of frequency of operation on axial
ratio is also examined in detail. It is found that circular
polarization is obtained only for a small frequency band.
For all other frequencies the polarization is elliptical
in shape. Circular polarization can also be produced at
other frequencies by simply trimming other flange parameters
like position; angle etc. Since the frequency of operation
is critical, the band-width of the present system is low.
Variation of axial ratio with frequency for the flange
$F_1$ and horn $H_1$ is shown in fig.4(7). These results are valid
for all other flanges and horns. From the data presented, it
may be seen that the antenna systems designed are having a
band-width of 1 GHz, ie., from 9 to 10 GHz.

4.2(v) Variation of axial ratio with azimuth ($\theta$)

Axial ratio is measured on other points of the
radiation pattern along the H-plane. Even though, the
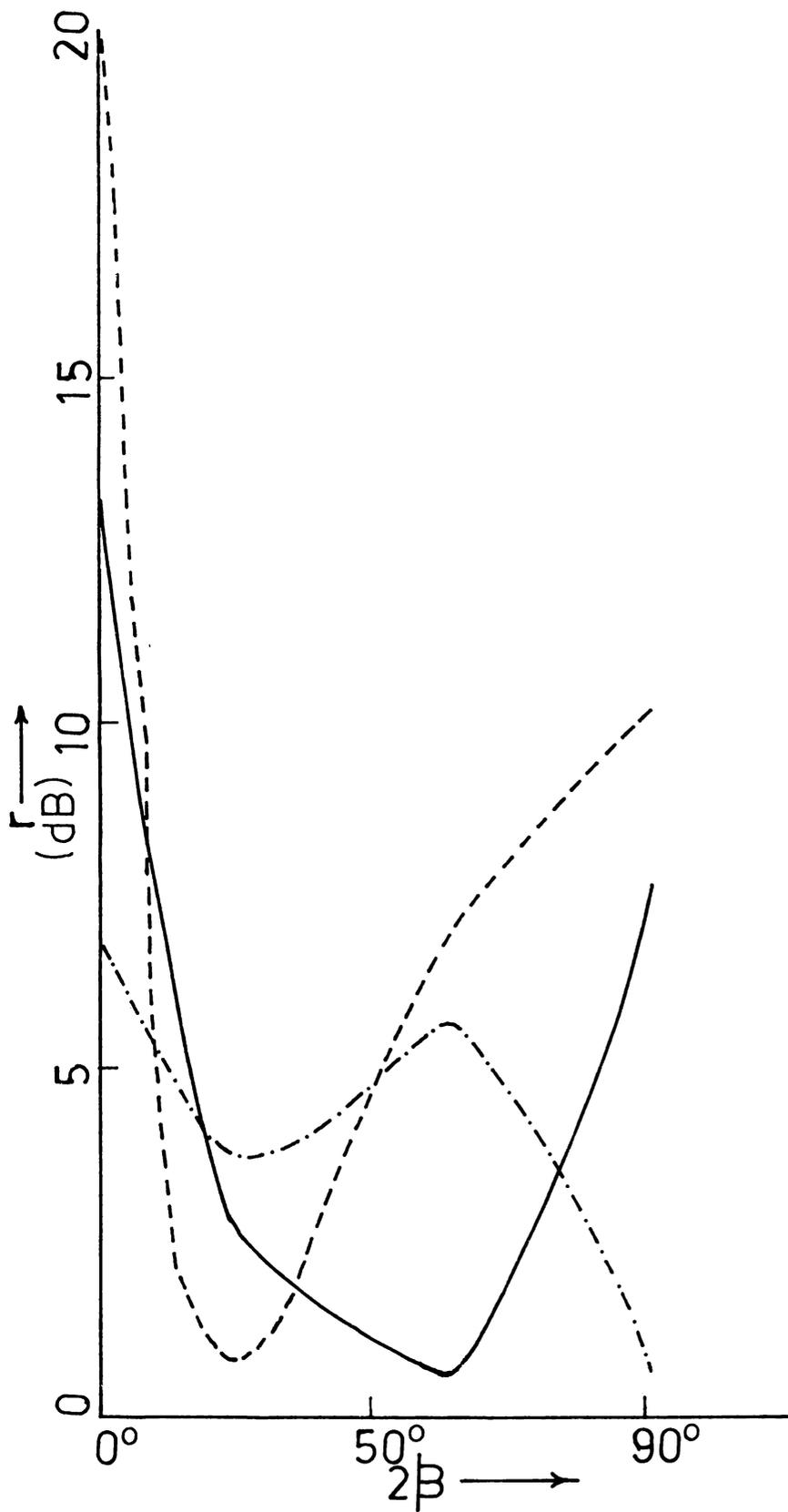
Fig.4.6: Variation of axial ratio with flange angle.

Horn H2,flange F1,frequency 9.375 GHz

——— Z=3.5  ----- Z = 4  -.-.-. Z=1.6
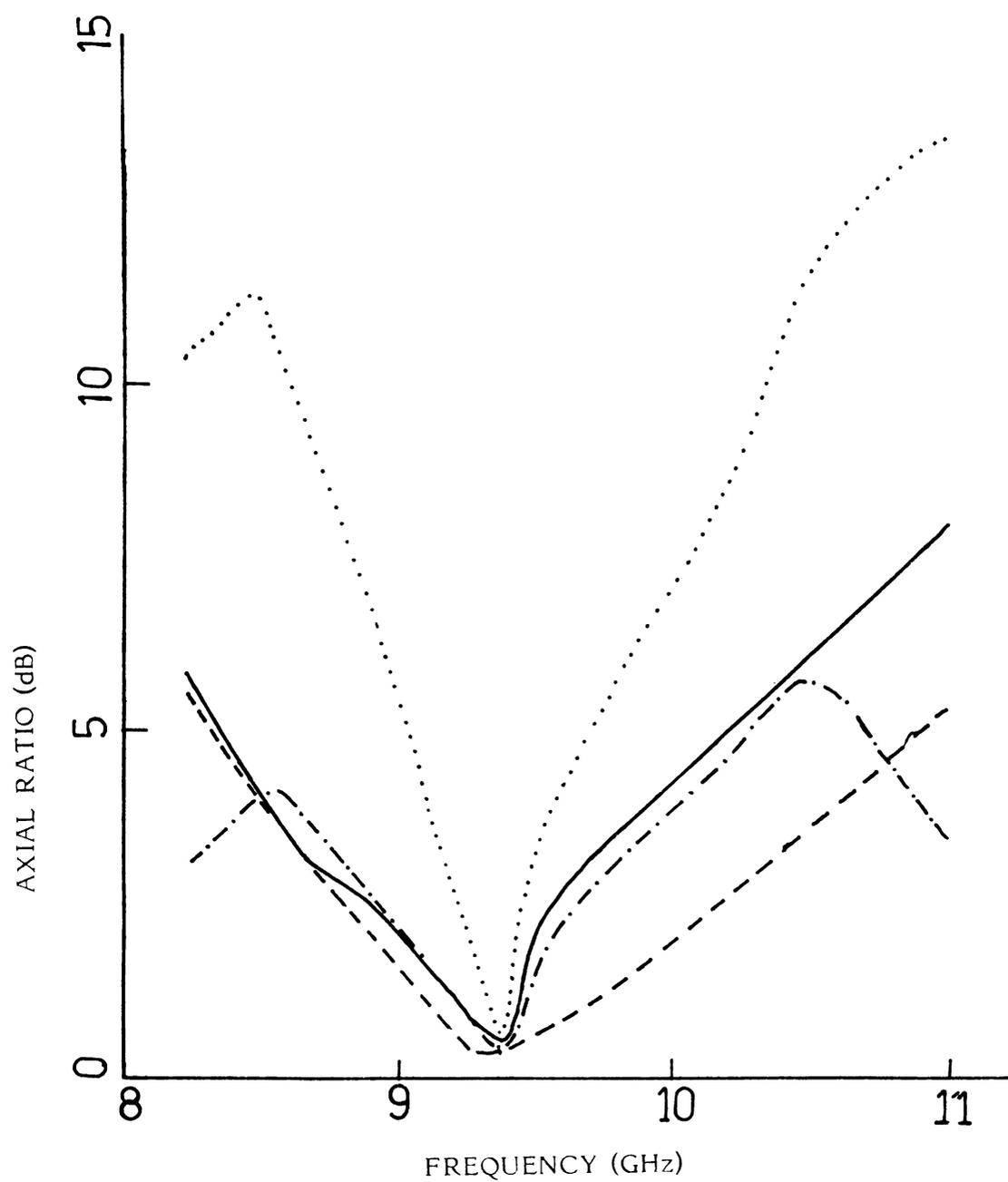
Fig.4.7: Variation of axial ratio with frequency. Horn H1,flange F1

——— 2β=60,Z=3.5 ----- 2β=45,Z=2.5 .....2β=90,Z=1.6 -.-.-.- 2β=30,Z=4.5

radiation from the flanged horn is circularly polarized along the axis, the polarization is elliptical in nature along the azimuth for most of the cases. In this case also, the axial ratio fluctuates from a maximum to minimum with azimuth angle. This variation of axial ratio is shown in fig.4(8) in the text.

4.2(vi)    Variation of axial ratio with width of
           corrugation (W/$\lambda$)

Axial ratio is measured along the axis of the flanged horn with the width of corrugations at the 'C' position of a particular flange. To study this effect corrugated flanges of different corrugation widths are used. Here the 'C' position for a particular flange is determined experimentally. Then the experiments are repeated with other flanges. Typical variation of axial ratio with W/$\lambda$ is shown in fig.4(9), where W is the width of corrugation and $\lambda$ is the operating wavelength. Again, axial ratio varies from a maximum to minimum with W/$\lambda$. But it may also be noted that by varying other flange parameters, circular polarization could be obtained. So, by proper trimming, the axial ratio can be adjusted to any desired value.
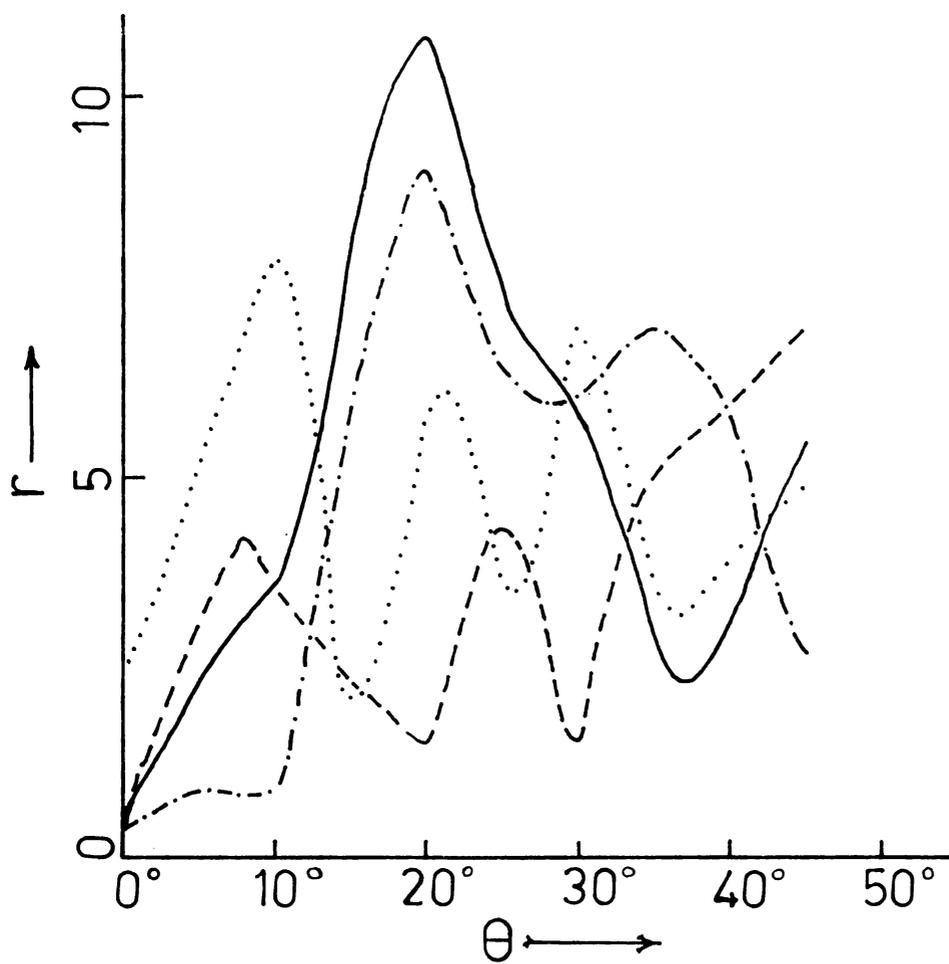
Fig.4.8: Variation of axial ratio with azimuth.

Horn H2,flange F1, frequency 9.375 GHz

——— 2β=60, Z=3.5 ------ 2β=45, Z=2.5

-.-.-.-2β=30, Z=4.5 ..... 2β=90, Z=1.6
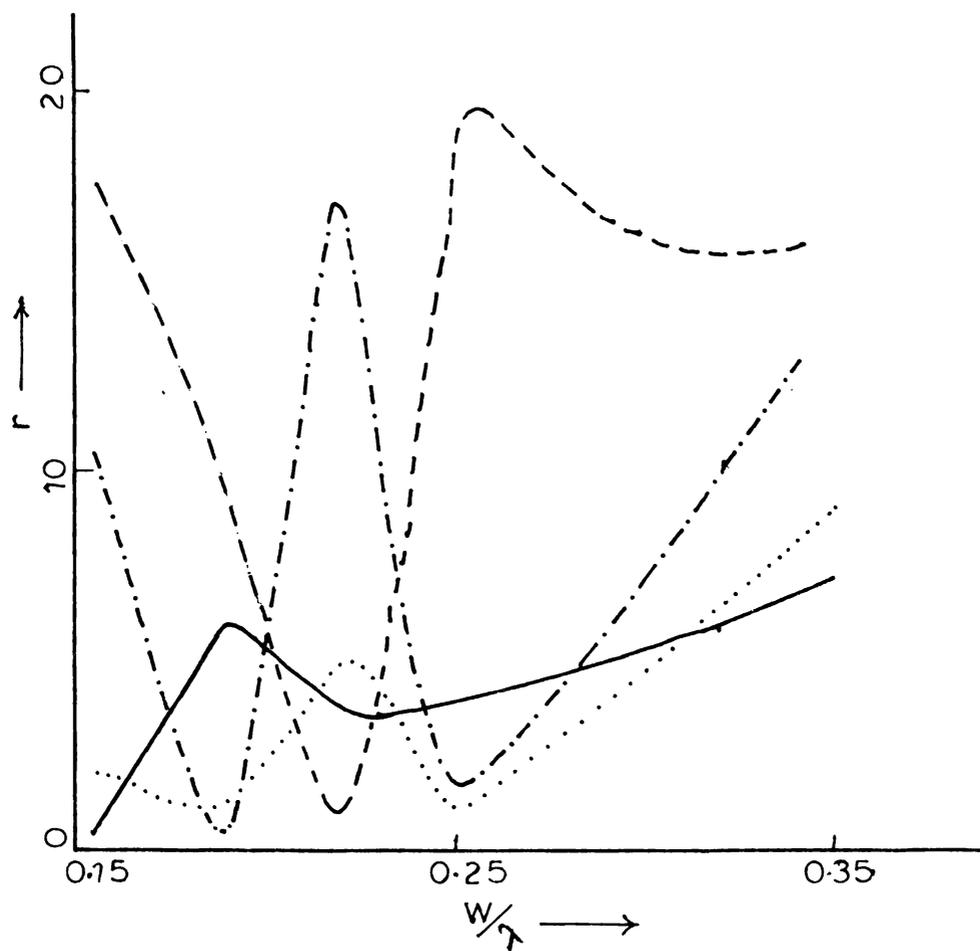
Fig.4.9: Variation of axial ratio with corrugation width.

Horn H2, frequency 9.375 GHz, $2\beta = 45$

———— Z=3.2 ---- Z=1.3 .... Z=9.4 -.-.-. Z=0.6

4.2(vii)  Variation of axial ratio with corrugation
          height (h/$\lambda$ )


Axial ratio is also measured for different
corrugation heights.  Variation of axial ratio with corru-
gation heights in wavelength (h/$\lambda$ ) is shown in fig.4(10).
Again, any desired axial ratio can be obtained for a
particular corrugated flange by simply adjusting the other
flange parameters.


4.3  Tilt angle of polarization ellipse


Another quantity which is of interest in ellipti-
cal polarization is the polarization orientation or tilt
angle.  The direction in which the major axis of the polari-
zation lies is called the tilt angle.  In this work, the tilt
angle is measured from the horizontal.


It is found that tilt angle is strongly dependent
on the position of the flange.  But at the circular polari-
zation position, the tilt angle is nearly zero, i.e., along
the co-polar direction (horizontal).  In general the
polarization ellipse is tilted through an angle with respect
to the horizontal.  Typical variation of polarization ellipse
with 'Z' is shown in fig.4(11).  It is also represented
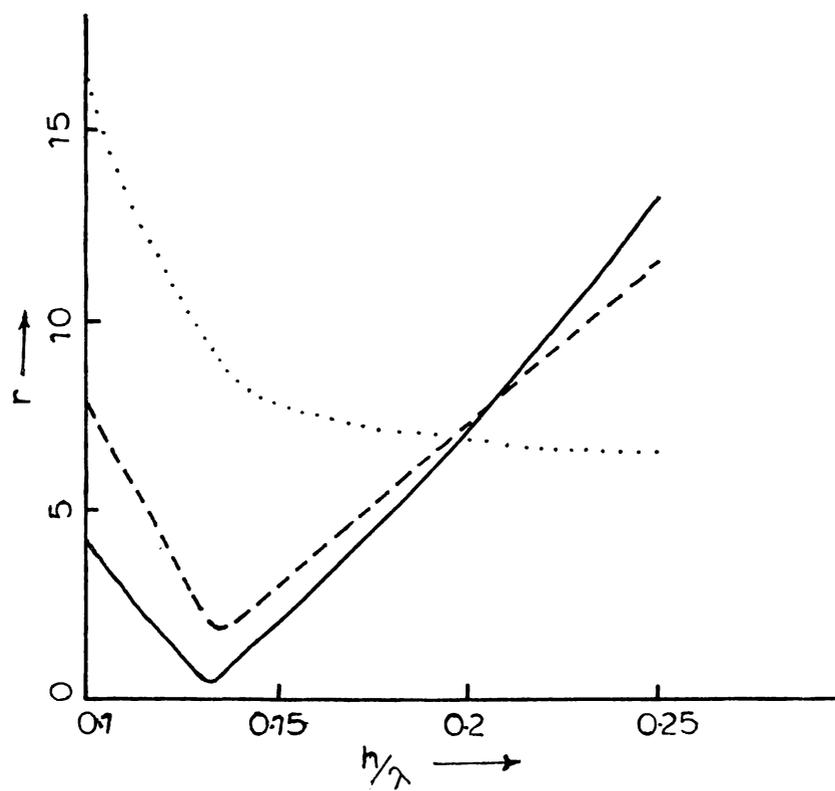
Fig.4.10: Variation of axial ratio with corrugation height.
HornH2, frequency 9.375 GHz, $2\beta = 45$
——— $Z = 2.5$ ---- $Z = 9.4$ .... $Z = 4.9$
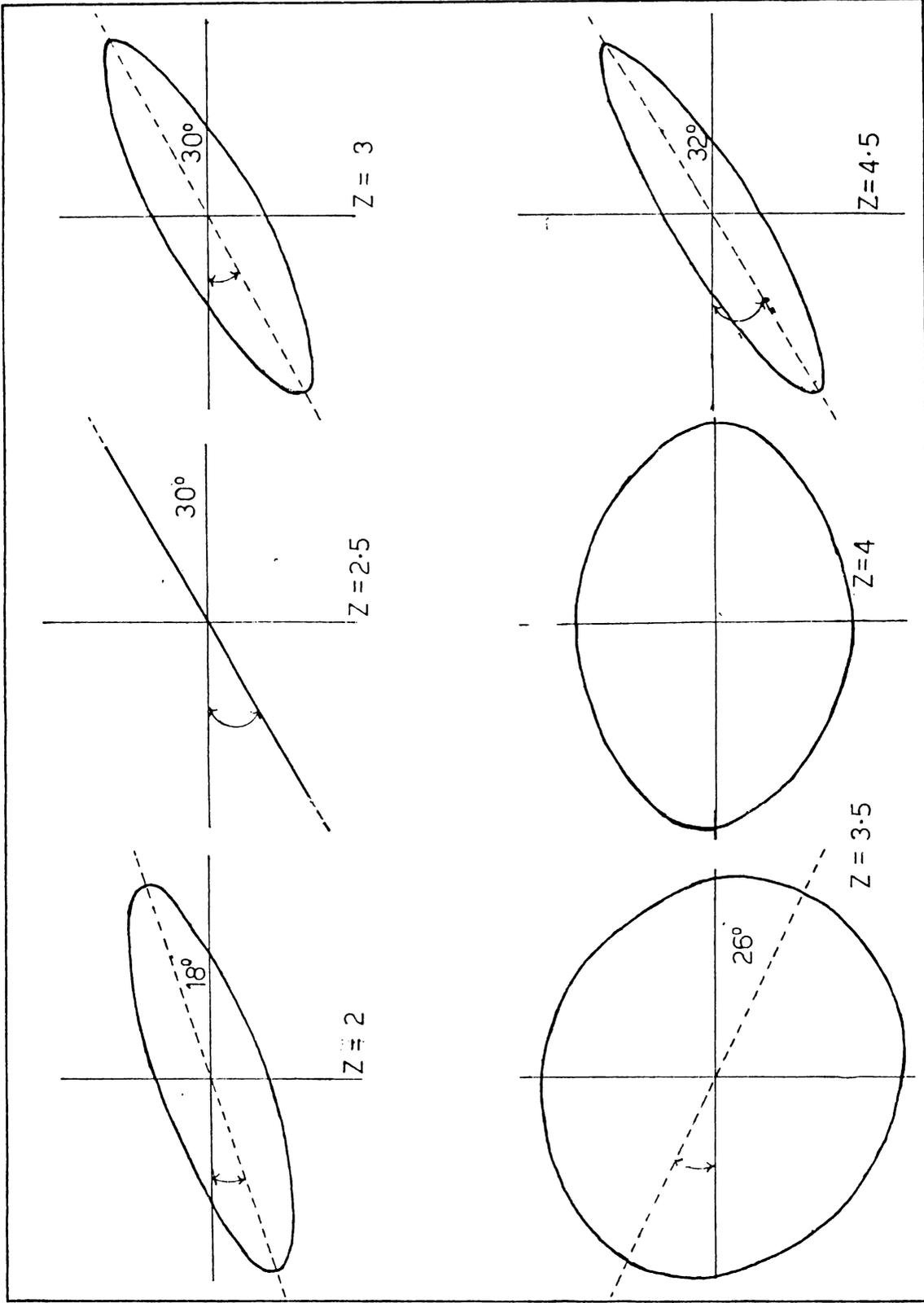
Fig.4.11: Variation of polarization ellipse with flange position. Horn H2, flange F1, frequency 9.375 GHz, $2\beta = 60$

graphically in fig.4.12(a&b). In azimuth the polarization ellipses are oriented in different direction. This variation is shown in fig.4(13) and 4(14). Again it is found that the tilt angle is varied with the tilt of corrugation. From the observations it is found that when the tips of the corrugations are oriented 45° with respect to the H-vector, the tilt angle is small. Variation of polarization ellipse with corrugation tilts are shown in fig.4(15) and 4(16). Dependence of polarization ellipse with frequency is shown for flange $F_1$ in fig.4(17 and 18). Again at certain frequency nearly circular polarization with zero tilt angle is obtained. From these observations it is clear that any desired polarization can be obtained by this simple flange technique.

## 4.4   Direction of polarization

One important parameter to be investigated for elliptical polarization is the sense of rotation of the polarized wave. The sense of rotation of the elliptically polarized wave is experimentally determined by the use of two identical helical antennas of opposite sense as described in the previous chapter.

## 4.4(1)   Variation with the position (Z) of the flange

The variations of on-axis power received by left handed circularly polarized and right handed circularly
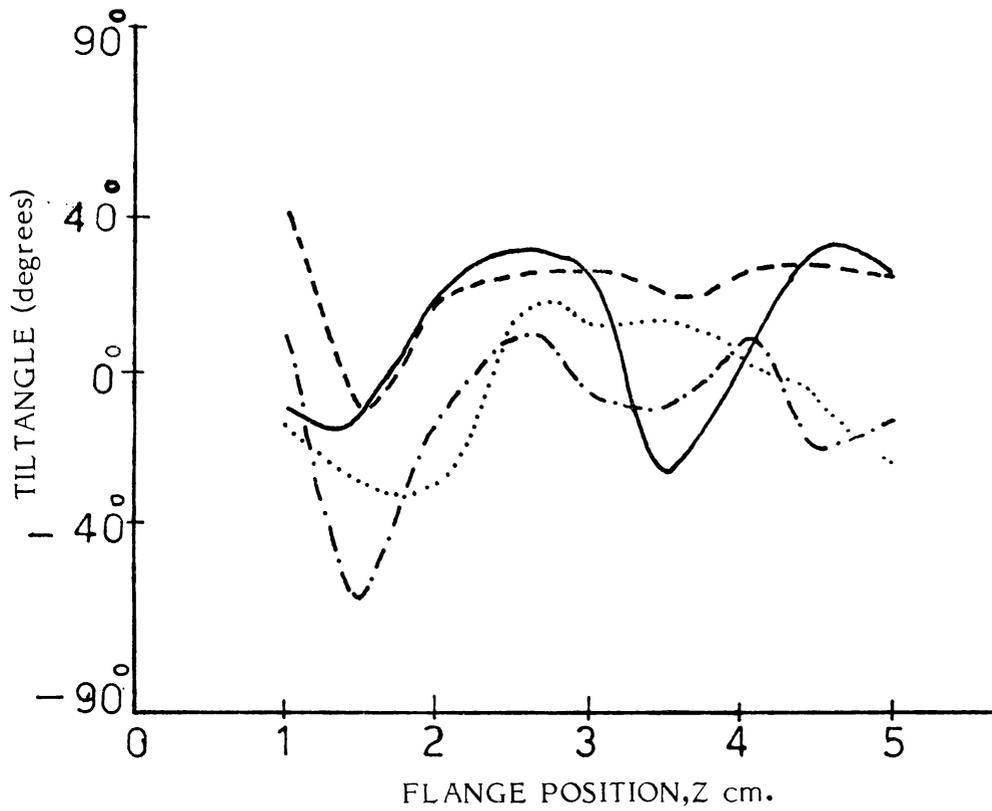
Fig. 4.12(a): Variation of tilt angle with Z.Horn H2,flange F2,frequency 9.375 GHz

———— $2\beta = 60$, ------ $2\beta = 45$, -.-.-.-.$2\beta = 90$,......$2\beta = 30$
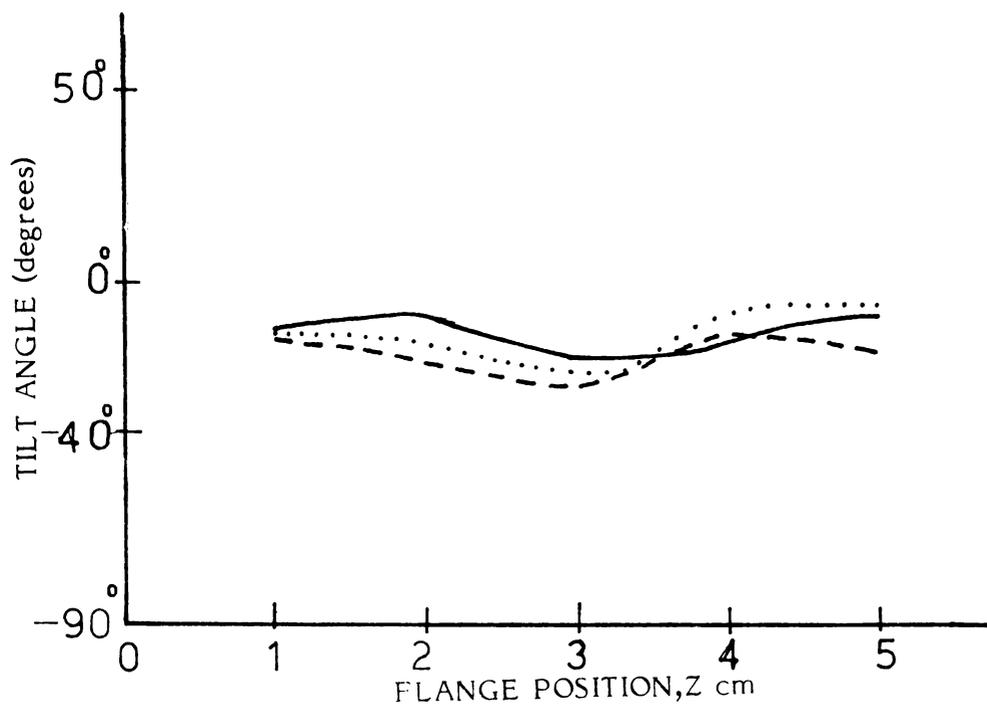


Fig.4.12(b): Variation of tilt angle with Z.Horn H1,flange F1,frequency 9.3 GHz

———— $2\beta = 60$, ------ $2\beta = 30$, ...... $2\beta = 45$
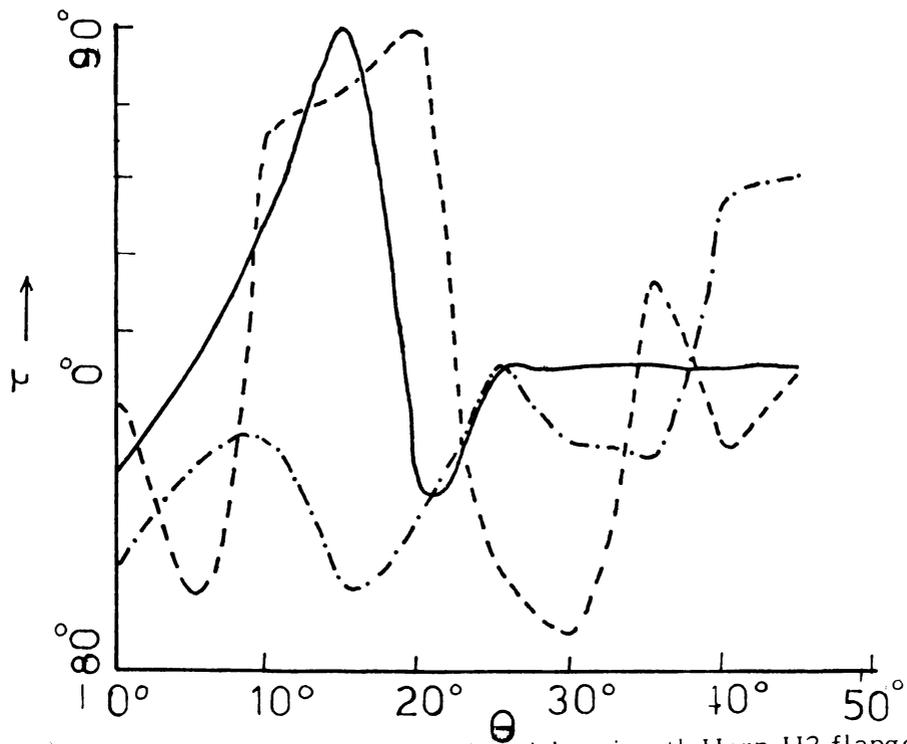
Fig.4.13 :Variation of tilt angle with azimuth.Horn H2,flange F1

——— $2\beta=60,Z=3.5$ ------ $2\beta=30,Z=4.5$ ......$2\beta=90,Z=1.6$
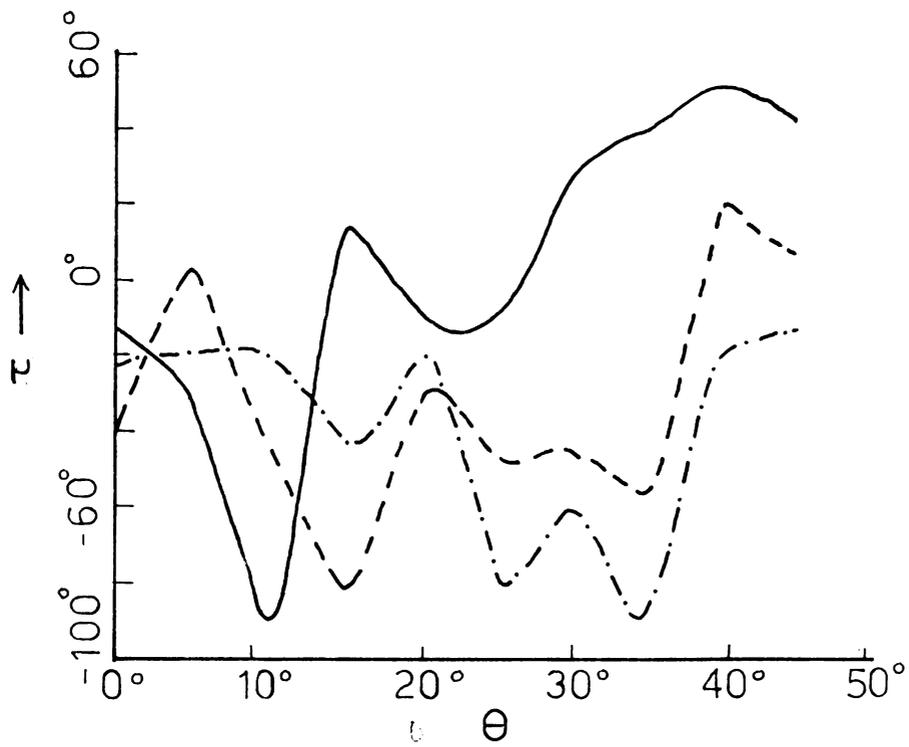


Fig.4.14. Variation of tilt angle with azimuth.Horn H4,flange F1

Frequency 9.165 GHz. ——$2\beta=90,Z=1.5$ ----$2\beta=30,Z=2$ -.-.-.$2\beta=60,Z=3$

93
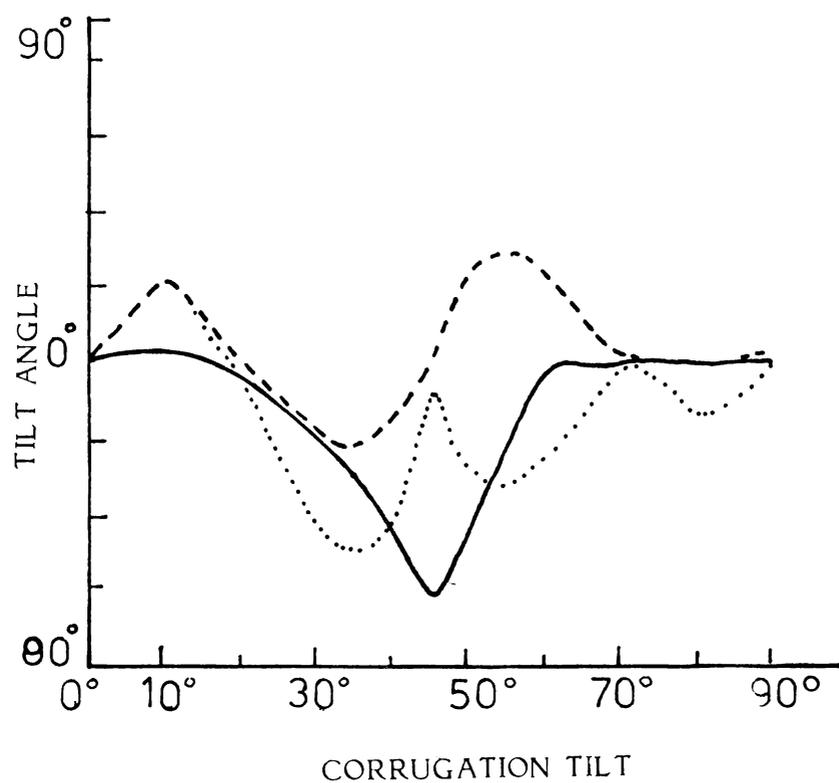
Fig.4.15:Variation of tilt angle with corrugation tilt.Horn H2,flange F1,frequency 9.375 GHz
——— Z=1.6,2β=90 ------ Z=3.5,2β=60 ...... Z=4.5 2β=30
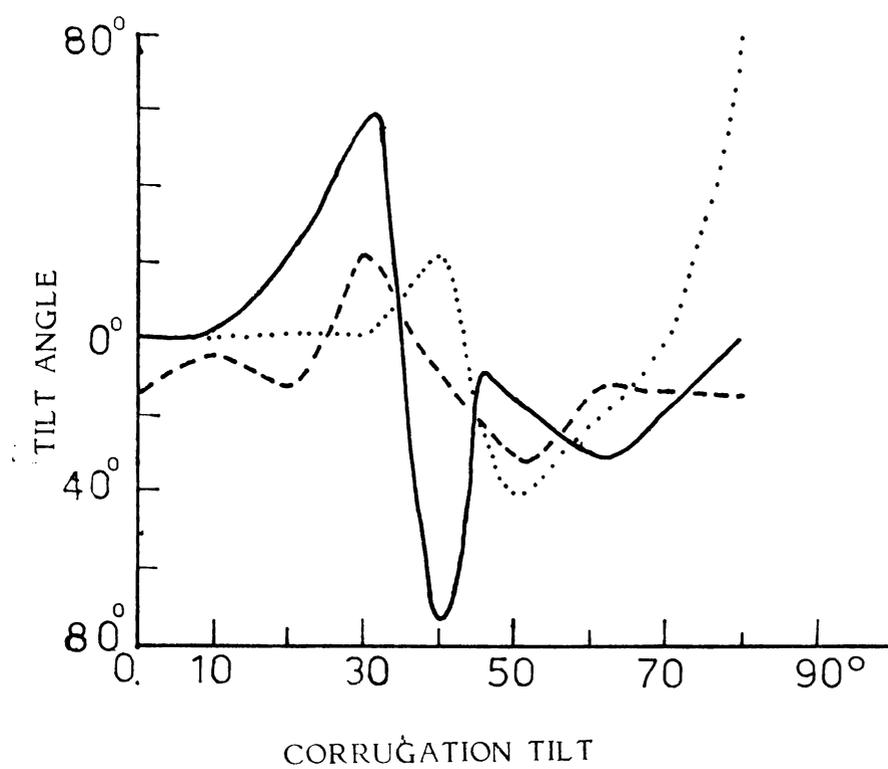


Fig.4.16: Variation of tilt angle with corrugation tilt.Horn H1,flange F1,frequency 11.67 GHz
——— Z=1.5,2β=90 ------ Z=7,2β=30 ...... Z=3.3,2β=60

Fig : 4.17: Variation of tilt angle with frequency.

———— Horn H2, Flange F1, 2β=60, Z=2.2

-·-·-··Horn H2,Flange F1, 2β= 90, Z= 1.6

--------Horn H2, Flange F1, 2β= 30, Z= 4
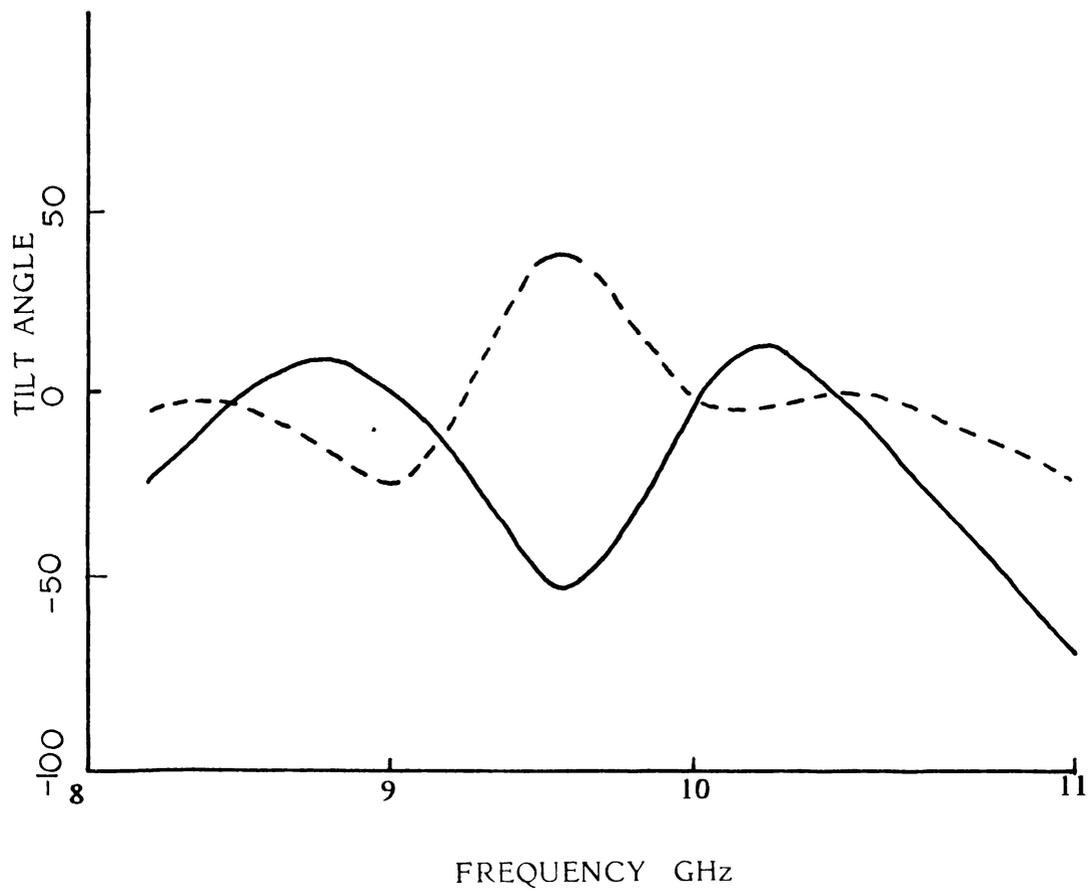
FREQUENCY  GHz

Fig.4.18: Variation of tilt angle with frequency.Horn H4,.

_____ Z =3.5, 2β = 30  ------------  Z = 1.4, 2β = 90

polarized helical antennas with the position of the flange

from the aperture of the horn are shown in fig.4.19(a,b and c).

In fig.4.19(a) the tilt of corrugation is 45° with the H-vector.

From the curve, it is obvious that the flanged horn acts as

an elliptically polarized radiator in the right handed sense.

But in 4.19(c) the tilt of corrugation is 135°. Here, the

wave is polarized in the opposite sense. Therefore, by simply

adjusting the corrugation tilt, the sense of polarization

can be altered.

4.4(2)  Variation with corrugation tilts ($\alpha$)

In this case the radiation pattern of the flanged

horn is plotted using helical antennas as a receiver for

different corrugation tilts. Typical variations of such

radiation pattern with tilt of corrugations are shown in

fig.4(20). The results again confirm that the beam is almost

circularly polarized when the tilt of corrugation is 45° or

135°. When the tilt of corrugation is 45°, it is polarized

in the right handed sense and it is polarized in the left

handed sense when the tilt of corrugation is 135°.

4.4(3)  Variation with frequency (f)

In fig.4(21), the variations of power received

by LHCP and RHCP helical antennas with Z for different
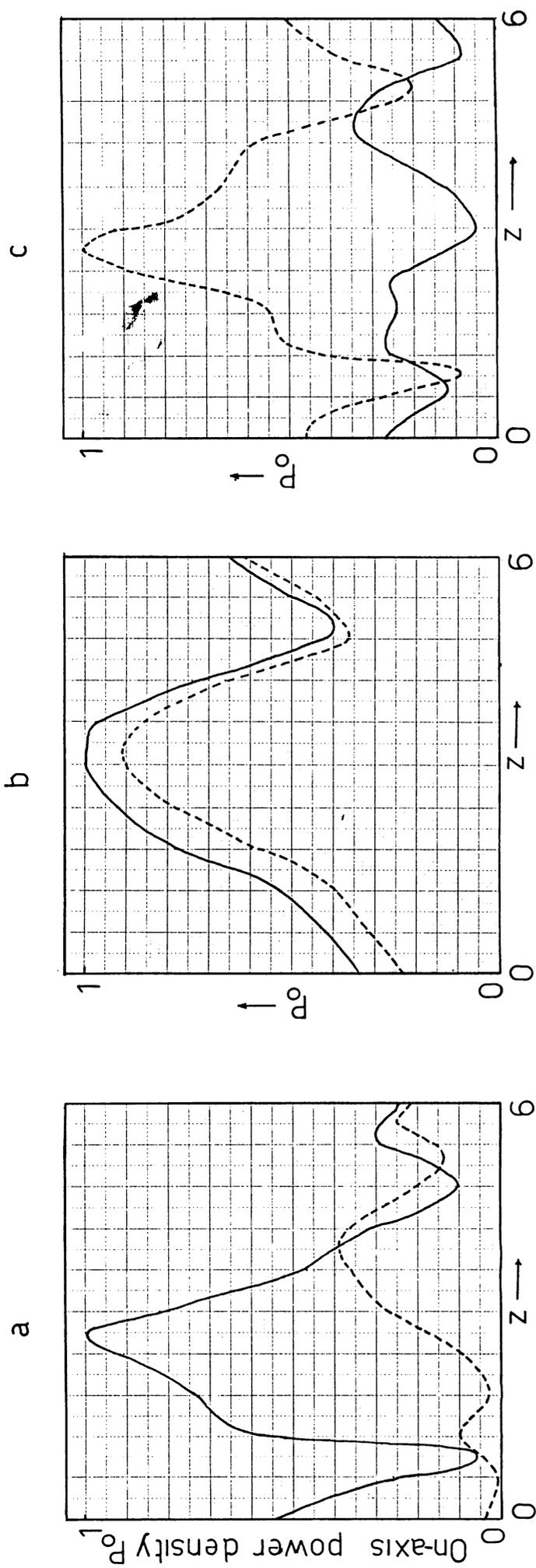
Fig. 4.19: Variation of on-axis power density received by LHCP & RHCP helical antennas with Z.
a. $\alpha=45°$, b. $\alpha=0°$, c. $\alpha=135°$, —— LHCP, —--— RHCP, Horn H2, Flange F1, Freq. 9·375 GHz, $2\beta=45°$.

98
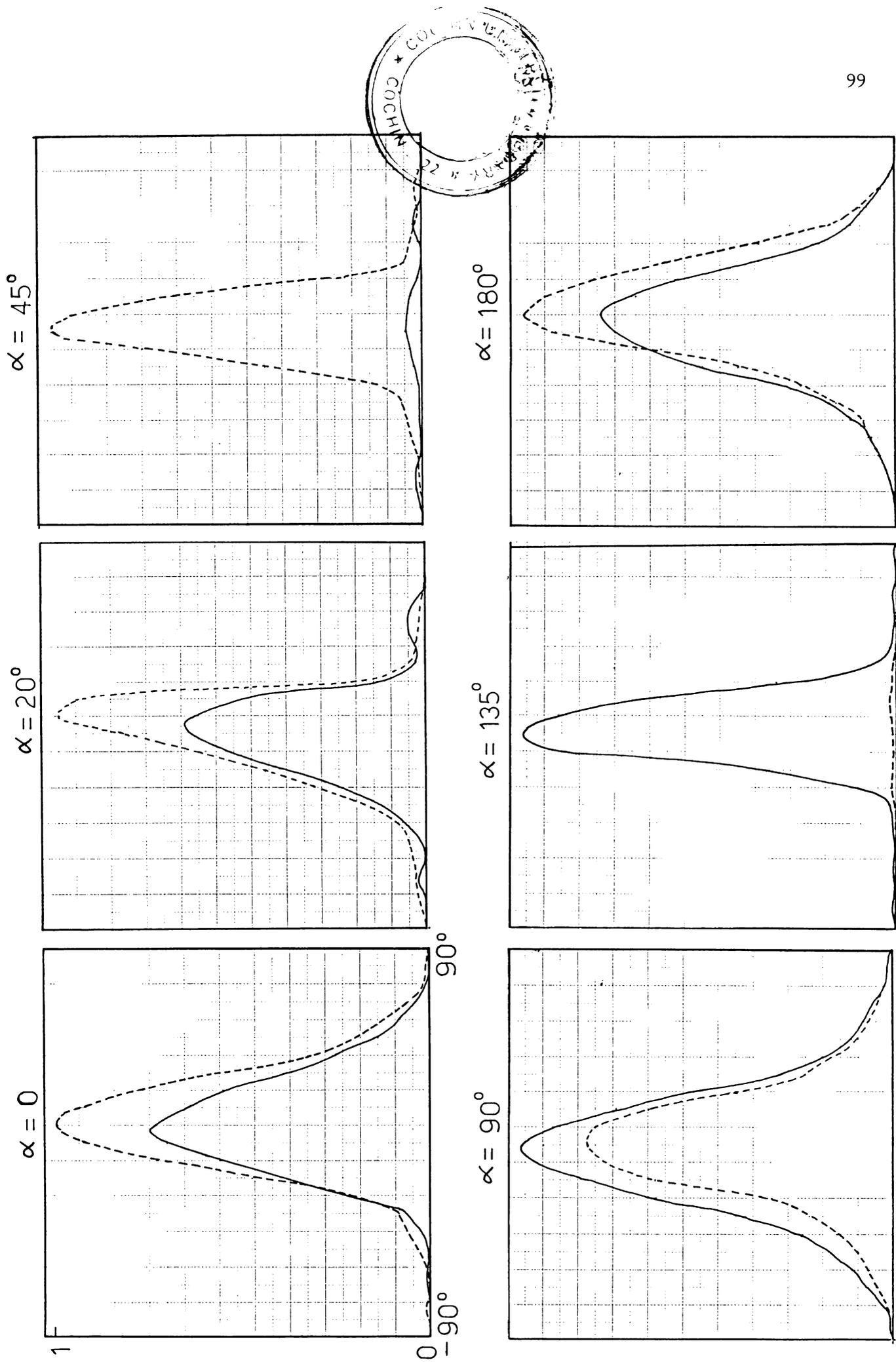
Fig. 4.20: Radiation patterns received by LHCP & RHCP helical antennas for different corrugation tilts.
Horn H2, Flange F1, Frequency. 9.375 GHz , 2B = 45°. – – – – LHCP ——— RHCP.
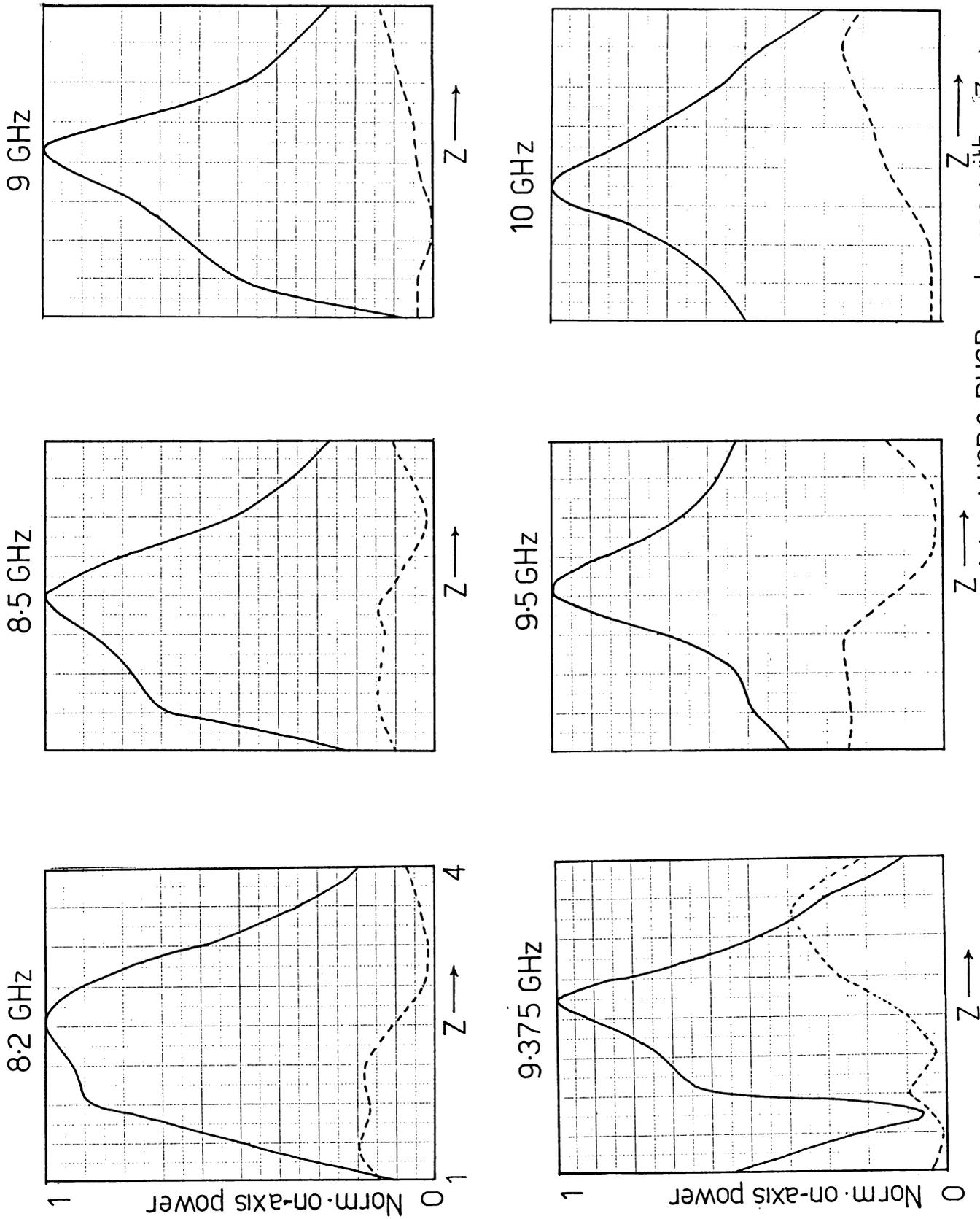
Fig. 4.21: Variaiation of on axis power received by LHCP & RHCP antennas with Z for different frequencies. Horn H2, Flange F1, 2β = 45°, ——— LHCP, − − −RHCP.

frequencies for a corrugation tilt of 45°, are shown. From the observations it is found that there is no change in the sense of rotation when the frequency is varied i.e., the antenna is always polarized in the right handed sense when the corrugation tilt is 45°.

4.5   Representation of polarization by different ways

As far as elliptical polarizations are considered there are a number of problems of its representation. In an elliptically polarized wave we have to represent two orthogonal field components and their phase difference. Different methods are described in literature to represent elliptical polarizations. Some of the exper..nental results are represented by the methods described in chapter 2.

Typical variation of polarization with the position of the flange from the aperture of the horn is shown in fig.4(22) by Ramsays q-plane representation. Typical p-plane representation of polarization of the flanged horn for different frequencies are shown in fig.4(23). Similarly the polarization of the wave from the above antenna with frequency is represented in Carter chart in fig.4(24).

Fig.4.23: Variation of polarization state of the flangedhorn with freq.: Horn H2,Flange F1,2β= 45,Z = 2.5.
a) 8.2 GHz, b) 8.5 GHz, c) 9 GHz, d) 9.375 GHz, e) 9.5 GHz, f) 10 GHz.
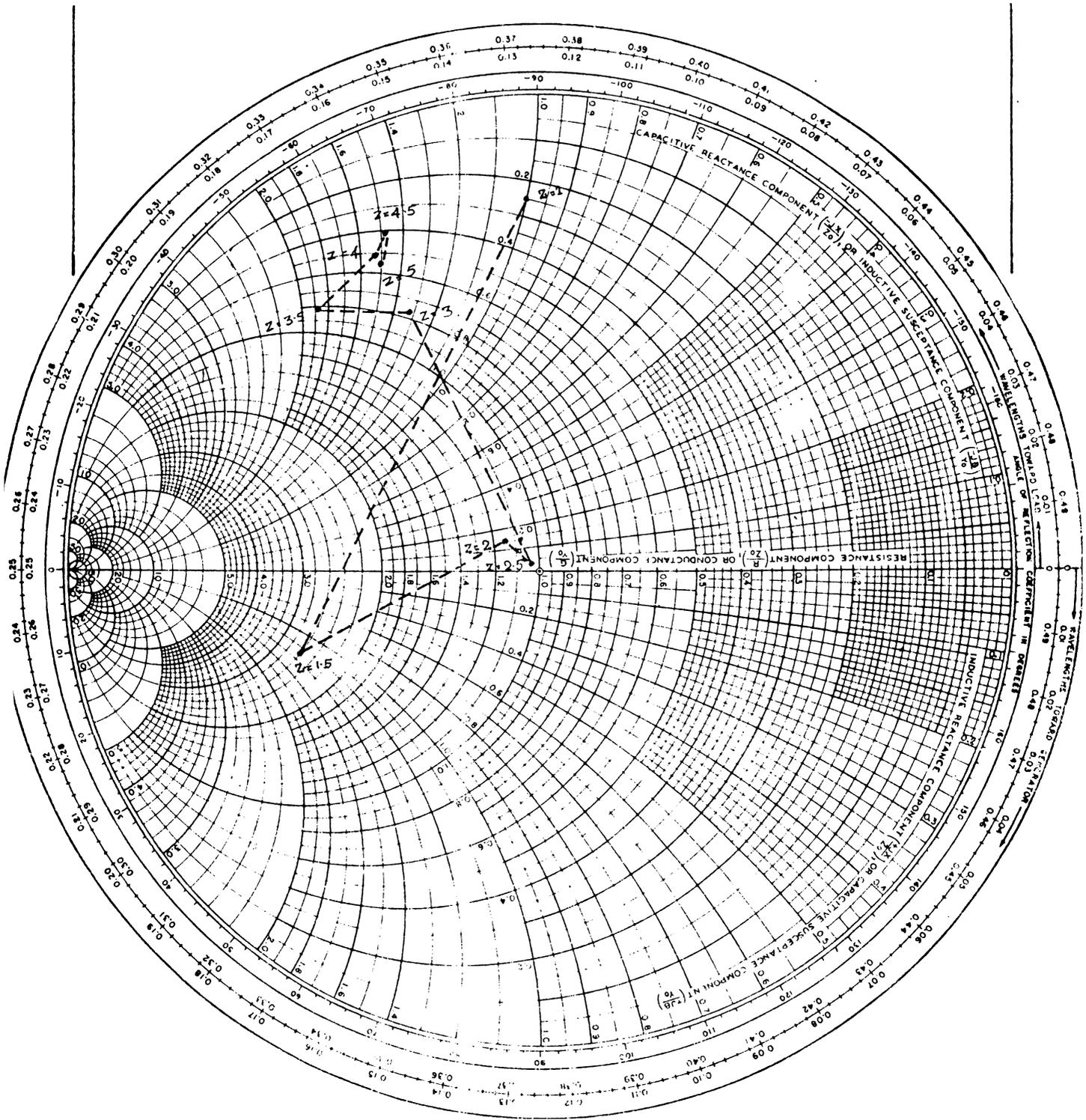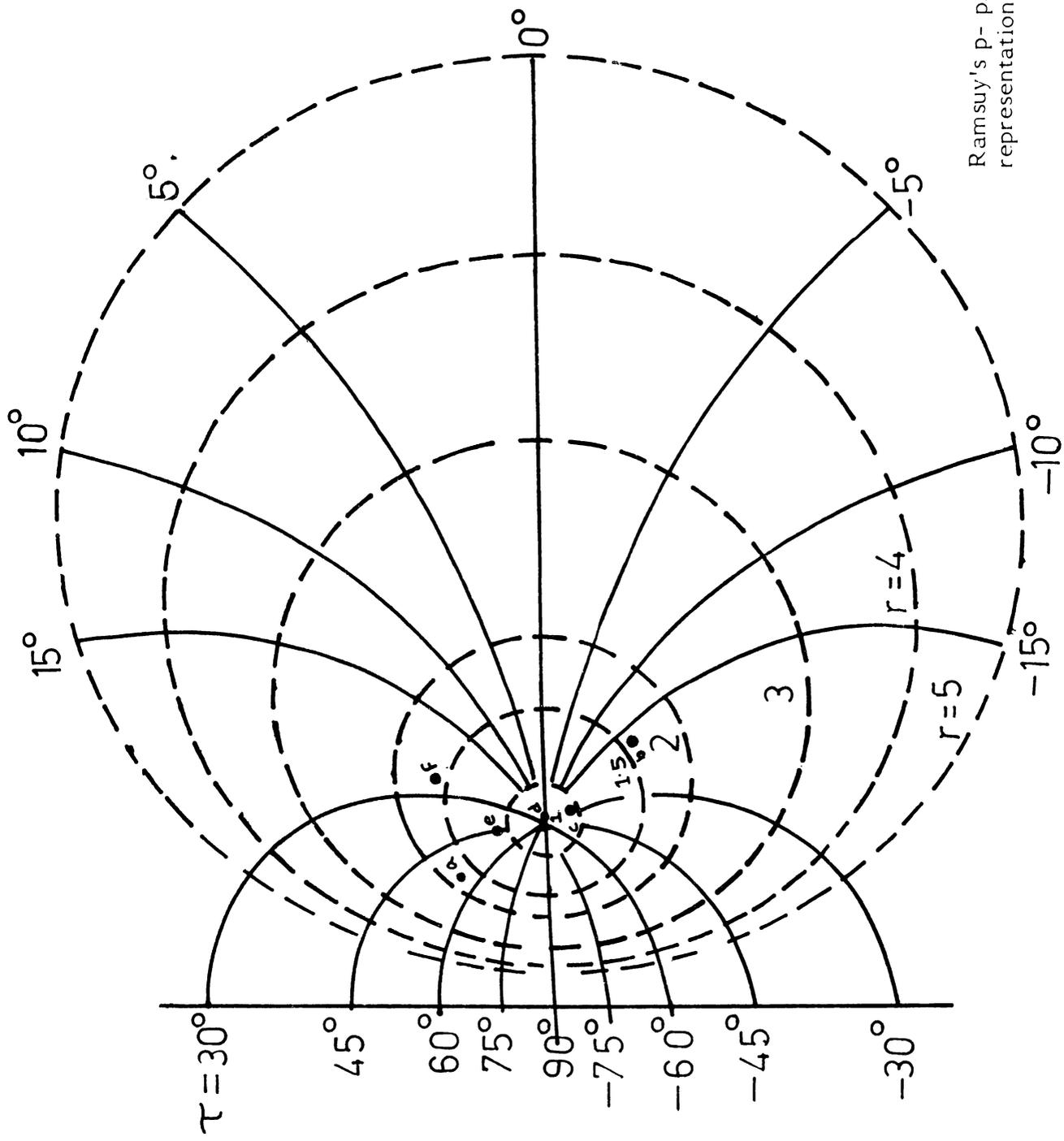
Ramsuy's p- plane
representation
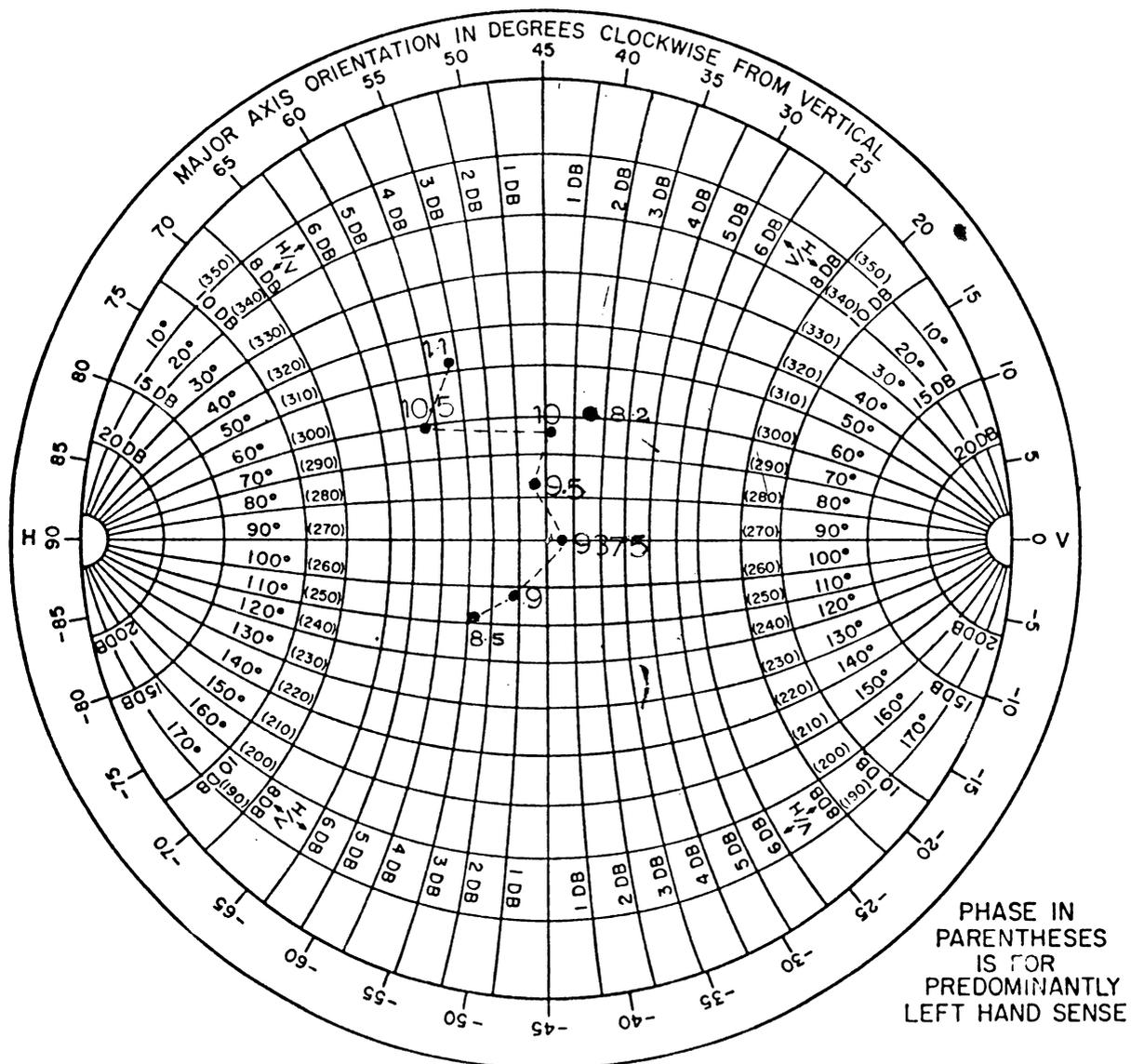
Polarization chart.

Fig.4.24: Variation of polarization with frequency. Carter chart representation.Horn H2, Flange F1, $2\beta=45$, $Z=45$, $\alpha=45$.

## 4.6  Voltage standing wave ratio (VSWR)

Another important parameter taken for the present investigation is the voltage standing wave ratio. From the VSWR data, a fairly good knowledge of matching of the system can be obtained. Therefore, the dependence of VSWR on various flange parameters are studied in detail.

It is observed that VSWR of the system is strongly dependent on the position of the flange. Va iations of VSWR with Z for different corrugation tilts are shown in fig.4(25). Natural VSWR (i.e., VSWR of the horn without flanges) is also shown for comparison. From the curves it may be found that VSWR fluctuates with Z. At the aperture, the VSWR is found to be less than the natural one. Then it is increased to a high value and decreased. At the circular polarization position the VSWR is low. Therefore, we may conclude that at the circular polarization position, better matching is achieved. It is also found that at 'C' position the gain is found to be increased. This may be partly due to the low VSWR. It is again found that VSWR is a function of corrugation tilt. When the tilt of corrugation is 45° the VSWR is found to be minimum. Typical VSWR variation with corrugation tilt is shown in fig.4(26). The observation shows that flanged horns are suitable to produce circular polarization with good matching.
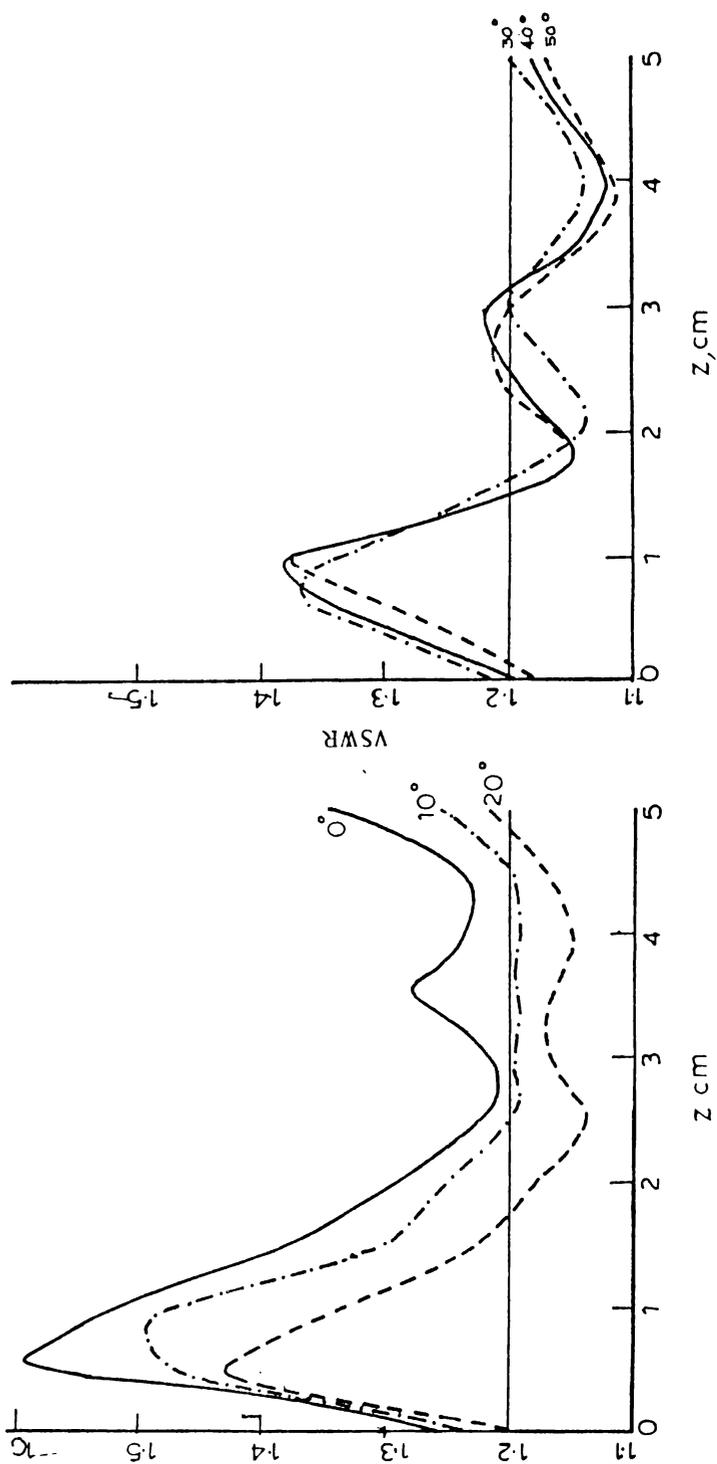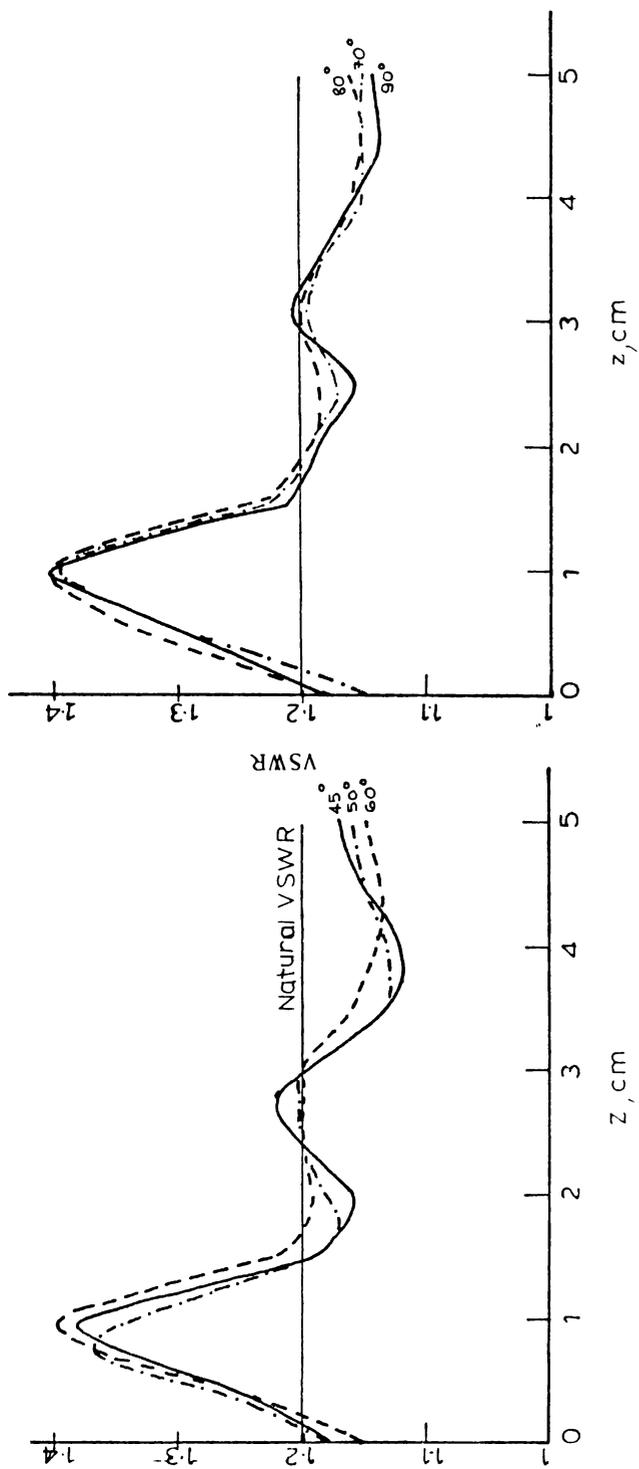
Fig. 4.25: Variation of VSWR with flange positions for different corrugation tilts.i
Horn H2, Flange F1, 9·375 GHz, 2β=45°.
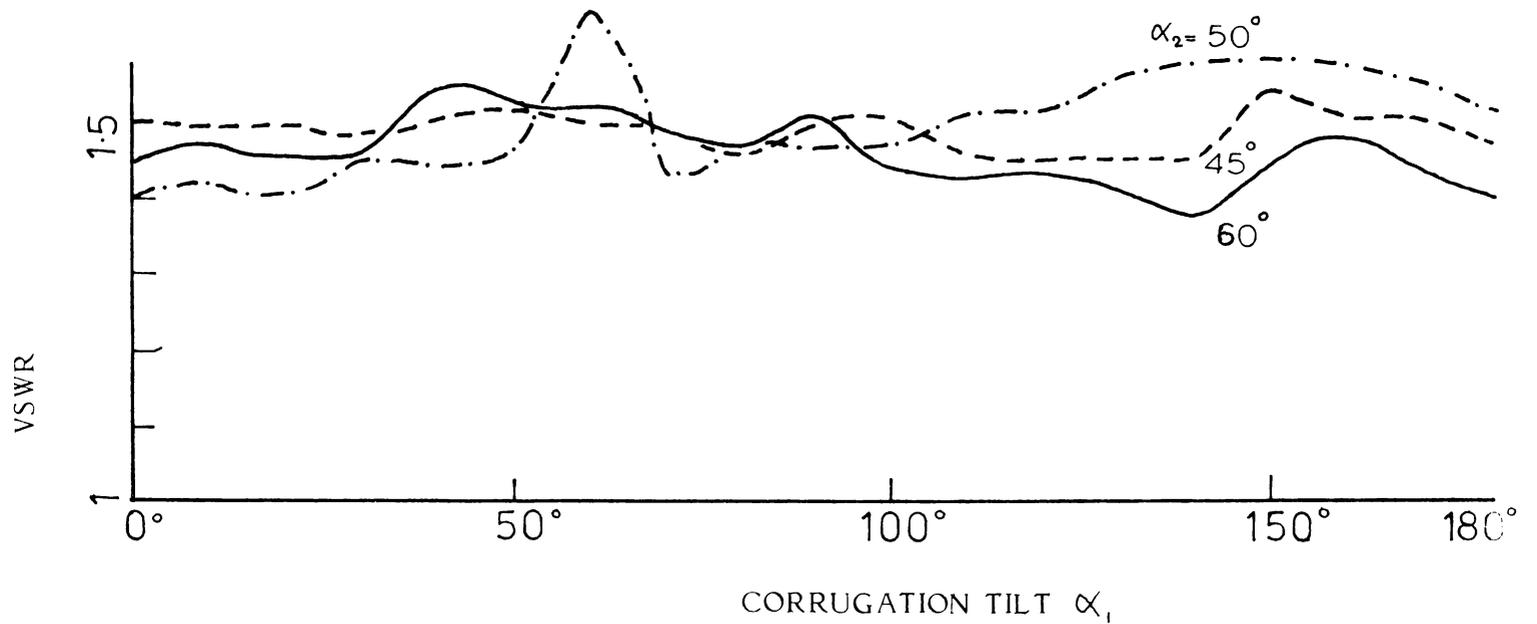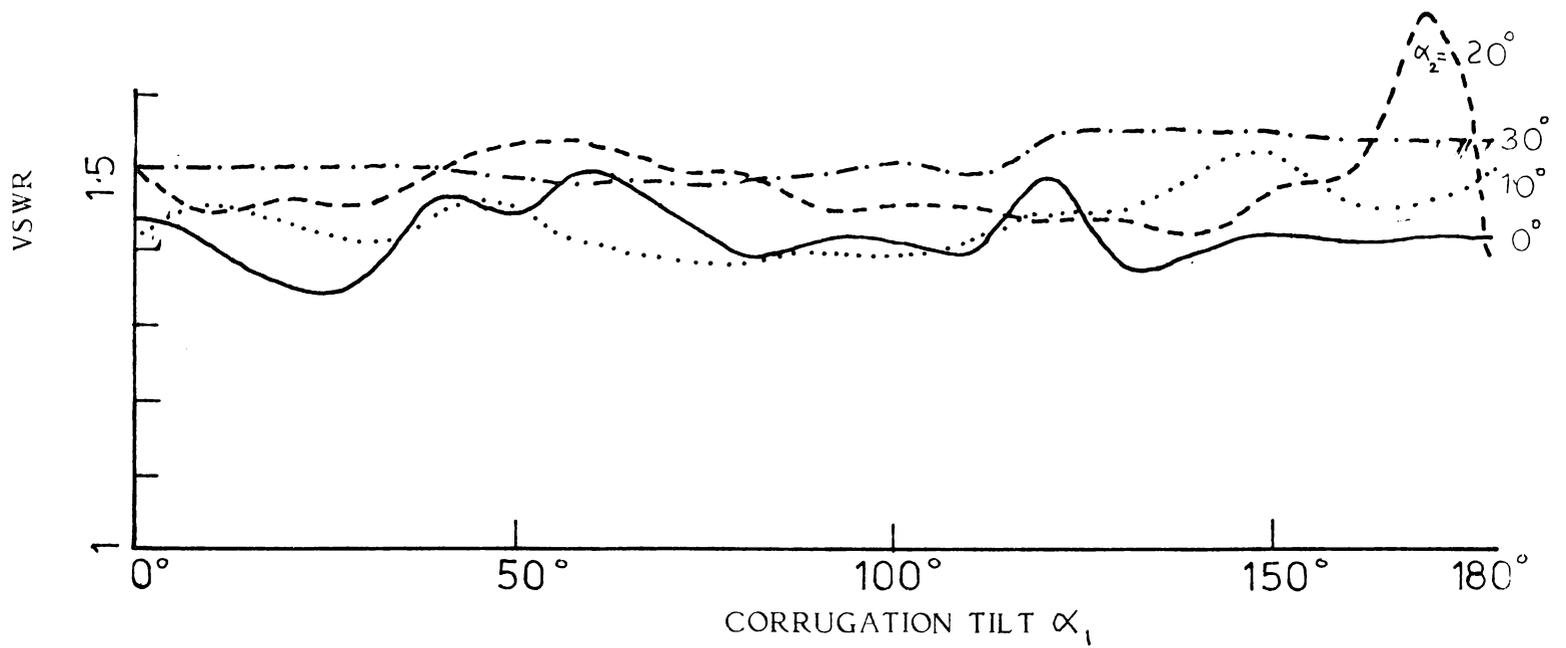
Fig.4.26: Variation of VSWR with corrugation tilt.Horn H1,flange F1,frequency 9.375 GHz,Z=2.5

4.7  Radiation patterns

Most interesting effect of the corrugated flanges
lies in their ability to control the polarization of a
linearly polarized horn radiator.  Depending upon the flange
parameters any desired polarization can be produced.  A
qualitative idea of this variation is also obtained from the
radiation patterns.


4.7(i)  Effect of position on radiation pattern

Drastic changes occur to the polarization of the
radiated energy when the position of the flange relative to
the aperture of the horn is varied.  It is found from the
preliminary observations that at certain position of the flange
the co-polar and cross-polar powers are equal.  Depending upon
the position of the flange a cross-polar component is obtained.
Hence radiation patterns are also affected by the position of
the flange.  Radiation patterns are taken in four different
planes namely, co-polar, cross-polar, 45° plane and 135° plane.

Typical variations of radiation patterns, with the
position of the flange are shown in fig.4(27).  At certain
position of the flange (Z = 6 cms) the cross-polar component
is very small.  At this position it is linearly polarized along
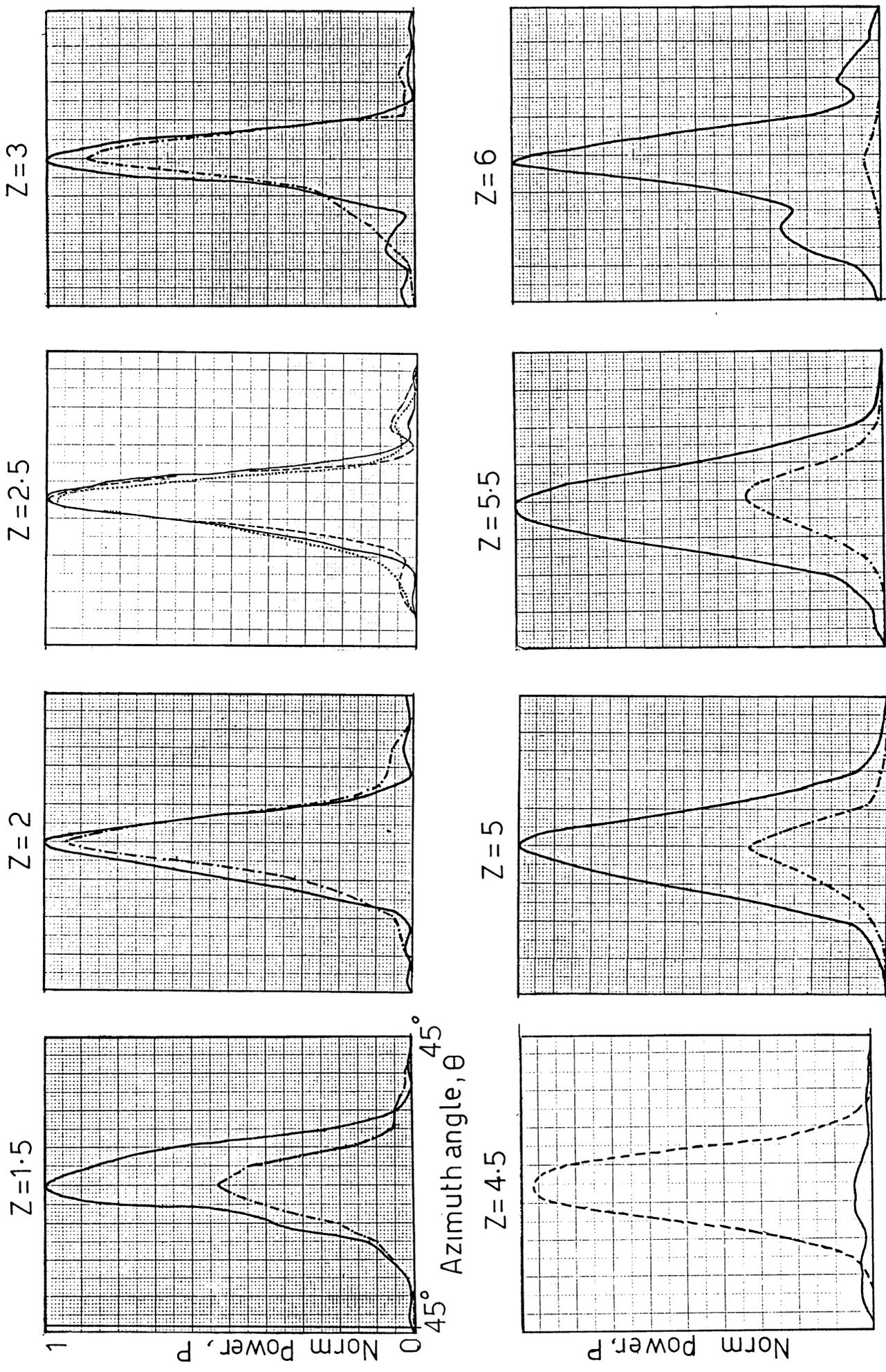
Fig. 4.27: Typical variation of radiation patterns with Z. Horn H2, Flange F1, Freq. 9.375 GHz, 2β=45°.
—— Co polar, – – – –Cross polar, ·········· 45°Polar.

the co-polar plane with low cross-polar component. But when the position of the flange is changed to 4.5 cms from the aperture of the horn the co-polar component is very small. At this position it is polarized in the orthogonal plane. At Z = 2.5 cm from the aperture, all the three patterns are nearly equal. At this position the axial ratio is found to be 0.5 dB. It is found from the experiments, for a particular corrugation period there is an optimum position for circular polarization position. E-plane radiation pattern of the flanged horn at 'C' position along with its natural pattern is also shown in the same figure. It is found that E-plane radiation pattern is also modified by this technique. Typical variation of E-plane radiation pattern with the position of the flange when the corrugation tilt is 0° (i.e., orthogonal to E-vector) is shown in fig.4(28). At certain positions, the beam is narrowed down. The on-axis power density is increased. This position of the flange is called 'O' position. But when the flange is moved to the minimum on-axis power position the beam broadens or splits into major lobes.

The variation of radiation pattern with the position can be qualitatively explained as follows. Since the tips of the corrugations are inclined, the incident electric field is split into two components, one parallel to the corrugation

111
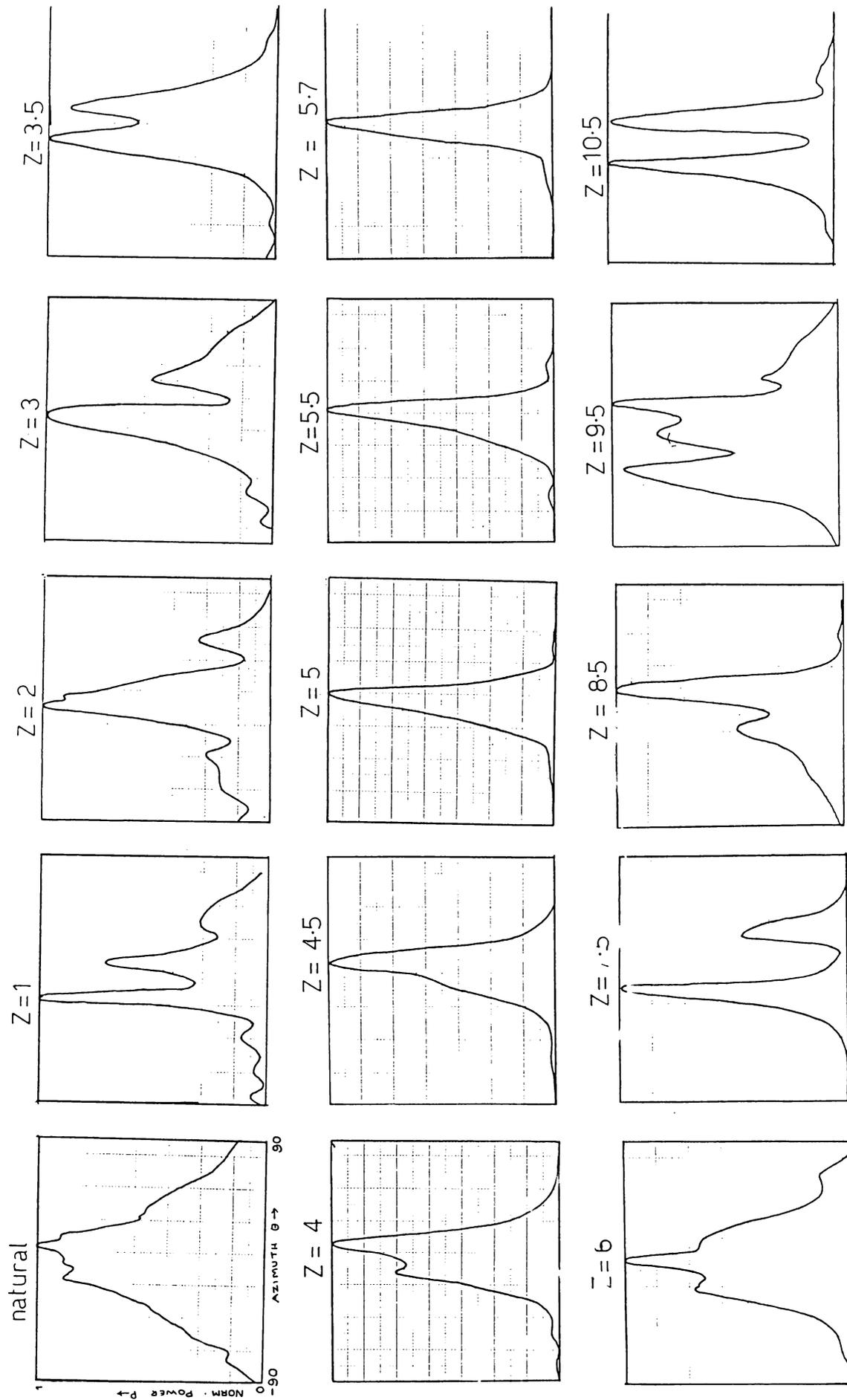


Fig 4 2 8 : Variation of E plane radiation patterns with Z · Horn H2, Flange F1 , 2β=45, Freq.9·375 GHz , α = 0°.

and other orthogonal to the corrugation. The first one is called TE component and the other as TM component. Here the TE component is totally reflected from the corrugation tips. But the other component will go into the corrugations and gets reflected from the bottom. These two with the primary will interfere at the far field and results in circular polarization. Since the amplitude and phase of the radiation from the flange is strongly depending on the position of the flange, the radiation pattern varies with the position. These theoretical aspects are considered in detail in the next chapter.

## 4.7(ii)  Effect of corrugation-tilt on radiation patterns

From the preliminary observations regarding co-polar and cross polar power density, it may be found that they are highly dependent on the tilt of corrugations. This aspect is illustrated in fig.4(29). It is evident that the circular polarization is obtained only when the tips of the corrugations are inclined at 45°. Similar variations, when both the flanges are rotated in the same way, are shown in fig.4(30).

## 4.7(iii)  Effect of frequency

It is also important to study the band-width of the antenna system. The typical variations of radiation pattern

113
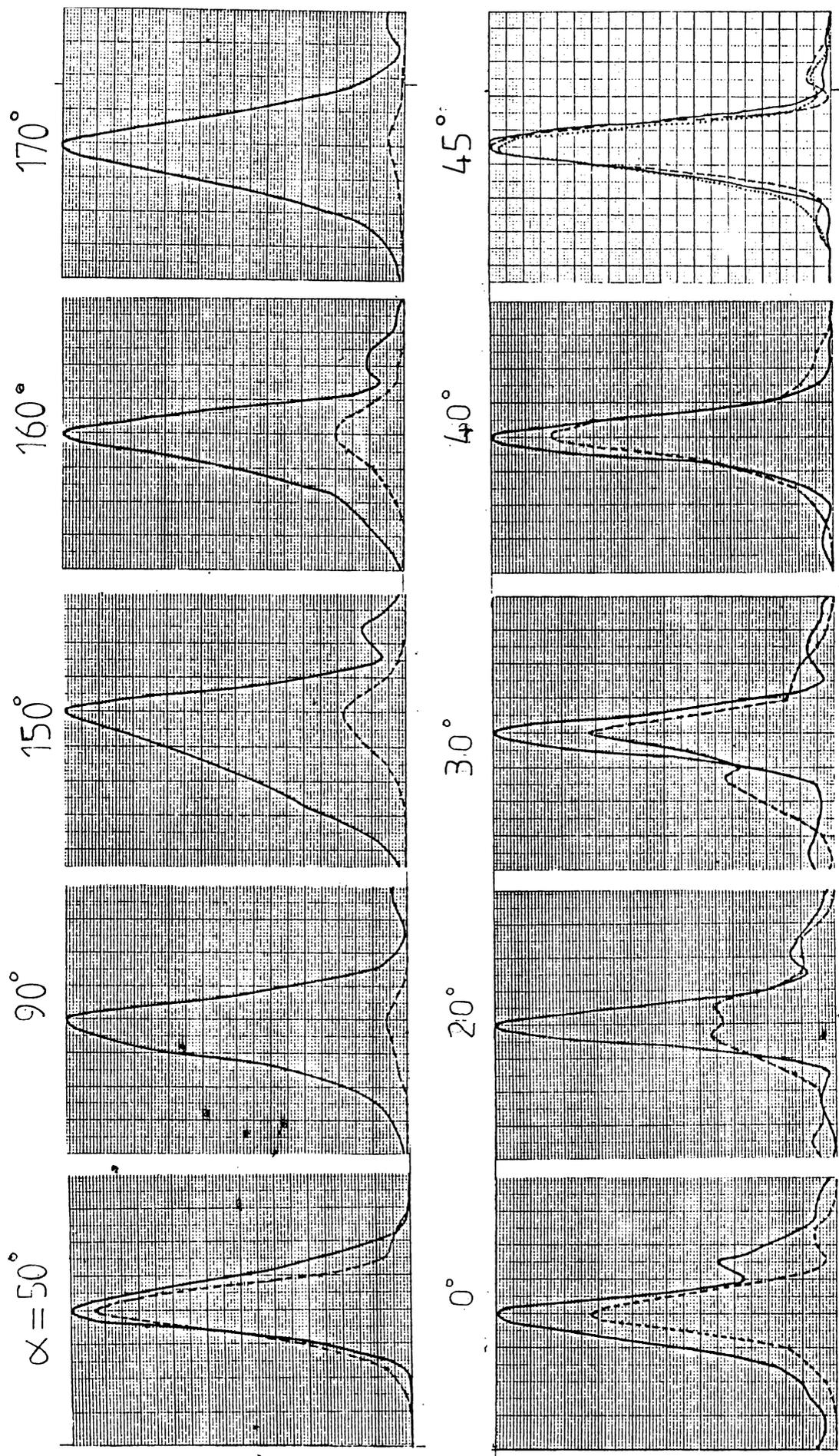
Fig. 4·29· Variation of radiation pattern with corrugation tilts. Horn H2, Flange F1, 2β= 45°

Frequency 9·375 GHz ——— Co ----- Cross ······· 45° Polar

α = 50°  90°  150°  160°  170°

0°  20°  30°  40°  45°
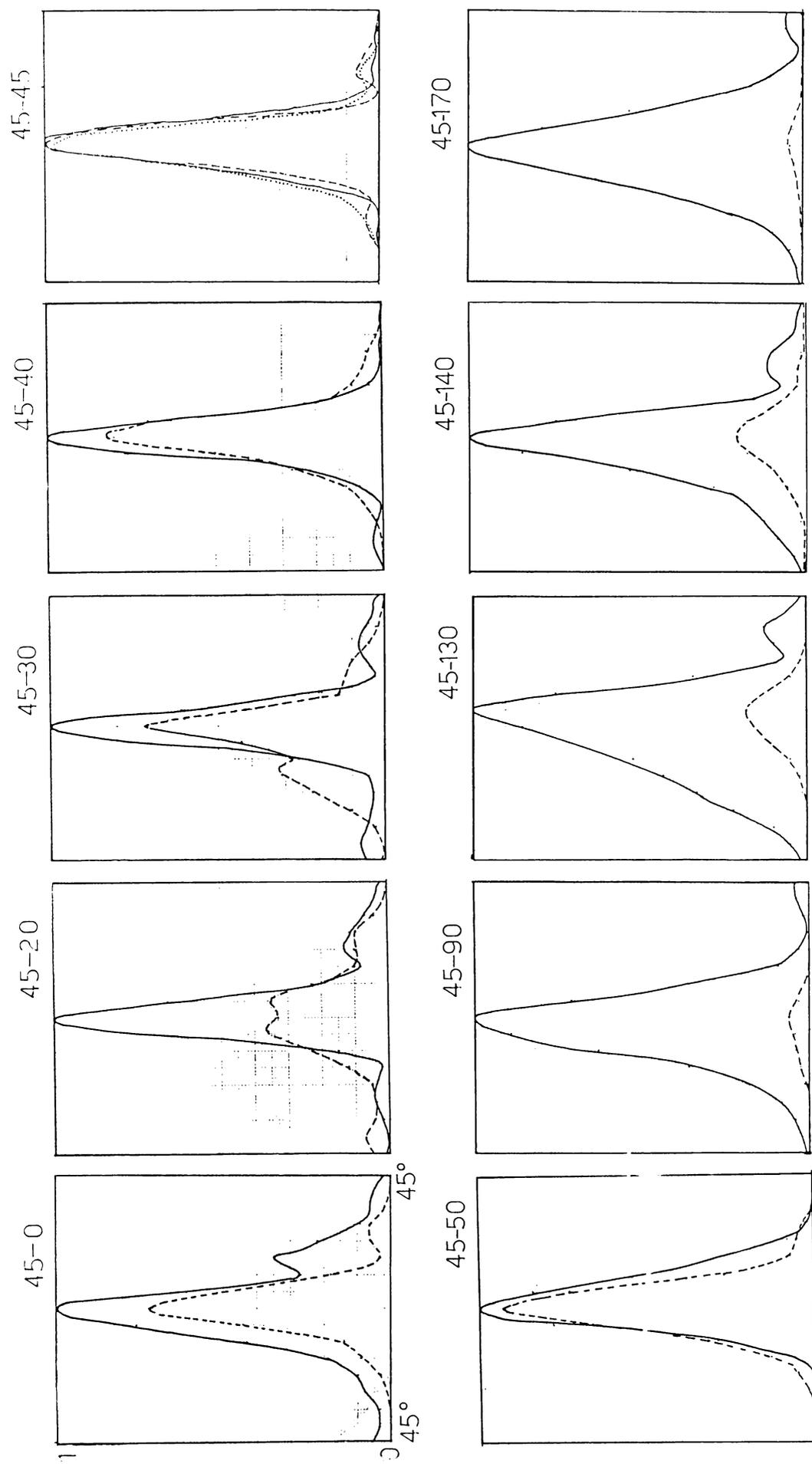
Fig. 4.30: Variation of radiation patterns with corrugation tilts. Horn H2, Flange F1, 2β = 45°, Frequency 9.375 GHz.
—— Co-polar, –––– Cross polar, ···· 45° polar.

with frequency are presented in fig.4(31). From the figure, the co-polar and cross-polar patterns are found to be nearly equal within the frequency band of 9 to 10 GHz. From the experiments it is also found that circular polarization is possible at other frequency by simply trimming the other flange parameters.

## 4.8  Half power beam width (HPBW)

Half power beam width of an antenna is directly related to gain and directivity. Variations of HPBW with flange parameters are invesitgated. This data is directly obtained from the radiation patterns.

It is stated earlier that the on-axis power density fluctuates with the position of the flange and naturally a change in HPBW is also expected. Co-polar, cross-polar and 45° plane HPBW are measured with the position of the flange. This variation is exhibited in fig.4(32). From the figure it is found that when the co-polar beam width is small the cross-polar width is large. But at the 'C' position, all the three beam widths are nearly equal. It is also supported by the VSWR measurements, because at this position a low VSWR is obtained.

116
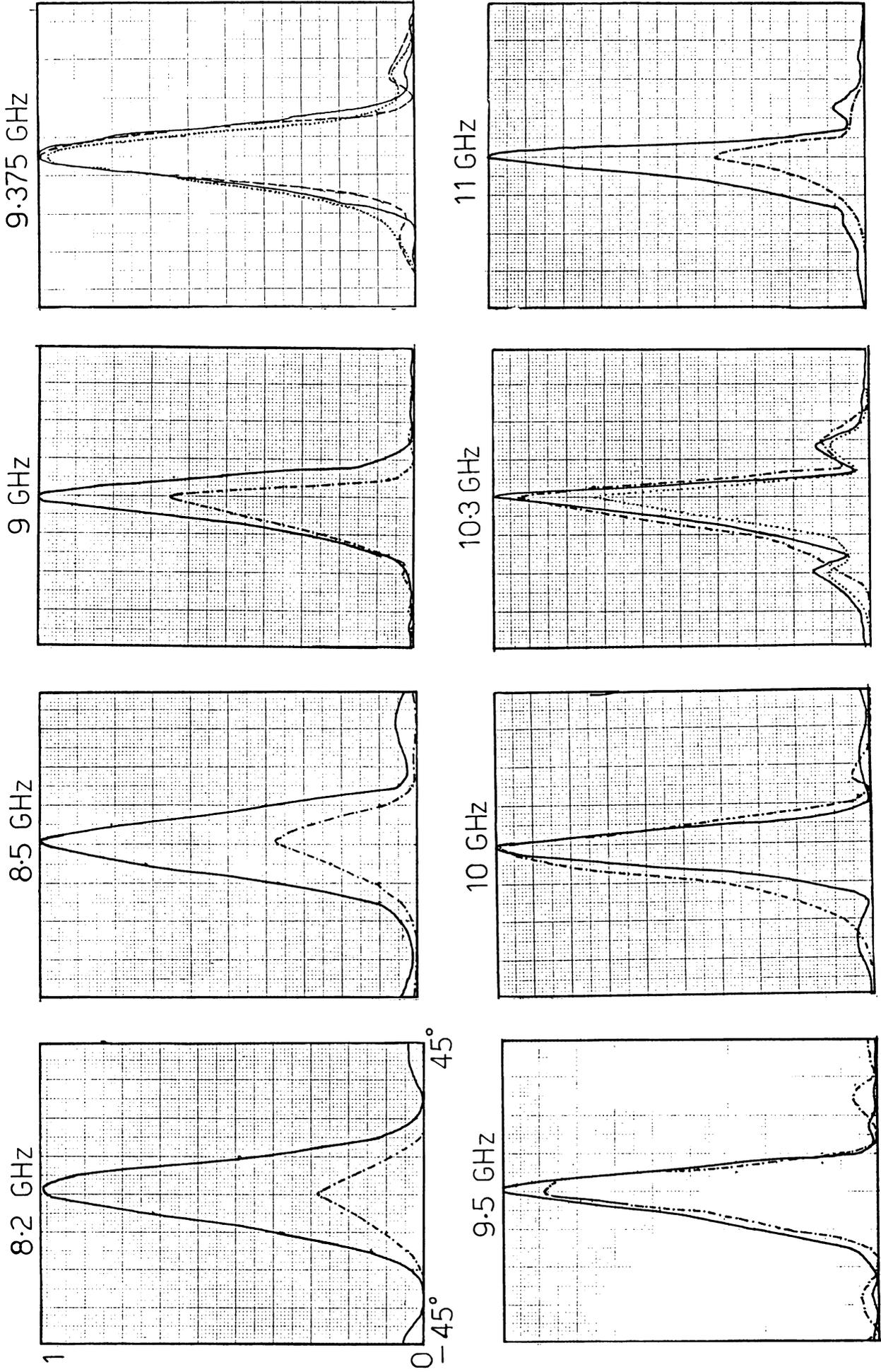


Fig. 4.31: Variation of radiation patterns with frequency. Horn H2, Flange F1, 2β=45°, α=45°.
——— Co-polar, — · — · — Cross-polar, · · · · · · · · · 45 polar.
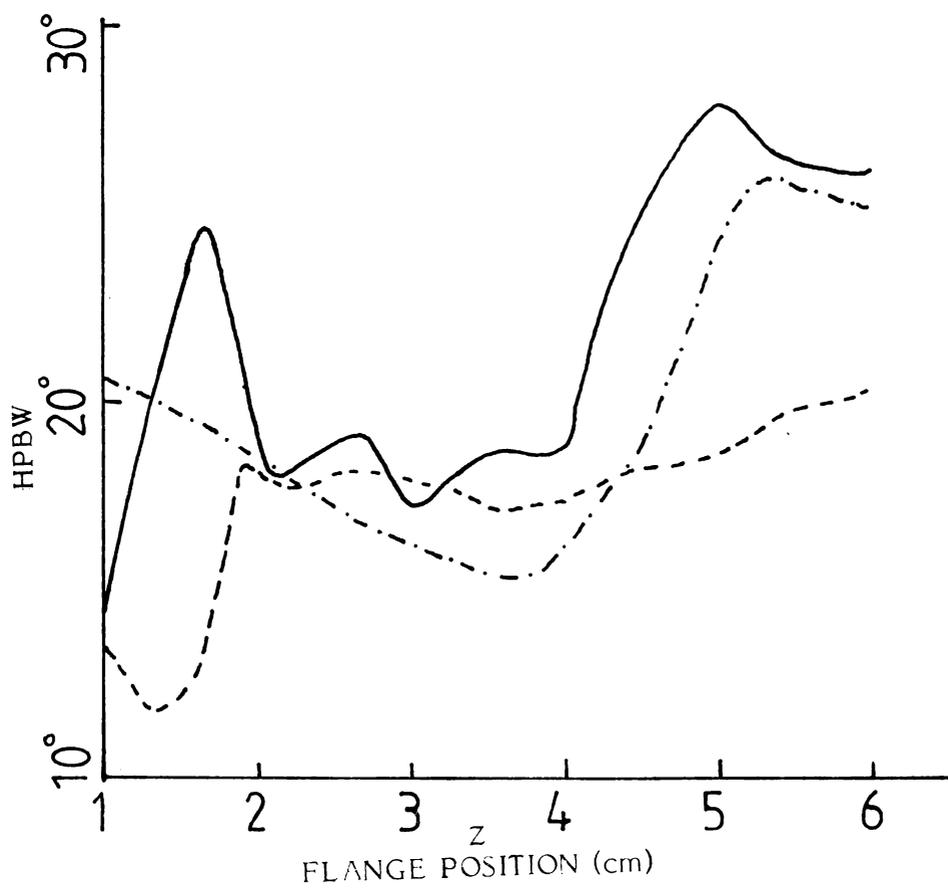
Fig.4.32: Variation of HPBW with flange position.Horn H2
Flange F1, 2β= 45, Frequency 9.375 GHz
———— Co-polar ---------Cross-polar -.-.-.-. 45°polar

Influence of corrugation tilt on the HPBW is shown in fig.4.33 and 4.34. Again the beam widths are nearly equal when corrugations are inclined through an angle of 45°. Frequency dependence of HPBW is shown in fig.4.35. In all cases the natural half power beam width of the horn is also shown for comparison. From the above results it may be concluded that the flange technique is a very effective tool for trimming the antenna polarization.

## 4.9 Antenna gain

The "gain", in this work refers to the directive gain. The gain of the antenna system is highly influenced by the position of the flange. The variation of gain with the position of the flange is shown in fig.4.36. When the flange is near the aperture, large variation of gain is obtained. When the co-polar gain is minimum the cross polar gain is found to be maximum at this range. But at 'C' position all the three gains (co-polar, cross-polar and 45° plane) are nearly equal. This is ascertained from the VSWR and HPBW data also. At 'C' position VSWR and HPBW of the antenna are found to be low. So, the gain is found to be increased. At other positions, matching is not obtained and this results in decrease in gain. Similarly, depending
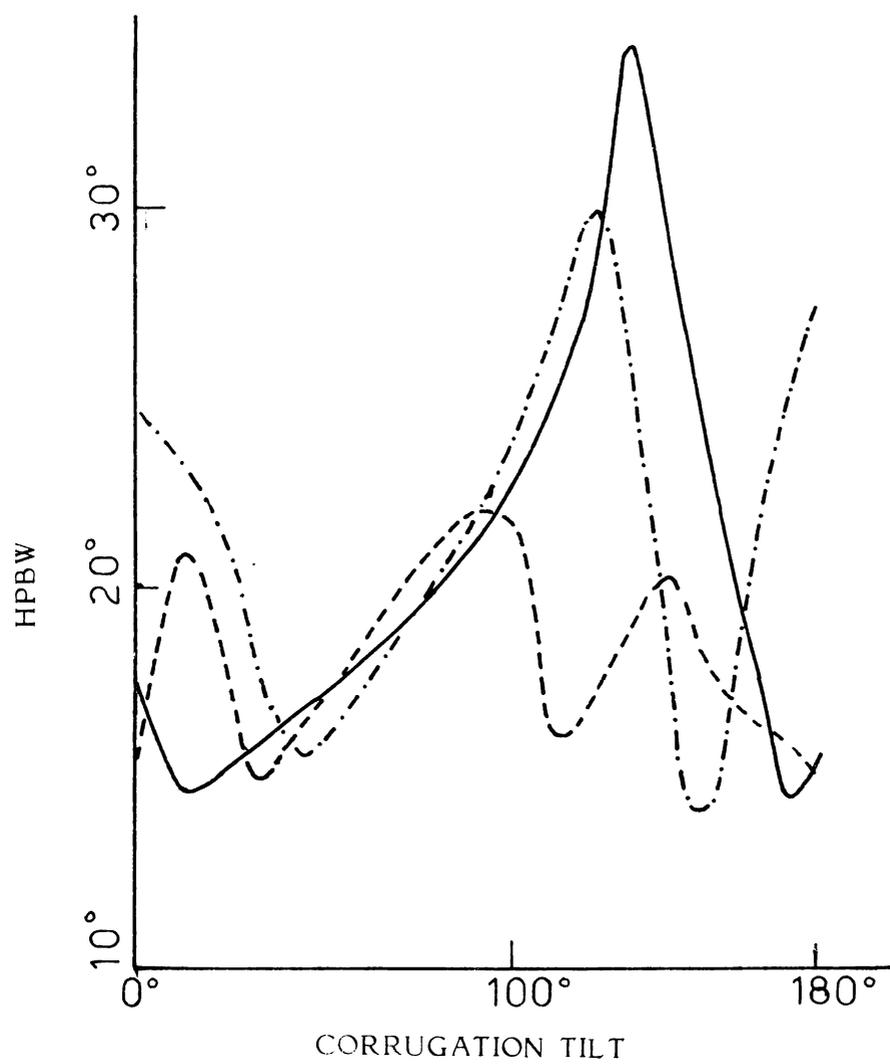
Fig.4.33: Variation of HPBW with corrugation tilt.Horn H2,flange F1,Z=2.5,2β=45
—— Co-polar, ------ Cross-polar, -.-.-.-. 45 deg.polar.
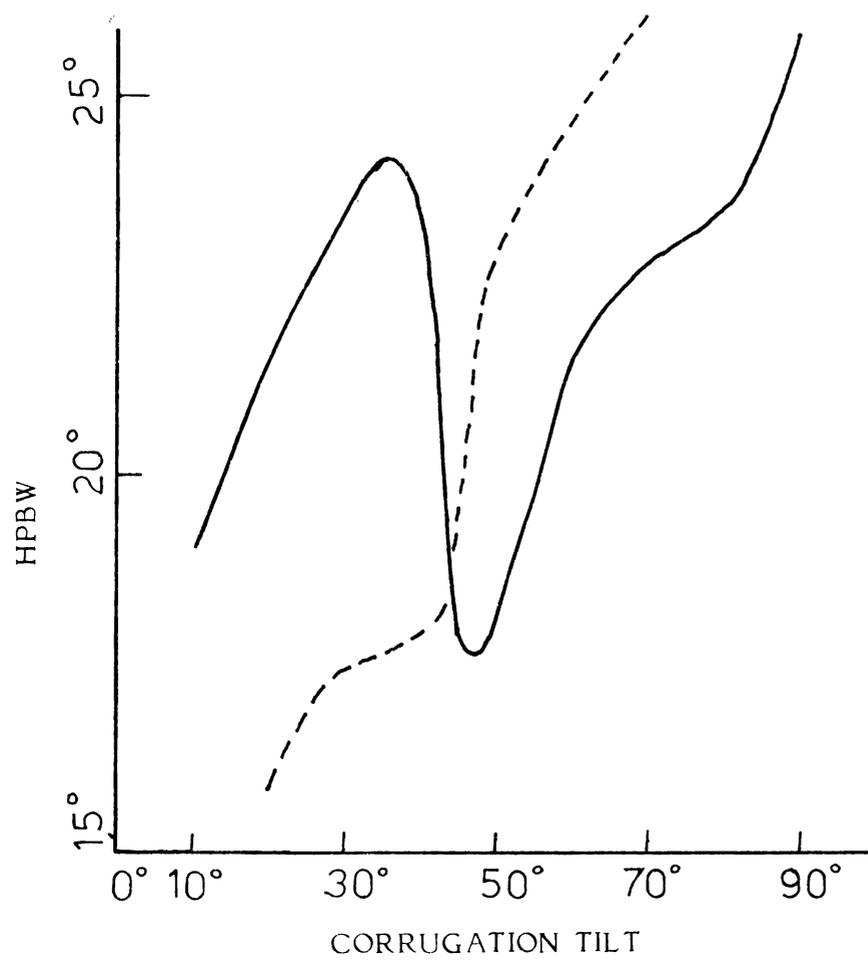
Fig.4.34:Variation of HPBW with corrugation tilt

Horn H2,flange F1,frequency 9.375 GHz,Z=2.5,2$\beta$=60

———— Co-polar, – – – – Cross-polar
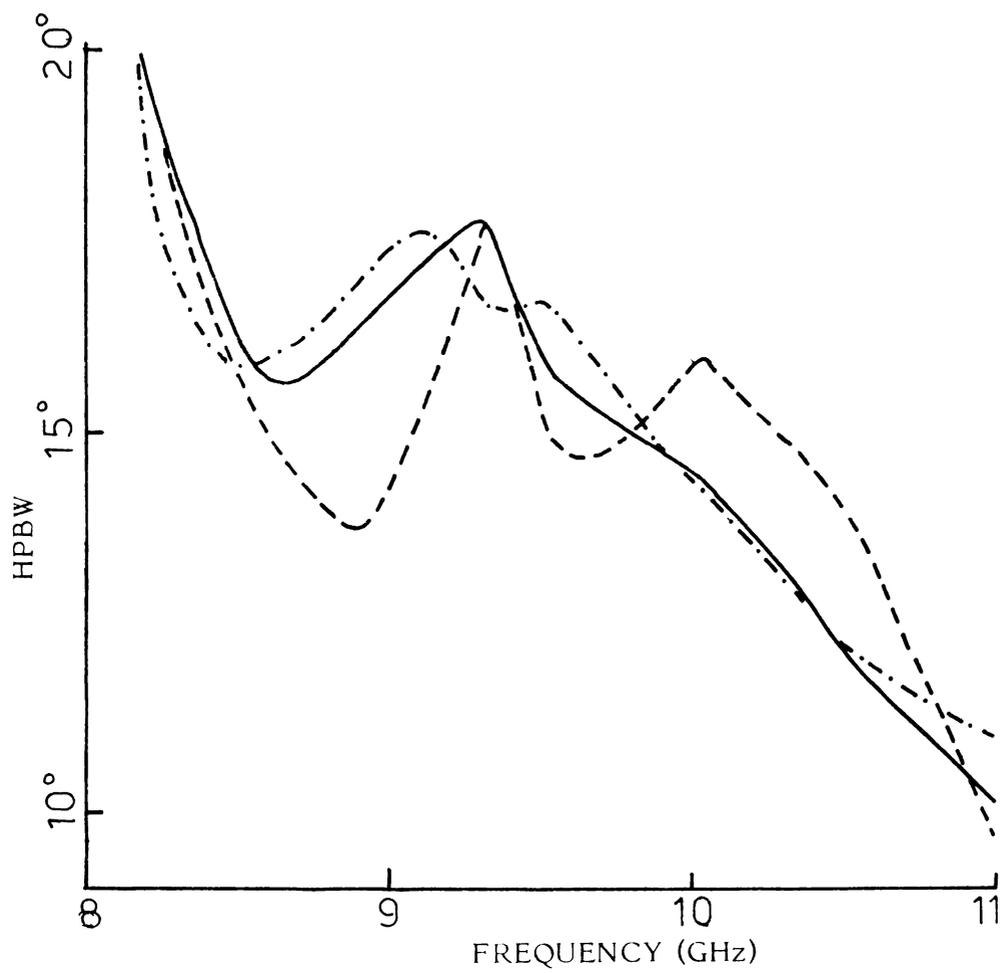
Fig.4.35: Variation of HPBW with frequency.Horn H2,Flange F1,2β=45,Z=2.5.
———— Co-polar, ------- Cross-polar, -.-.-.-.-. 45 deg.polar.
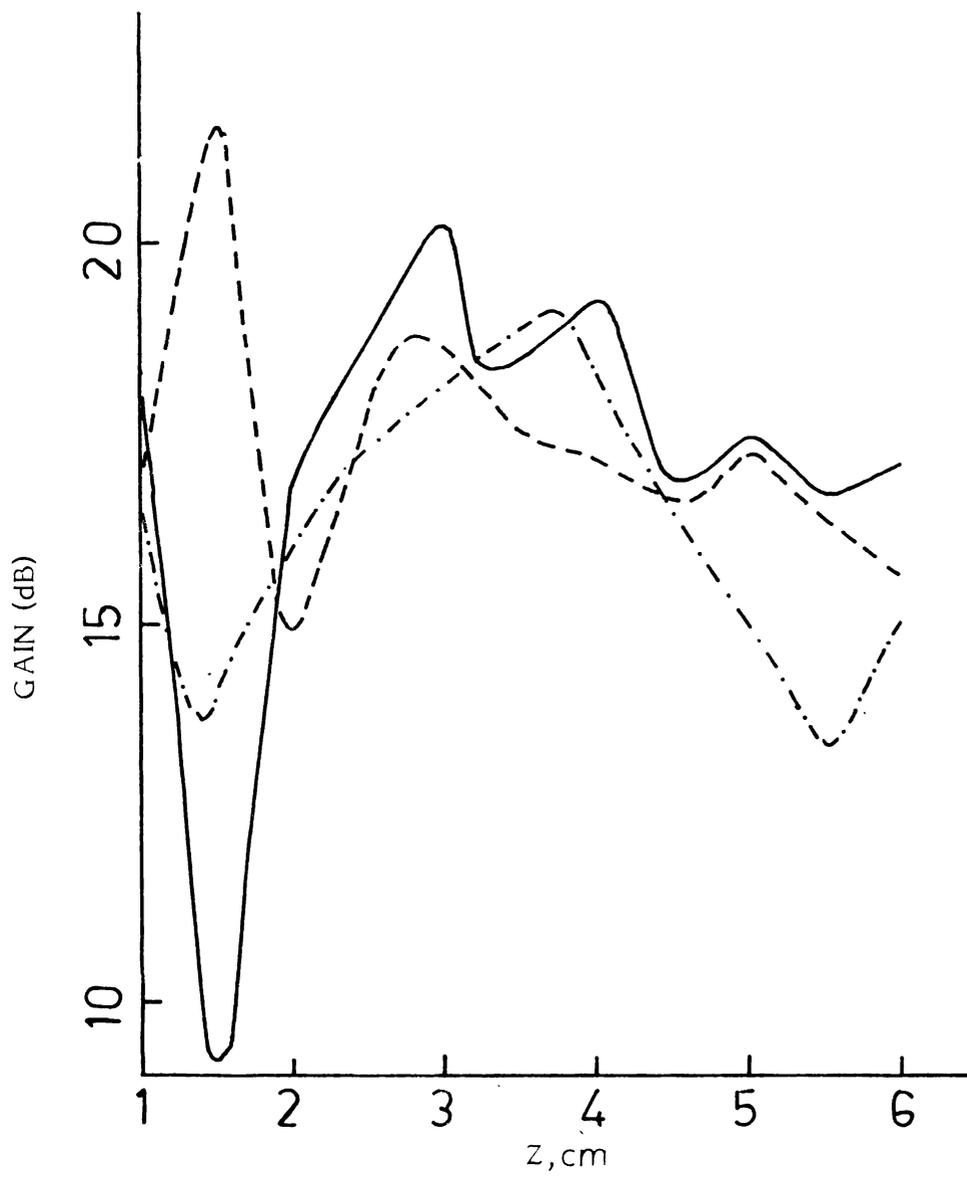
Fig.4.36: Variation of directive gain with Z.Horn H2,Flange F1

Flange angle 2β=45, Flange position

——— Co-polar, —————— Cross-polar, -.-.-.-.-. 45 deg.polar.

upon the position of the flange, the radiation from the
sources will interfere constructively at this position and
hence the gain is increased. In the above experiments, a
maximum gain of 18 dB is obtained at the 'C' position, with
a horn of natural gain 14 dB.

4.9(ii)  Dependence of gain on the tilt of corrugation

On axis power and HPBW of the present system are
found to depend upon the tilt of corrugation. Therefore a
corresponding variation of gain with corrugation tilt is
also investigated. Fig.3.37(a&b) show typical variation
of gain with tilt of corrugation. Again, it is observed
that the corrugations on the flange, when inclined at 45°
will result in equal values of the three gains, which are
nearly equal to that at the 'C' position.

4.9(iii)  Variation with frequency

Another factor which is investigated in this study
is the dependence of gain on frequency. It is found from
the earlier observations that the corrugated flanges are
usually frequency sensitive. This is shown in fig.4.38.
Gain of the system is found to be unaffected by frequency
within the band of 9 to 10 GHz. So the band width of the
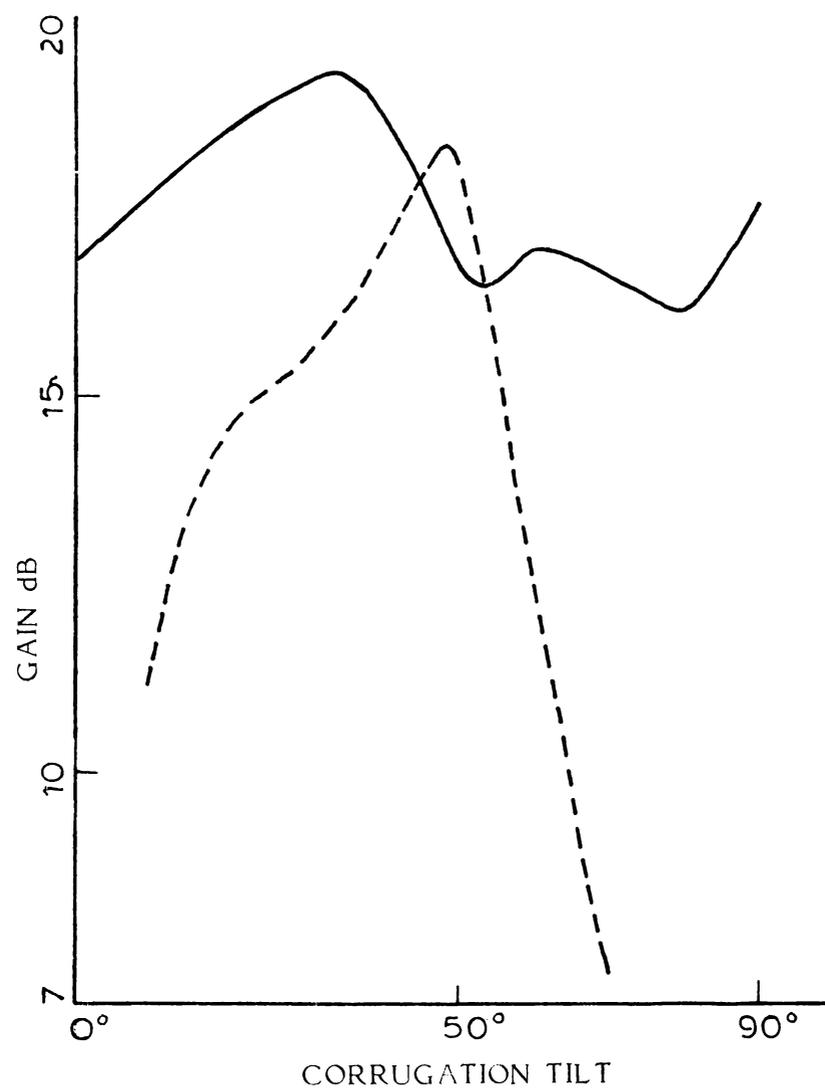
Fig.4.37(a) Variation of Gain with corrugation tilt.Horn H1,Flange F1.

Frequency 9.375 GHz, $2\beta = 45$, $Z = 2.5$.

———— Co-polar, ------ Cross-polar.
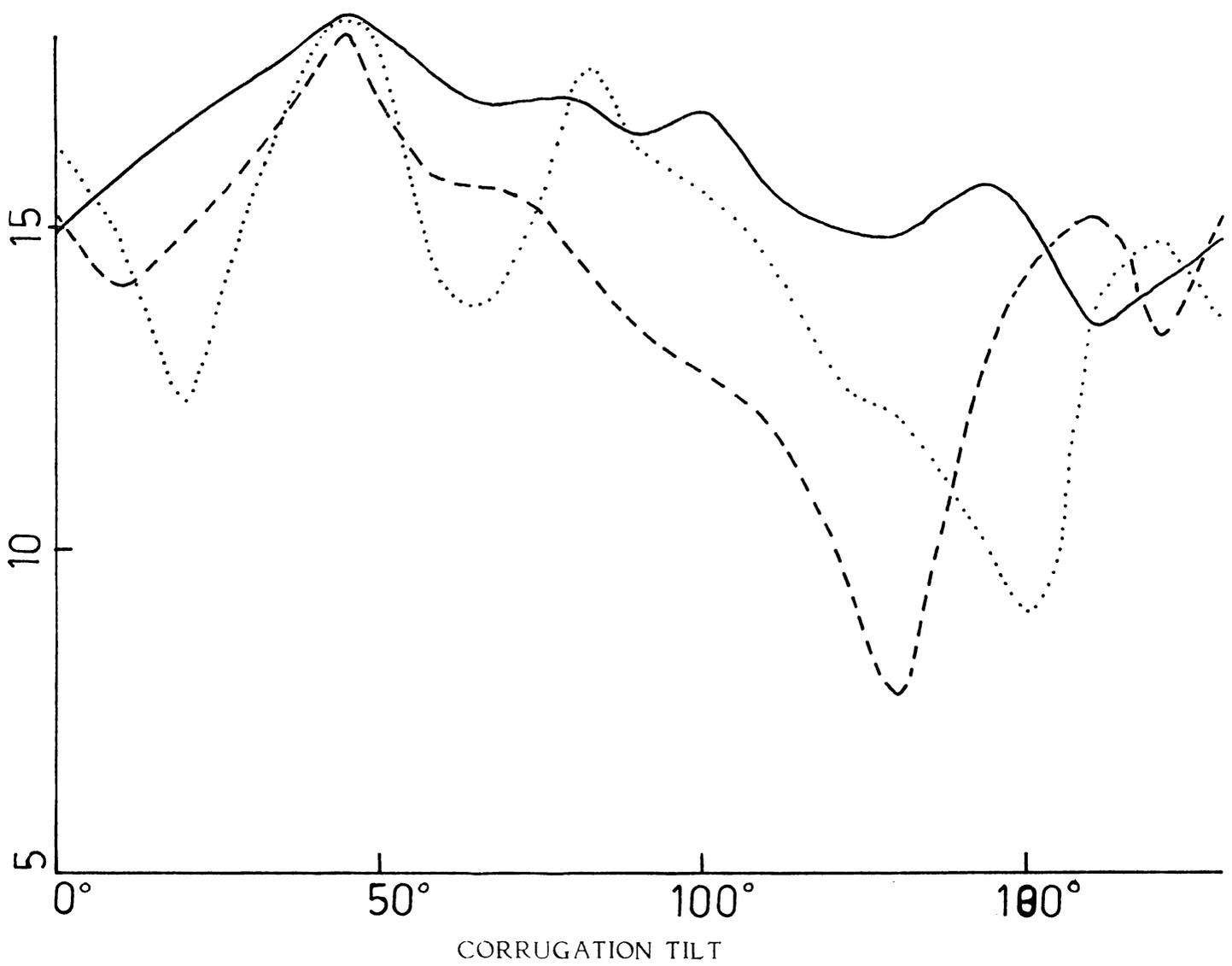
Fig.4.37(b): Variation of Gain with corrugation tilt.Horn H2,Flange F1,2$\beta$=45,Z=2.5,Freq.9.375 GHz.
———— C0-polar, —————— Cross-polar, ……… 45 deg.plane.
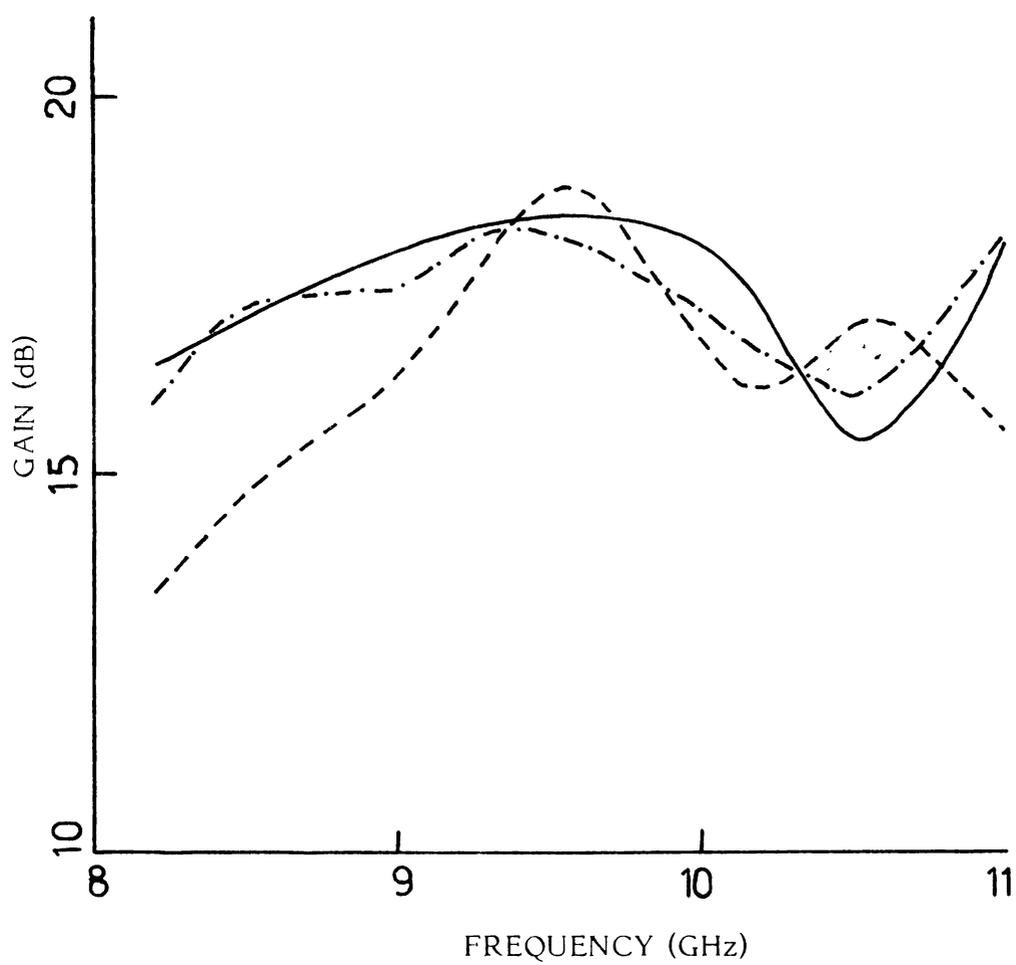
Fig.4.38: Variation of Gain with frequency.Horn H2,Fla. F1,2β=45,Z=2.5.
——— Co-polar, ------- Cross-polar, -.-.-.-. 45 deg.polar.

system is found to be very low. This is also predicted by the theory in the next chapter. If the frequency is varied, the path difference of the individual secondary radiators are disturbed and hence destructive or constructive inter-ference will take place and hence the decrease and increase of the gain.

The experiment is also conducted using a dielectric corrugated flange (F8). In that case it is found circular polarization is not possible. The result is also true with plane metallic flange. But when a dielectric corrugated flange is coated with aluminium, circular polarization is obtained. The variation of axial ratio with Z for the flange $F_{12}$ is shown in fig.4.39. Typical radiation pattern at the 'C' position is shown in fig.4.40. This result again confirms the action of corrugations on flanges. Typical co-polar and cross-polar radiation patterns of different flanges at 'C' position are shown in fig.4.41.

Thus from the above results it is clear that this system provides a simple and efficient technique for producing elliptically polarized antenna like horns with high gain and better matching. A probable theoretical analysis on the basis of line source theory and method of images are presented in the next chapter.
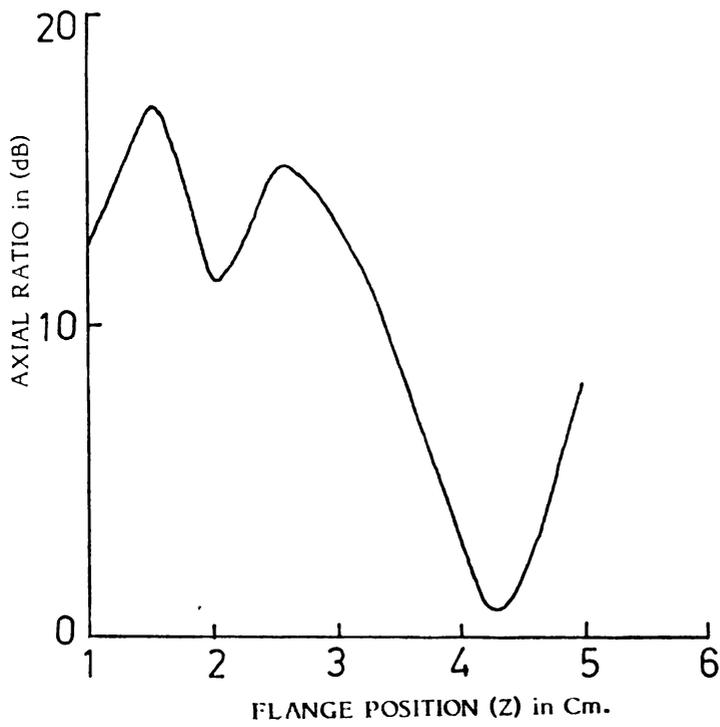
Fig.4.39: Variation of axial ratio with flange position.
Horn H2, Flange F12, 2β=45, Freq. 9.375GHz,
This is a aluminium coated perspex flange.



Co polar
Cross polar
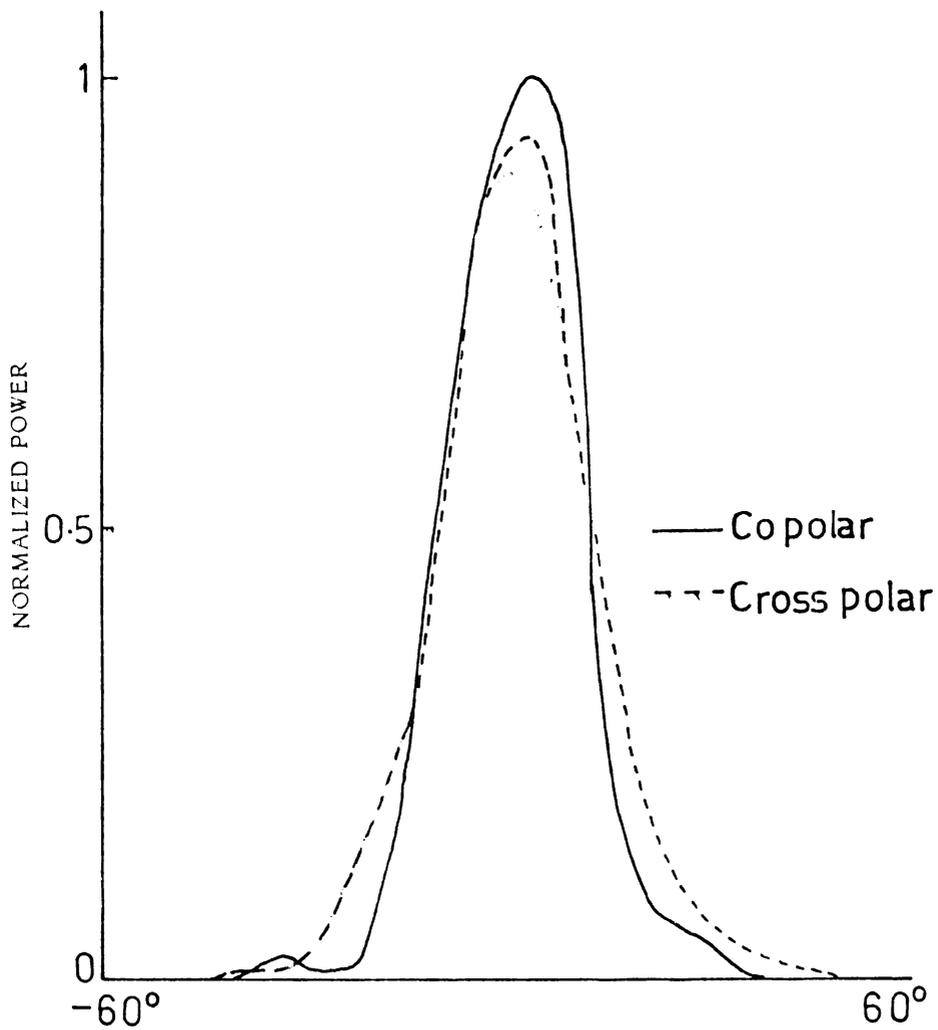
Fig.4.40: Typical radiation pattern of the above system.

horn H2,F1 i3,5...

H2,F13,8 GHz,Z=4,2β...

H2,F14,8·3GHz,Z=39,2β=45·

H2,F14,8·2GHz,Z=37,2β=30

1

H2,F2,9·5GHz,Z=4,2β=45·

H2,F3,11·365GHz,Z=5,2β=45·

H2,F5,9GHz,Z=6·7GHz,2β=60

H2,F4,9·5GHz,Z=6·4,2β=45·

−45

H2,F6,9·5GHz,Z=5·8,2β=10·

H2,F6,10GHz,Z=4,2β=30·

H2,F7,9·375GHz,Z=74 2β=60·

H2,F10,9·5GHz,Z=37,2β=60·

0

−45

45
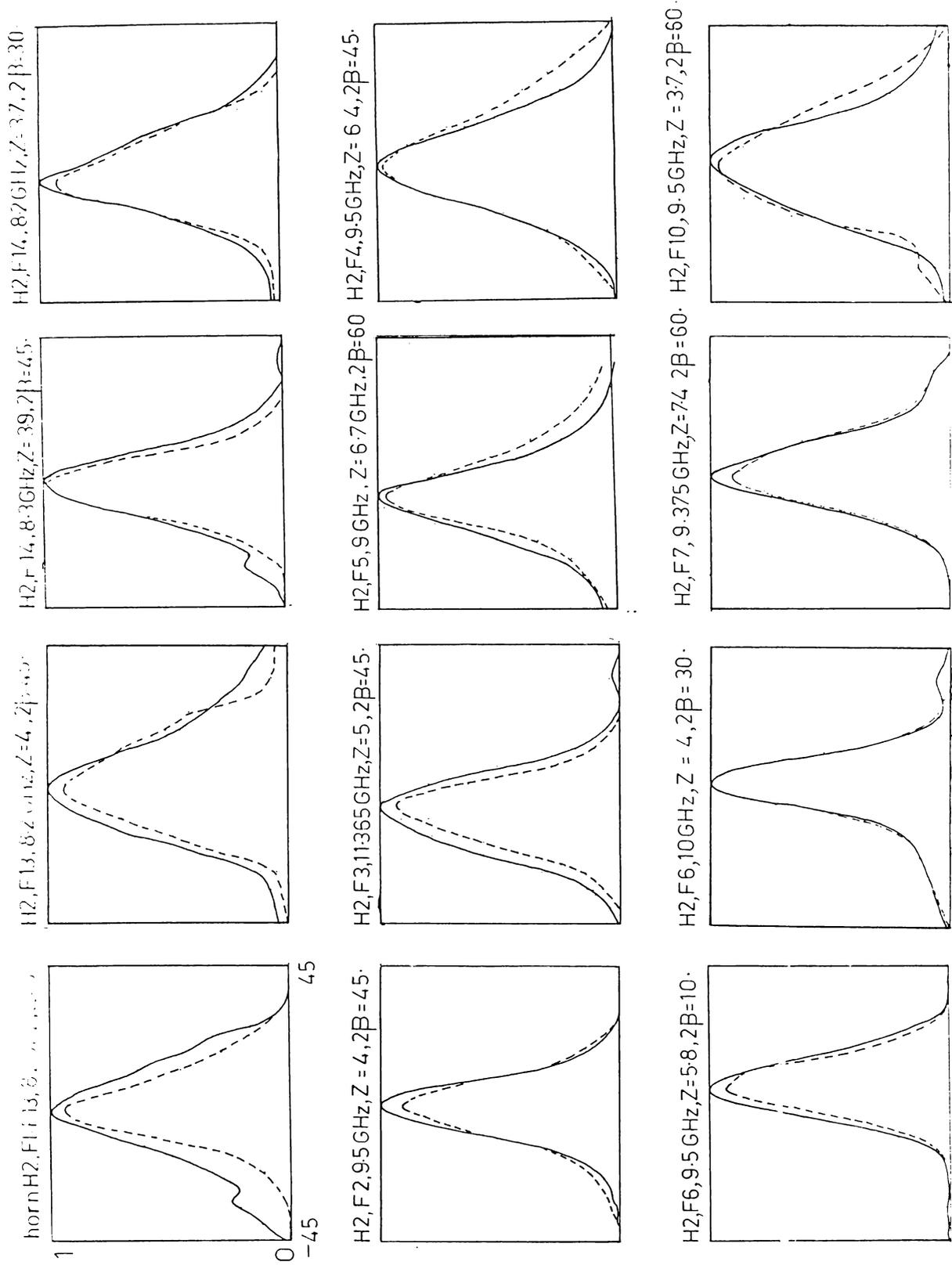
Fig 4·41 Typical co polar and cross polar radiation patterns at C-position for different flanges.
co polar, cross polar

GHAPTER : 5

**Theoretical analysis**

Chapter 5

THEORETICAL ANALYSIS


Theoretical analysis of axial ratio of elliptically
polarized wave from horns fitted with tilted corrugated flanges
is presented in this chapter.  The theoretical approach is on
the basis of secondary radiators and method of images.  A
comparison between the experimental and theoretical results
is given at the last part of this chapter.


5.1  Horns fitted with straight corrugated flanges


Owen and Reynolds[72] proposed the "Line source theory"
to explain the effect of plane metallic flanges on sectoral
horns.  Later, Butson and Thomson[73] adopted this method to
explain their experimental results.  Recently Zachariah and
Vasudevan[88] modified this theory to explain the radiation from
horns fitted with corrugated flanges.  Here, the narrow aperture
of the feed horn is treated as a line source.  The above theory
is adopted to explain the observed results.  Geometry of a horn
fitted with corrugated flanges is shown in figs.5.1(a) and
5.1(b).  All the flange parameters are marked in the figure.
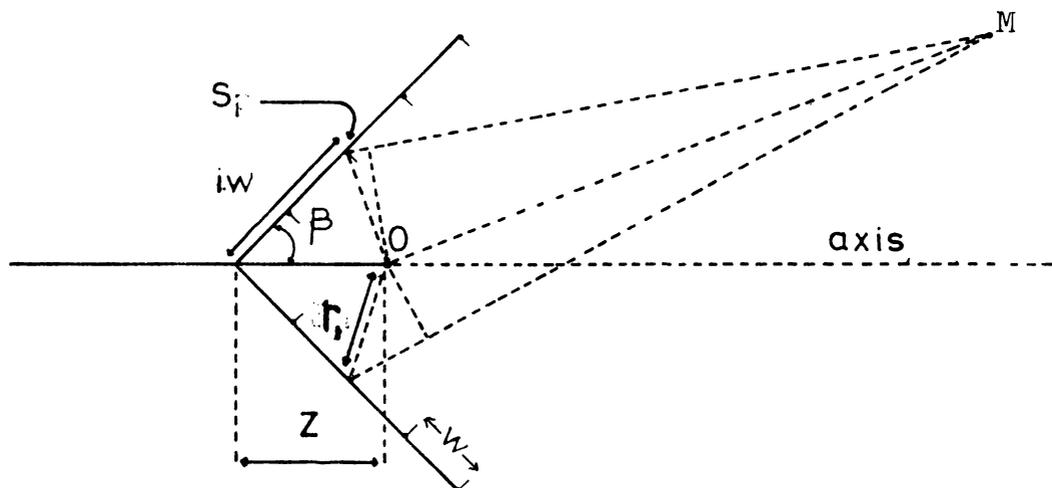

130

Fig.5.1 (a) Geometry of the corrugated flange mounted sectoral horn. O is the horn aperture. $s_i$ is the $i^{th}$ element on the flange surface. $r_i$ is the distance of the $i^{th}$ element from the horn aperture. Z is the distance between the point where the flanges are kept and the horn aperture.



Fig.5.1 (b) Geometry of the flange mounted sectoral horn. O is the horn aperture. I and I' are the images of O cast by the flange elements.

Fig.5.1 (a) Geometry of the corrugated flange mounted sectoral horn. O is the horn aperture. $s_i$ is the $i^{th}$ element on the flange surface. $r_i$ is the distance of the $i^{th}$ element from the horn aperture. Z is the distance between the point where the flanges are kept and the horn aperture.
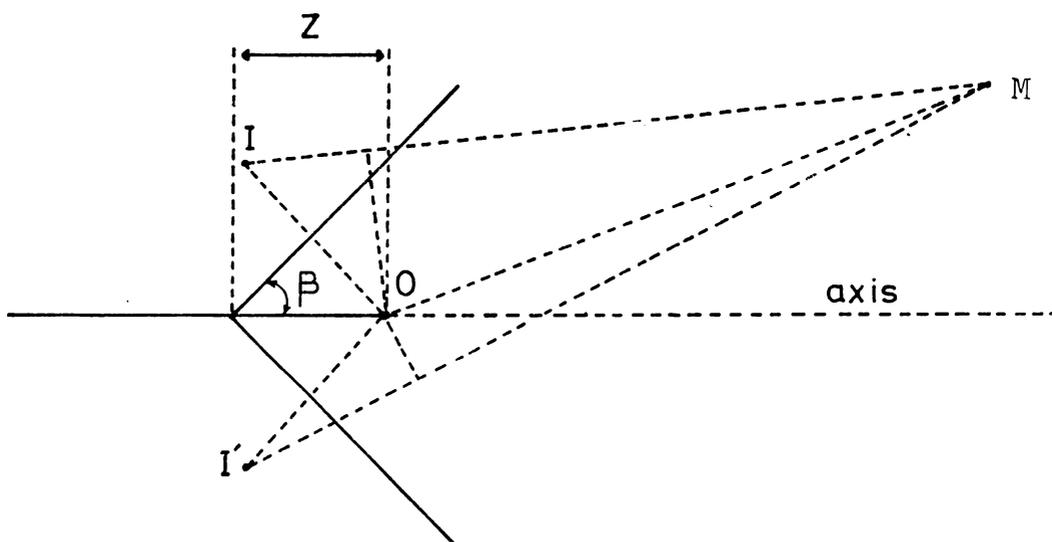
Fig.5.1 (b) Geometry of the flange mounted sectoral horn. O is the horn aperture. I and I' are the images of O cast by the flange elements.

The tips of the corrugations are orthogonal to the E-vector. Here 'O' is the aperture of the horn. Let there are 'N' corrugation-elements in each flange. All these elements are excited by the aperture of the horn (treated as a line-source) and act as secondary radiators. The amplitude and phase of these secondary sources vary from element to element. The amplitude of excitation of $i^{th}$ element is proportional to $\frac{1}{r_i^2}$ where $r_i$ is the distance of the $i^{th}$ element from the aperture of the horn.

From the figure, we see that

$$r_i = \left[ (z^2 + (iw - \frac{h}{\tan\beta})^2 - 2z(iw - \frac{h}{\tan\beta})\cos\beta \right]^{\frac{1}{2}} \tag{1}$$

where w is the width, and h is the height of the corrugation, $2\beta$ is the flange angle and Z is the distance of the flange from the aperture of the horn.

The phase difference between the radiation from the $i^{th}$ element and the aperture of the horn, as it reaches the far field point M,

$$\eta_i = \frac{2\pi}{\lambda} r_i \left[ 1 - \cos(\alpha_p - \theta) \right] \tag{2}$$

where $\alpha_p$ is

$$\cos^{-1}\left[\frac{(iw - h/\tan\beta)^2 - z^2 - r_i^2}{2zr_i}\right]$$

Similarly, the relative phase of the $i^{th}$ element from the second flange is

$$\eta_i' = \frac{2\pi}{\lambda} r_i [1 - \cos(\alpha_p + \theta)] \tag{3}$$

The amplitudes of these radiators are equal to $\frac{k}{r_i^2}$ where $k$ is a constant equal to 0.077 as estimated by Butson and Thomson[73].

The total contribution from all these elements from one flange is given by the vector sum of the amplitudes from all the elements.

The contribution from the first flange

$$K = \left\{\left[\sum_{i=1}^{N} \frac{k}{r_i^2} \sin\eta_i\right]^2 + \left[\sum_{i=1}^{N} \frac{k}{r_i^2} \cos\eta_i\right]^2\right\}^{\frac{1}{2}} \tag{4}$$

The resultant phase difference is given by

$$\emptyset = \tan^{-1}\left[\frac{\sum\limits_{i=1}^{N} \frac{k}{r_i^2} \sin \eta_i}{\sum\limits_{i=1}^{N} \frac{k}{r_i^2} \cos \eta_i}\right] \qquad (5)$$

Similarly the contribution from the second flange is

$$K' = \left\{\left[\sum\limits_{i=1}^{N} \frac{k}{r_i^2} \sin \eta_i'\right]^2 + \left[\sum\limits_{i=1}^{N} \frac{k}{r_i^2} \cos \eta_i'\right]^2\right\}^{\frac{1}{2}} \qquad (6)$$

and its phase

$$\emptyset' = \tan^{-1}\left[\frac{\sum\limits_{i=1}^{N} \frac{k}{r_i^2} \sin \eta_i'}{\sum\limits_{i=1}^{N} \frac{k}{r_i^2} \cos \eta_i'}\right] \qquad (7)$$

Therefore the total contribution from all the corrugation elements is

$$E_1 = K \angle \emptyset + K \angle \emptyset' \qquad (8)$$

$$= \left[(K \sin \emptyset + K'\sin \emptyset')^2 + (K \cos \emptyset + K'\cos \emptyset')^2\right]^{\frac{1}{2}} \qquad (9)$$

To satisfy the limiting condition, this is to be multiplied

by the overall space directivity factor $(\frac{\cos\theta}{\cos\beta} - 1)$

$$E = E_1(\frac{\cos\theta}{\cos\beta} - 1)^{\frac{1}{2}} \tag{10}$$

when the space factor is negative, E is unrealistic and

hence neglected. The resultant phase is

$$\epsilon = \tan^{-1}\left[\frac{K \sin \phi + K'\sin \phi'}{K \cos \phi + K'\cos \phi'}\right] \tag{11}$$

Due to the propagation of waves inside the corrugation

we have to consider the effect of images I and I'. The relative

phase of the image I is given by

$$\delta = \frac{2\pi}{\lambda} 2.z.\sin\beta \sin(\beta - \theta) \tag{12}$$

Similarly the phase of the image I' is

$$\delta' = \frac{2\pi}{\lambda} 2z.\sin\beta \sin(\beta + \theta) \tag{13}$$

Therefore, the resultant of the primary and the images is given by

$$E_\theta' = \left\{3+2\cos(\delta - \delta') + 2[\cos\delta\,(1+\cos(\delta - \delta') + \right.$$

$$\left. \sin\delta\,\sin(\delta - \delta')]\right\}^{\frac{1}{2}} \tag{14}$$

and its phase

$$\varepsilon' = \tan^{-1}\left[\frac{\sin\delta + \sin\delta}{1 + \cos\delta + \cos\delta}\right] \tag{15}$$

Therefore the resultant power at M is given by

$$P = \left\{[E_\theta\,\sin\varepsilon + E_\theta\,\sin\varepsilon']^2 + [E_\theta\,\cos\varepsilon + E_\theta'\,\cos\varepsilon']^2\right\}$$

$$X\,(1 + \cos\theta) \tag{16}$$

where $(1 + \cos\theta)$ is the directivity factor for directional antennas.

## 5.2 Calculation of axial ratio of tilted corrugated flanged horns

In general the tips of the corrugations are inclined at an angle $\alpha$ to the H-field. Then the incident radiation from the aperture of the horn can be split into two components, namely TM and TE waves. The component which is parallel to the tips of the corrugation is TE waves and the other orthogonal to the corrugation is called TM waves. It is diagrammatically shown in fig.5.2.

$$E_{TE} = E \cos \alpha \tag{17}$$

$$E_{TM} = E \sin \alpha \tag{18}$$

where E is the incident electric field. For normalized case E is taken as unity. TE waves are completely reflected from the tips of the corrugations; but TM waves propagate into the slots[98]. So the theory of secondary sources is taken to TE waves and method of images is taken for TM waves. The relative phase of the $i^{th}$ corrugation element along the axis is

$$\eta_i = \frac{2\pi}{\lambda} r_i [1 - \cos \alpha_p] \tag{19}$$
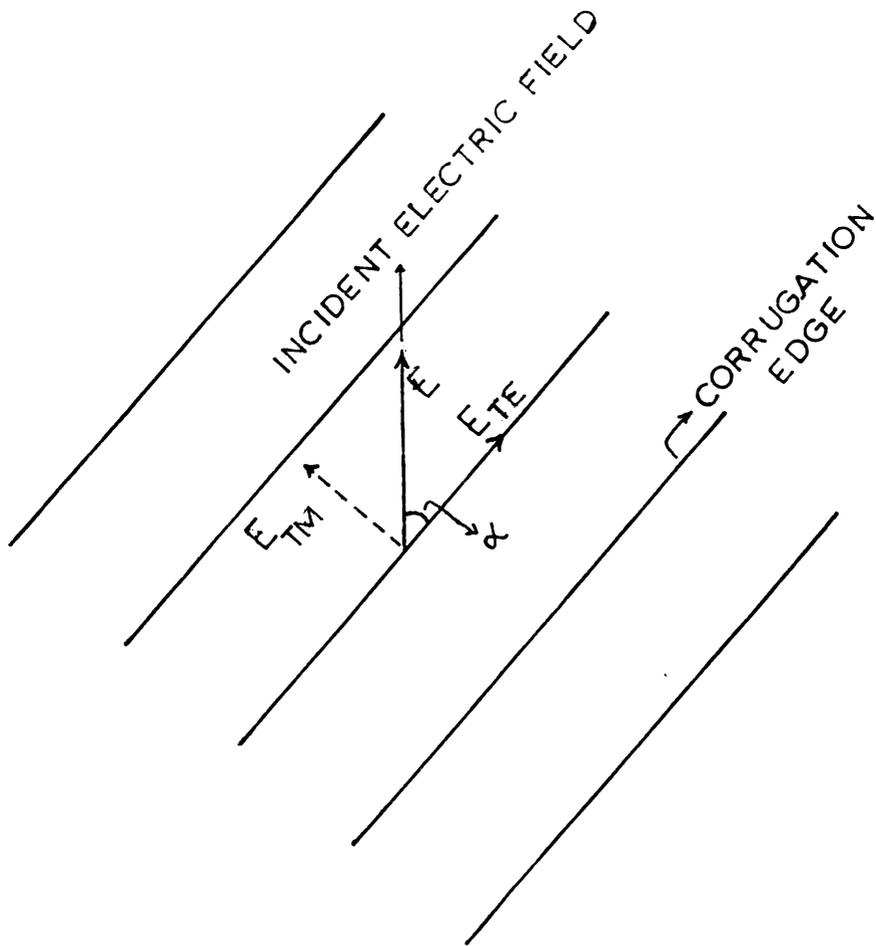
Fig.5.2:Schematic representation of the incident electric-fieldon the corrugated flange and it's component along and orthogonal to the corrugation edge.

where

$$r_i = [Z^2 + (iw - \frac{h}{\tan\beta})^2 - 2Z(iw - \frac{h}{\tan\beta})\cos\beta]^2 \qquad (20)$$

and

$$\alpha_p = \cos^{-1} [\frac{(iw - h/\tan\beta) - Z^2 - r_i^2}{2Zr_i}] \qquad (21)$$

Therefore the total TE component along the axis from all the corrugation element is

$$M = k\left\{[\sum_{i=1}^{N} \frac{E_{TE}}{r_i^2} \sin\eta]^2 + [\sum_{i=1}^{N} \frac{E_{TE}}{r_i^2} \cos\eta_i]^2\right\}^{\frac{1}{2}} \qquad (22)$$

and the phase

$$\psi = \tan^{-1}\left[\frac{\sum_{i=1}^{N} \sin\frac{\eta_i}{r_i^2}}{\sum_{i=1}^{N} \cos\frac{\eta_i}{r_i^2}}\right] \qquad (23)$$

The phase of the image is given by

$$D = \frac{12.56}{\lambda} [z\sin\beta + h]\sin\beta \qquad (24)$$

Therefore we have two components, one is parallel to the corrugation and other is perpendicular to it.

The component of M along the H-field is

$$P = M \cos \alpha \tag{25}$$

Similarly the perpendicular component is

$$Q = M \sin \alpha \tag{26}$$

The component of the image along the H-field is

$$S = E_{TM} \sin \alpha \tag{27}$$

Similarly the perpendicular component is

$$T = E_{TM} \cos \alpha \tag{28}$$

All these are represented in fig.5.3.

The total field along the H-field is the vector sum of P and S. The total field orthogonal to the H-field is similarly the vector sum of Q and T.

$$E_{cross} = E_{\rightarrow} = 2 \left[ (P \sin \psi + S \sin D_o)^2 + (P \cos \psi + S \cos D_o)^2 \right]^{\frac{1}{2}} \tag{29}$$

$$E_{\uparrow} = 2 \left[ (Q \sin \psi + T \sin D_o)^2 + (Q \cos \psi + T \cos D_o)^2 \right]^{\frac{1}{2}} \tag{30}$$
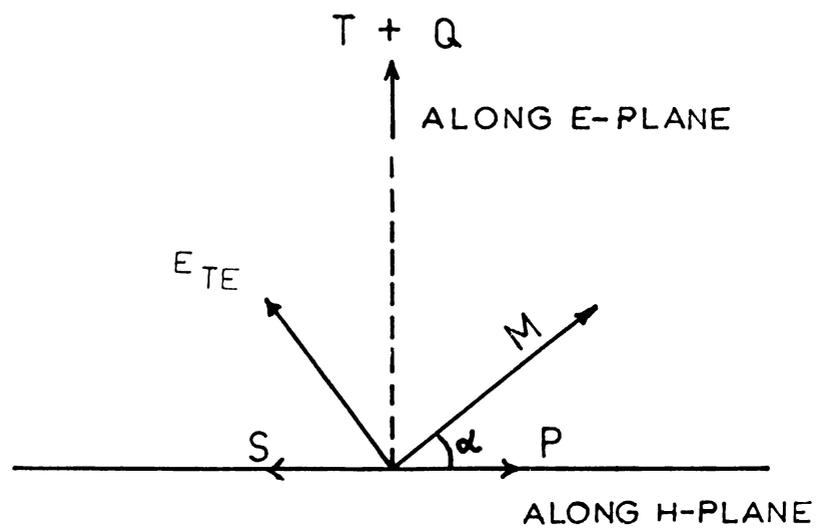
Fig.5.3: Field components along the E-plane and H-plane.

The term 2 is because of the contribution from both the flanges. However, for cross polar component, 1.5 is found to give more tangible values with respect to experimental patterns. The phases are

$$\emptyset_{\rightarrow} = \tan^{-1} \frac{P \sin + S \sin D_O}{P \cos + S \cos D_O} \qquad (31)$$

$$\emptyset_{\uparrow} = \tan^{-1} \frac{Q \sin + T \sin D_O}{Q \cos + T \cos D_O} \qquad (32)$$

But the vertical component will add with the direct radiation from the horn. The total co-polar field is

$$E_{copolar} = [(E_{\uparrow} \sin \emptyset_{\uparrow})^2 + (E + E \cos \emptyset_{\uparrow})^2]^{\frac{1}{2}} \qquad (33)$$

and the phase is

$$\emptyset_{co} = \tan^{-1} \frac{E_{\uparrow} \sin \emptyset_{\uparrow}}{E_{\uparrow} + E \cos \emptyset_{\uparrow}} \qquad (34)$$

The phase difference between the co-polar and cross-polar component is

$$\mathcal{P} = \emptyset_{\uparrow} - \emptyset_{co} \qquad (35)$$

The major axis of the polarization ellipse is given by[119]

$$OA = \frac{1}{2}[E_{co}^2 + E_{cross}^2 + (E_{co}^4 + E_{cross}^4 + 2E_{co}^2 E_{cross}^2)^{\frac{1}{2}}]^{\frac{1}{2}} \qquad (36)$$

The minor axis of the polarization ellipse

$$OB = \frac{1}{2}\left[E_{co}^2 + E_{cross}^2 - (E_{co}^4 + E_{cross}^4 + 2E_{co}^2 E_{cross}^2)^{\frac{1}{2}}\right]^{\frac{1}{2}} \tag{37}$$

Then the axial ratio is given by

$$\text{Axial ratio } \gamma = 20 \log \frac{OA}{OB} \tag{38}$$

and the tilt angle of the polarization ellipse[106,110]

$$\tau = \frac{1}{2}\tan^{-1}\left[\frac{E_{co}^2 \sin 2\rho}{E_{co}^2 + E_{cross}^2 \cos 2\rho}\right] \tag{39}$$

## 5.3 Results of the theoretical calculations

The axial ratios given by the above equation were computed using a computer, for various flanges and horns. The theoretical results are presented in this section.

Here the variation of on-axis axial ratio as the distance of the flanges from the aperture of the horn is presented. It has been observed that axial ratio fluctuates between a maxima and a minima as Z is varied. These typical variations are shown in fig.5.4(a,b,c, and d). Experimental curves are also shown for comparison. It is found that there
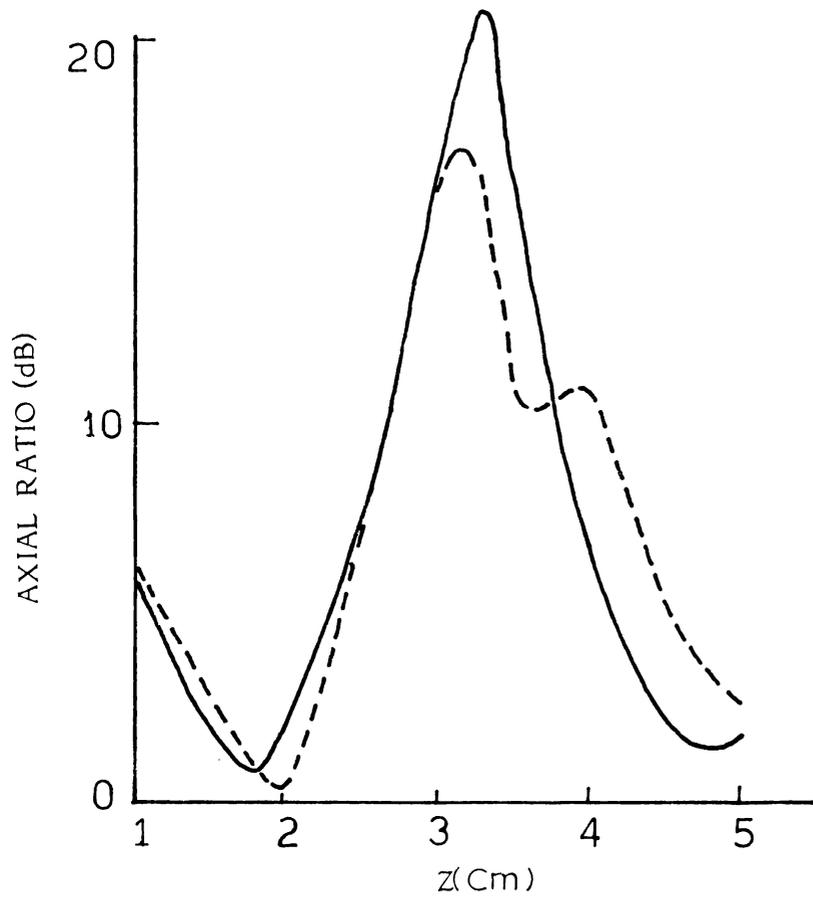
Fig.5.4(a): Theoretical and experimental variation of axial ratio with flange position.
Horn H2,Flange F1,Frequency 11.365 GHz,2$\beta$=90,$\alpha$=45.
———— Theory, --------- Experiment
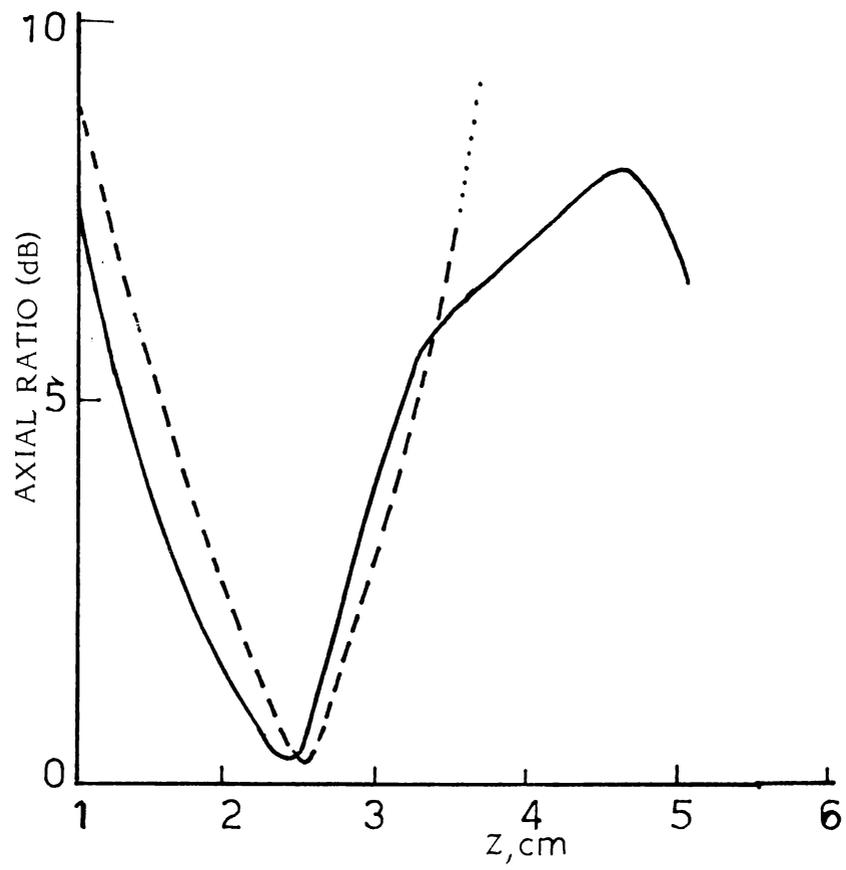
Fig.5.4(b): Theoretical and experimental variation of axial ratio
with flange position.
Horn H2,Flange F1,Fre.9.375 GHz,$2\beta=45,\alpha=45$.
——————— Theory, -------- Experiment.
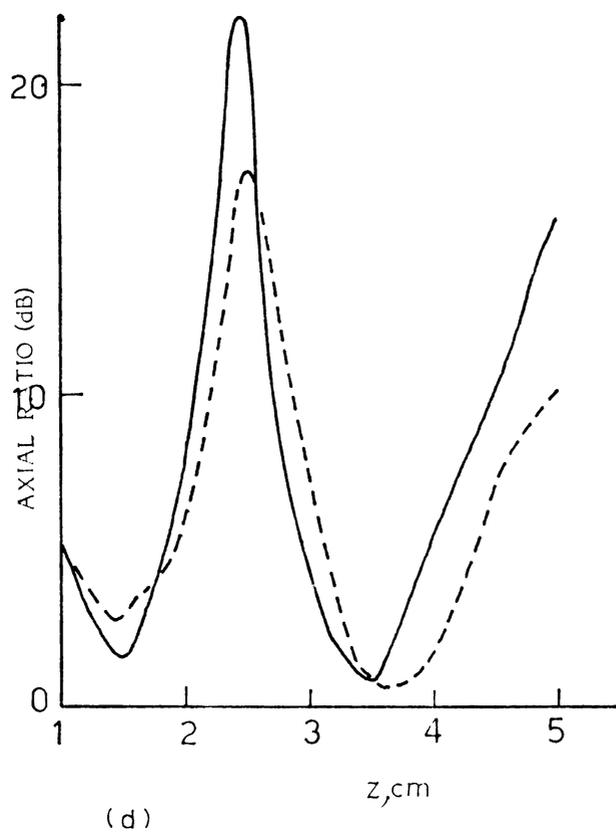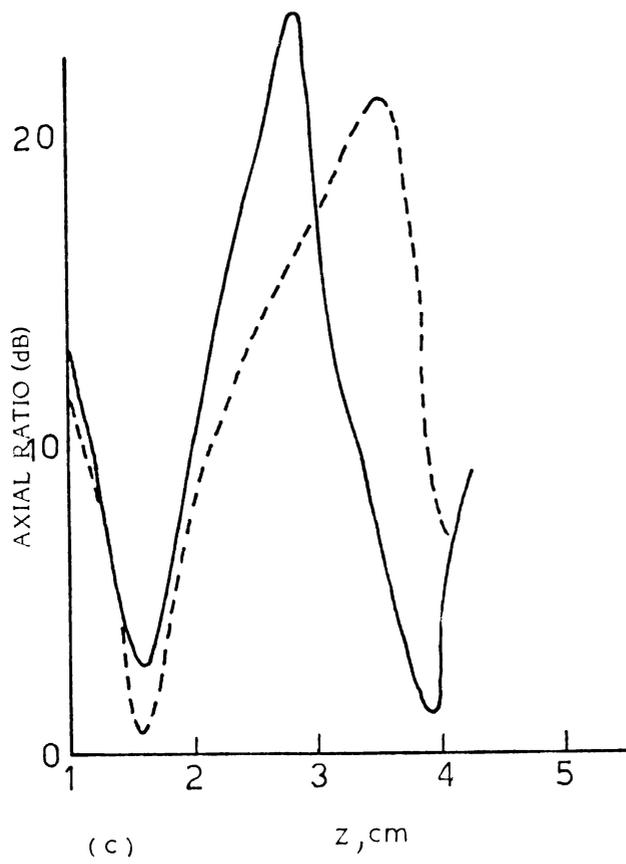
Fig.5.4: Theoretical and experimental variation of axial ratio with Z.
Horn H2, Flange F1, Frequency 9.375 GHz and $\alpha = 45$.
c) $2\beta = 90$, d) $2\beta = 60$ ———— Theory, ------ Experiment.

is fairly good agreement between theory and experiment at
the circular polarization positions.  Table 5.1 shows the
comparison between the theory and experiment for better
understanding.  The position of the flange for circular
polarization for different flanges is  shown in table 5(2).

Typical variation of axial ratio with frequency
is shown in fig.5.5(a,b and c).  It is again found that the
frequency response can also be roughly explained with this
simple theory.  Similarly the variation of axial ratio with
flange angle for a fixed position of the flange is shown
in fig.5.6.

In fig.5.7 the variation of polarization tilt
angle with the flange position is shown.  It is found that
all these variations can be explained by this theory.

The small difference between the theory and
experiment is found at certain points away from the 'C'
positions.  These are presumed to be due to various approxi-
mations made in the theory.  These facts are discussed further
in the next chapter. From the theoretical and experimental
curves, it may be observed that there is fairly good agreement
between theoretical and experimental results.

Table 5.1

### Theoretical and experimental results

Horn $H_2$, Flange $F_1$, Frequency 9.375 GHz, $2\beta = 60°$, $\alpha = 45°$

| Z | Theoretical axial ratio | Experimental axial ratio |
|---|---|---|
| 1 | 5.4 | 5 |
| 1.5 | 1.89 | 2.8 |
| 2 | 7.9 | 5.2 |
| 2.5 | 17.2 | 22.2 |
| 3 | 5 | 7 |
| 3.5 | 0.83 | 0.6 |
| 4 | 5.3 | 0.8 |
| 4.5 | 9.8 | 7 |

Table 5.2

Theoretical and experimental results
for different flanges and horns

| Horn | Flange | $2\beta$ | Frequency GHz | Experimental | | Theory | |
|------|--------|------|---------------|--------------|------|--------|------|
| | | | | 'C' position | Axial ratio | 'C' position | Axial ratio |
| $H_2$ | $F_1$ | 45 | 9.375 | 2.4 | 0.4 | 2.5 | 0.22 |
| $H_2$ | $F_1$ | 60 | 9.315 | 3.5 | 0.6 | 3.4 | 0.25 |
| $H_1$ | $F_3$ | 30 | 11.365 | 4.5 | 1.2 | 3.8 | 0.9 |
| $H_1$ | $F_3$ | 45 | 11.365 | 1.4 | 1.07 | 1.8 | 1.1 |
| $H_1$ | $F_3$ | 60 | 11.365 | 3.0 | 0.79 | 2.6 | 1.12 |
| $H_3$ | $F_1$ | 30 | 11.365 | 3.9 | 0.92 | 4.2 | 1.15 |
| $H_3$ | $F_1$ | 45 | 11.365 | 2.2 | 0.62 | 2.0 | 1.006 |
| $H_3$ | $F_1$ | 60 | 11.365 | 2.5 | 0.83 | 2.6 | 1.15 |
| $H_3$ | $F_1$ | 90 | 11.365 | 4.4 | 1.8 | 3.8 | 1.5 |
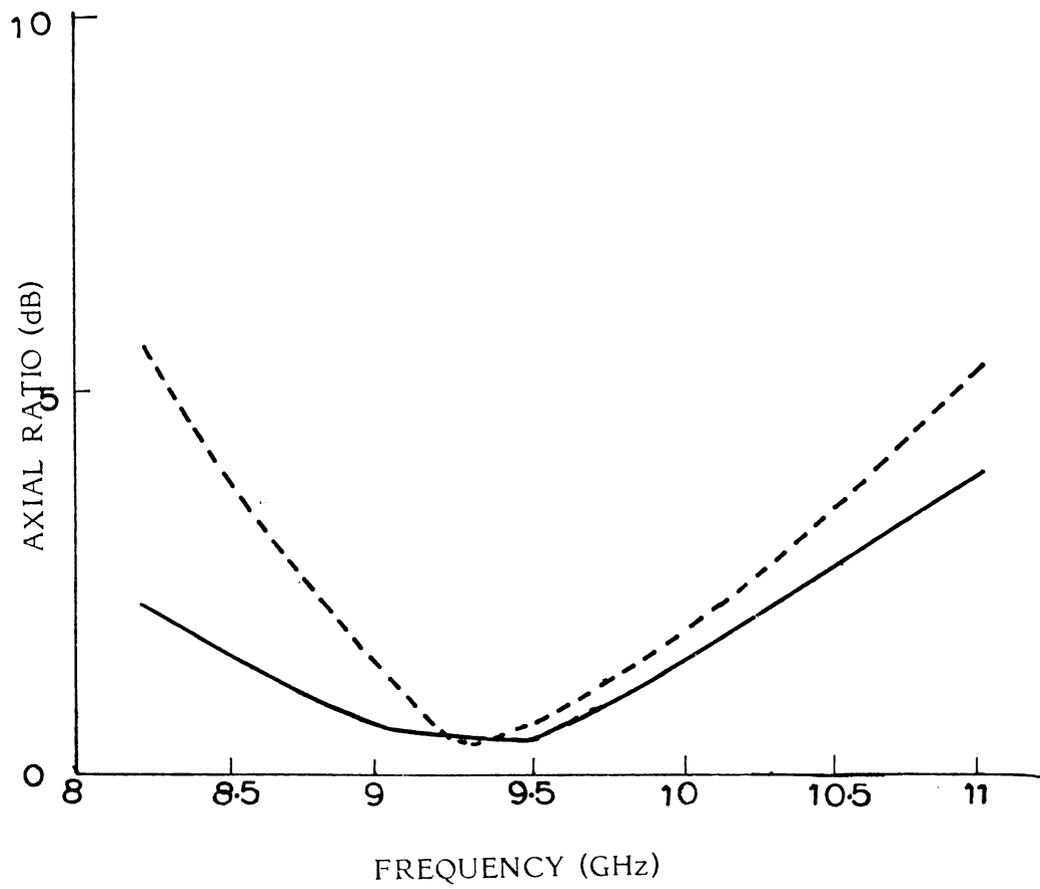
Fig.5.5(a): Variation of axial ratio with frequency.Horn H2,Flange F1.
Z=2.5,∝=45,2β=45,———Theory,------Experiment.
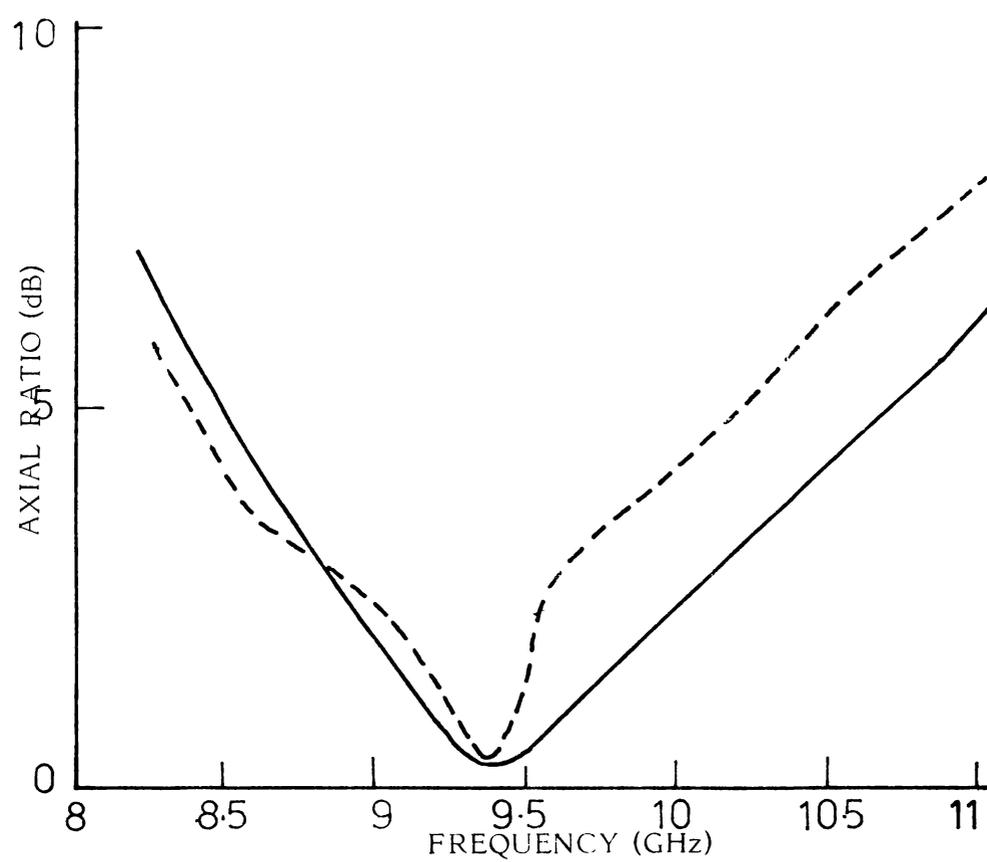
Fig.5.5.(b): Variation of axial ratio with frequency.
Horn H2,Flange F1,2$\beta$=60,Z=3.5,$\alpha$=45.
———— Theory, ------ Experiment.
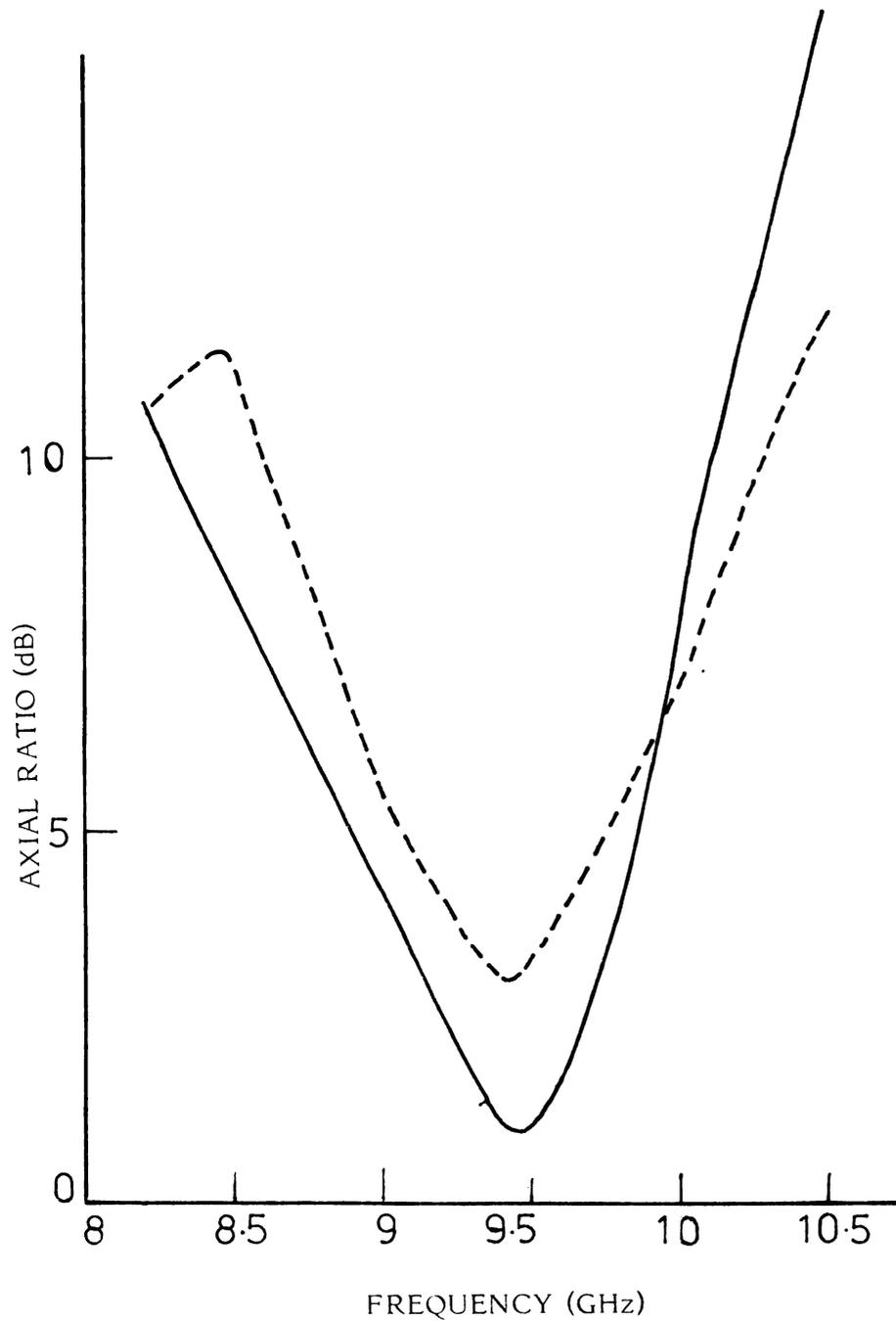
Fig.5.5(c): Variation of axial ratio with frequency.Horn H2,Flange F1,
z=1.6,2β=90, α=45.———Theory, ------ Experiment.
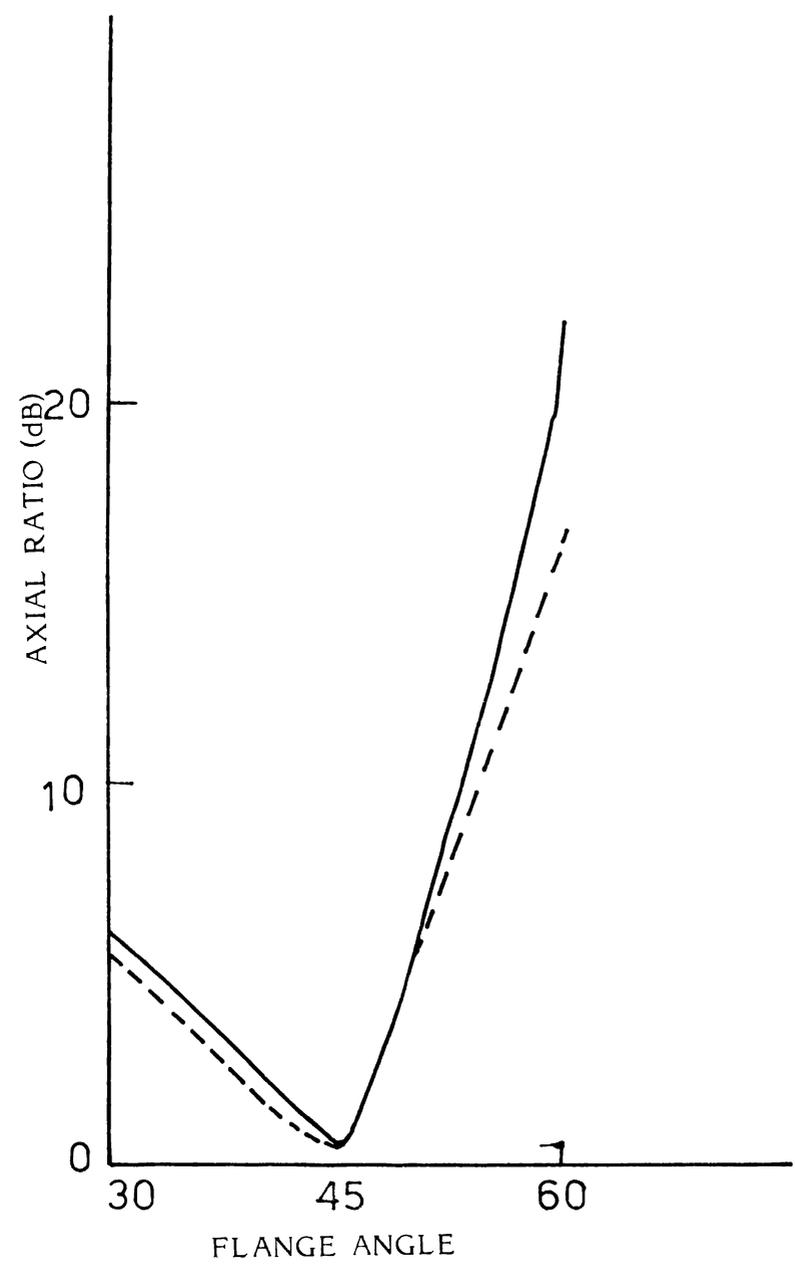
Fig.5.6: Variation of axial ratio with flange angle.
Horn H2,Flange F1,Freq.9.375 GHz,Z=2.5.
——— Theory, ------- Experiment.
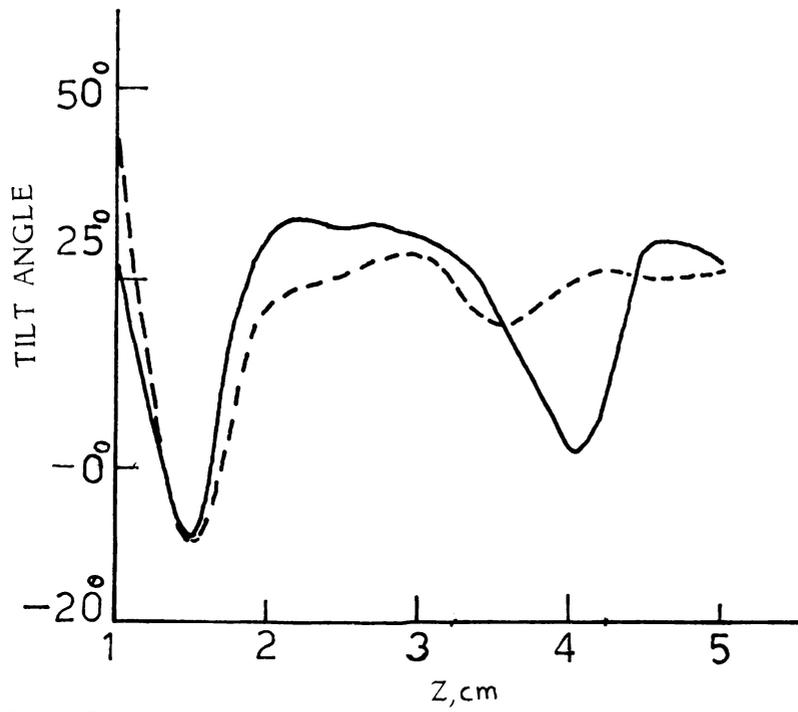
Fig.5.7: Variation of tilt angle of the polarization ellipse with Z.
Horn H2,Flange F1,Freq.9.375 GHz,2B=45,$\alpha$=45.
Theory, ------- Experiment.

CHAPTER : 6

**Conclusions**

Chapter 6

## CONCLUSION

This concluding chapter presents the summary
of the investigations carried out and comments of the
results obtained. The advantages of the present system
over other existing systems are examined in this chapter.
The chapter concludes with the description of the scope
of further work in continuation with the work presented
in this thesis.

6.1      The variations of co-polar and cross-polar
on-axis power density with the position of the flange from
the aperture of the horn for different corrugation tilts
are presented in fig.4(1) and 4(2). From there it is found
that there is a possibility of achieving circular polariza-
tion when the corrugation tilt is 45°.

Variations of on-axis axial ratio with different
flange parameters are shown in figs.4(3) to 4(16). From
these, it may be found that by carefully controlling the
flange parameters, any desired polarization can be synthesized
using the techniques developed in this thesis. It is found

155

that for circular polarization, the optimum corrugation tilt
angle is 45° and the band width of the system is nearly 9 to
10 GHz.

From the variations of axial ratio with azimuth,
it is found that the beam is circularly polarized only along
the axis. From the experiments it is found that when the
tilt of corrugation is 45°, the sense of rotation is right
handed one. But when the corrugation tilt is 135°, it is
polarized in the opposite sense. Again from VSWR measurements
it is found that the matching is improved at the circular
polarization position.

From figs.4(32) - 4(36) it is found that the half
power beam-width is also improved by this technique. At the
'C' position the beam-width is found to be less than the
natural horn. Similarly from figs.4(37) - 4(39), it is clear
that the directive gain is increased from the natural one.

When the corrugation tilt is zero degree, i.e.,
the tips of the corrugation, are orthogonal to the E-vector,
very good improvement in antenna characteristics is obtained
with negligibly small cross-polar component, that is a highly
linearly polarized wave is obtained from the flanged horn.
When the flange is at the optimum 'O' position, a sharp narrow

beam with low sidelobe is obtained. But when the flange is moved to the minimum position (M-position) a split beam with a null along the axis is obtained in the E-plane. So, the radiation characteristic can be conveniently controlled by trimming the flange parameters.

From the experimental investigations, it has been observed that a horn with tilted corrugations are very effective in trimming the antenna characteristics.

Compared to other existing systems, the present system is not a fixed device. Therefore, it is easy to achieve any desired polarization by simply adjusting the flange parameters. Hence, the same system can be used for obtaining a beam with a specific polarization characteristic.

6.2 Sources of errors in the theory

The results of the numerical computation show that there is good agreement with theory and experiment. However, at certain positions of the flange away from the circular polarization position (C-position) there exists some differences between theory and experiments. These are, presumably due to different approximations made in the theoretical calculations. The main sources of errors are the following:

1.      In the theoretical model, the aperture of the horn is treated as a line source.  But in actual case it is not a line source.  Therefore, the radiation from the aperture of the horn is taken into account.

2.      In calculating the distance of corrugation elements from the aperture, an error factor is also present.  Since the corrugations are tilted, the portions of the same element are at different distances away from the aperture.  But in the theory the distances are calculated from the centre of each corrugation element.

3.      In the theoretical model, only two images are taken into account.  But the number of images formed will depend on the flange angle.  This fact is not taken into consideration in the theory.

4.      Thickness of the corrugations is considered to be negligibly small, even though it has a finite value.  However, this theoretical model with the approximations, could explain the position of the flange for circular polarization precisely.

6.3  Suggestion for further work

Topics and problems for further investigation in continuation with the work presented in this thesis are suggested in this section.

A more accurate theoretical model can be developed, taking into account the radiation pattern of the aperture, edge diffraction from the corrugation tips etc.

The polarization can be electronically controlled by placing PIN diodes on dielectric flanges instead of corrugations. A dielectric flange with PIN diodes arranged in the form of a matrix can be employed. By proper excitation of diodes, polarization can be varied.

The flange technique can be adopted in microstrip antenna using parasitic elements close to the patch to control the polarization state.

Another possible direction of work is the use of horns having walls with tilted grooves to develop circularly polarized shaped beams.

The effect of dielectric material in the slots of the flanges can be studied in detail.

Frequency scanning of the radiation pattern can be done by using asymmetric metallic flanges.

The effect of the present system as primary feed on secondary reflectors can be taken as a topic for further

investigations. Various radiation and polarization chara-
cteristics can be modified using this technique.

From the observations it is found that horns fitted
with corrugated flanges provide an effective and simple
directional antenna as feed for fine adjustments of antenna
characteristics. These systems may find wide application in
radar and radio astronomy.

APPENDIX

# APPENDIX - A

## Axially symmetric radiation patterns from flanged sectoral horns

A modified sectoral horn antenna with identical E- and H-plane patterns over the X-band frequency is discussed in this appendix. Axially symmetric radiations from horns are reviewed in chapter 2. From the above review it is evident that such feed systems are important in antenna technology.

It is reported that an H-plane sectoral horn with corrugated flange can have a beam with adjustable characteristics[88]. Hence, axially symmetric radiation can be obtained from sectoral horns by properly trimming the flange parameters. The possibility of axially symmetric radiation patterns from sectoral horn is explored here. The effect of corrugated flanges on E-plane sectoral horn has not been reported in literature. This factor is also taken into account for the present investigation. The work presented in this appendix is the effect of plane and corrugated metallic flanges on both H- and E-plane sectoral horns.

161

A.1  Experimental set up

Geometry of the flanged H-plane sectoral horn
is shown in fig.A.1(a) and A.1(b).  The flanges are mounted
with their corrugation edges orthogonal to the E-vector.
The width of the flange is greater than the wavelength used,
and nearly equal to $3\lambda$ , where $\lambda$ is the free space wavelength.
The height h of the corrugation is of the order of $\lambda/4 < h < \lambda/2$,
to prevent surface waves.  The slot walls are vanishingly
thin compared to the slot width.  The parameters of different
flanges used in this studies are shown in table A.1.  Experi-
mental arrangement for plotting radiation pattern, VSWR etc.
are same as described in chapter 3.


A.2  Experimental results

This section is split into two parts.  The first
part deals with the effect of flanges on H-plane sectoral horns,
while the second part is the study on E-plane sectoral horns.


A.2.1  H-plane sectoral horns


A.2.1(a)  Variation of on-axis power density and VSWR with
          the position of the flange from the aperture of
          H-plane sectoral horns

Typical variation of on-axis power density and
VSWR of the flanged H-plane sectoral horn with the position

163
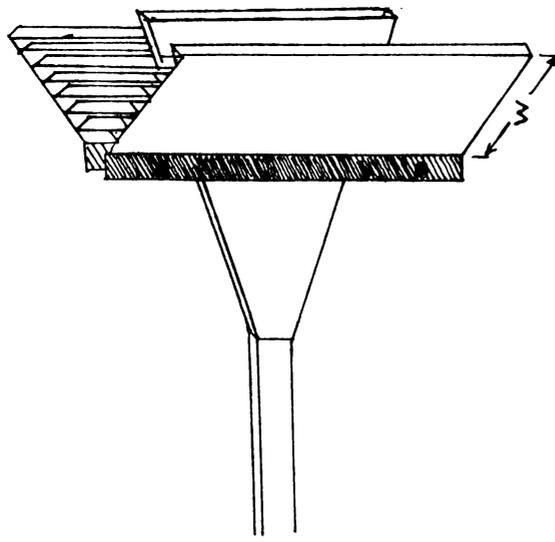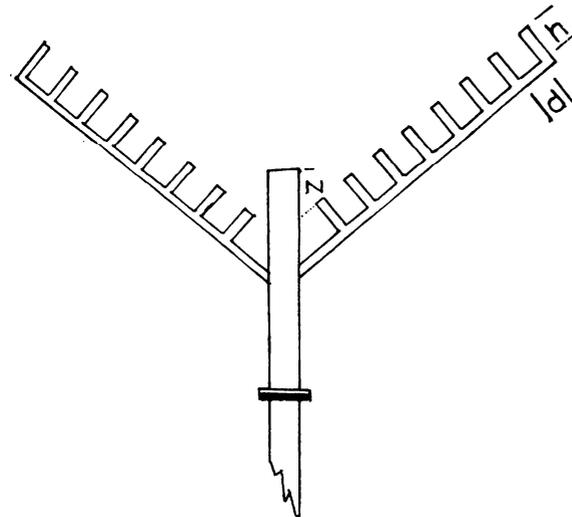


a) E - PLANE VIEW

b) H - PLANE VIEW

Fig.A.1: Geometry of the flanged H-plane sectoral horn. w= width of the flange, d= corrugation width, h= corrugation depth, Z= flange position from the aperture.

Table A.1

Parameters of different
corrugated flanges used

--------------------------------------------------------

| Flange<br>Number | Number of<br>corrugations<br>(n) | Corrugation<br>width (d) |
|---|---|---|
| 1 | 0 (Plane) | -- |
| 2 | 6 | 1.66 |
| 3 | 8 | 1.25 |
| 4 | 11 | 0.90 |
| 5 | 14 | 0.714 |
| 6 | 19 | 0.526 |

--------------------------------------------------------

of the flange from the aperture is shown in fig.A.2. It is observed that depending upon the position of the flange the on-axis power density fluctuates from a maximum to minimum. The position of the flange (Z) corresponding to the maximum on-axis power density is called optimum position (O-position). The minimum on-axis power density position of the flange is called the minimum position (M-position)[75]. The E-plane radiation pattern at the 'O' position is found to be sharp with low sidelobes. But at the 'M' position a split beam with null along the on-axis is obtained. From the VSWR data it is found that at 'O' position the matching is improved. Similarly at the 'M' position the VSWR is found to be large. From the experiments it is found that the radiation is axially symmetric at the second 'O' position. Again at this position the VSWR is found to be less than the natural horn (i.e. horn without any flanges), with enhanced on-axis power. These results are true with different horns and flanges.

A.2.1(b)  Radiation pattern

The radiation patterns of corrugated flanged H-plane sectoral horn at the $O_2$ position of the flanges are shown in fig.A.3. The natural H and E-plane radiation pattern of the horn is also shown in fig.A.4. From the observations it is found that the pattern is axially symmetric only at

the second 'O' position (O-position). The radiation patterns
of the horn without flanges are also shown for comparison.
It is believed that a corrugated flange with corrugation
edges perpendicular to the E-vector will not modify the
H-plane radiation pattern. But from the experiments it is
found that flanges can modify the H-plane radiation pattern.
The natural half power beam width (HPBW) in E- and H-plane
respectively are 91.56° and 28.09°. But with flanges at the
$O_2$ position it is 20.19° each.

A.2.1(c)  Half power beam width (HPBW)

Typical variation of HPBW in both planes with
corrugation period is shown in fig.A.5. It is evident from
the figure that the two beam widths are nearly equal for a
critical region. This region is called the optimum periodicity
region. From the figure the optimum periodicity is $\lambda/8$ to $\lambda/4$.

Variation of HPBW with flange angle is shown in
fig.A.6. Here the flange angle is varied at the $O_2$ position.
From the curve it is evident that symmetric radiation is possible
for a particular flange angle. It is found from the experiments
at other flange angles the $O_2$ positions are changed.
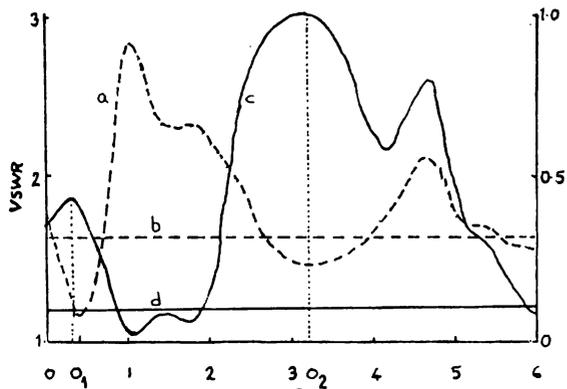
Fig.A.2:Variation of $^Z$VSWR andP with
Z.Freq.9.5 GHz,2$\beta$= 60, N= 9.

a) VSWR, b) on axis power,
c) Natural VSWR, Natural P.
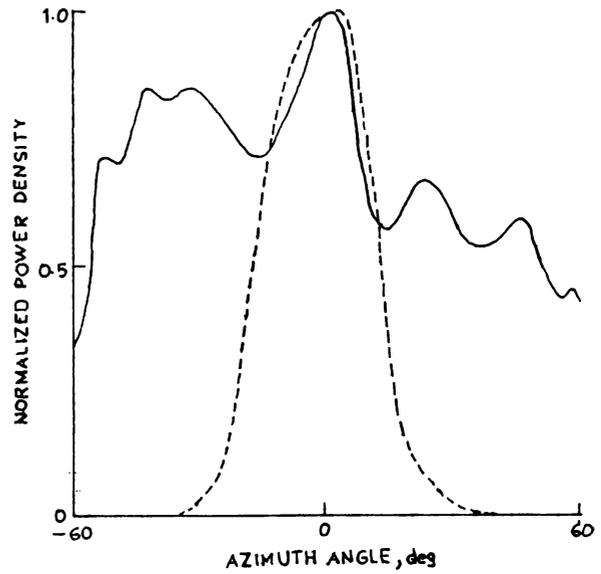
Fig.A.4: Natural radiation pattern of the H-plane
sectoral horn at 9.5 GHz.
....... H-plane, ——— E-plane.
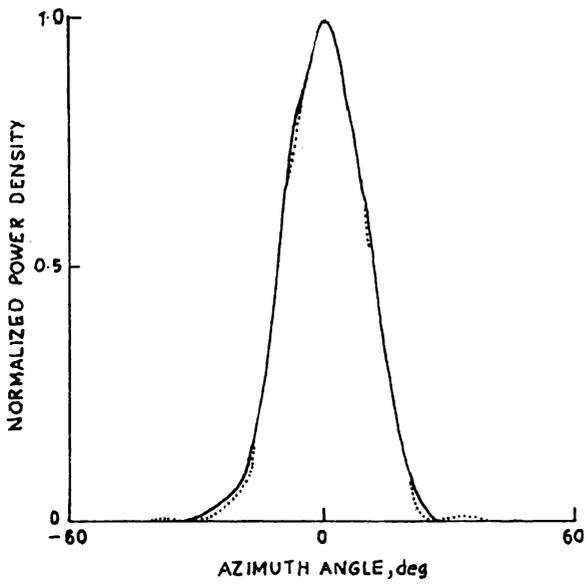
Fig.A.3: Typical radiation pattern at the
second optimum position.
..... H-plane,——— E-plane.
Freq.9.5 GHz,2$\beta$= 60,N= 9. Z=3·2
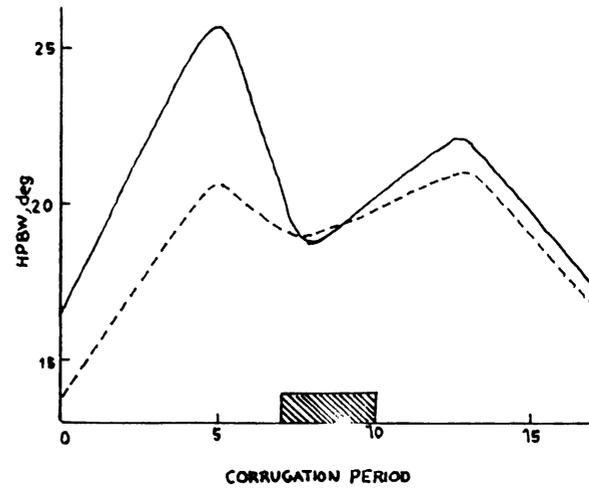
Fig.A.5: Variation of HPBW with N.
Freq. 9.5 GHz, 2$\beta$= 60, Z=3·2
....... H-plane, ——— E-plane
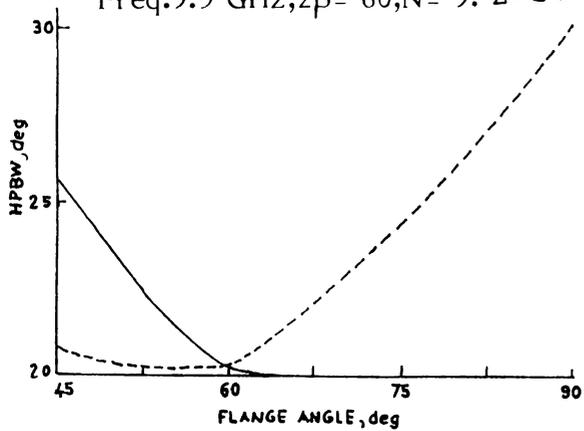
Fig.A.6: Variation of HPBW with 2B.
....... H-plane ——— E-plane.
Freq.9.5 GHz, N= 9, Z=3·2
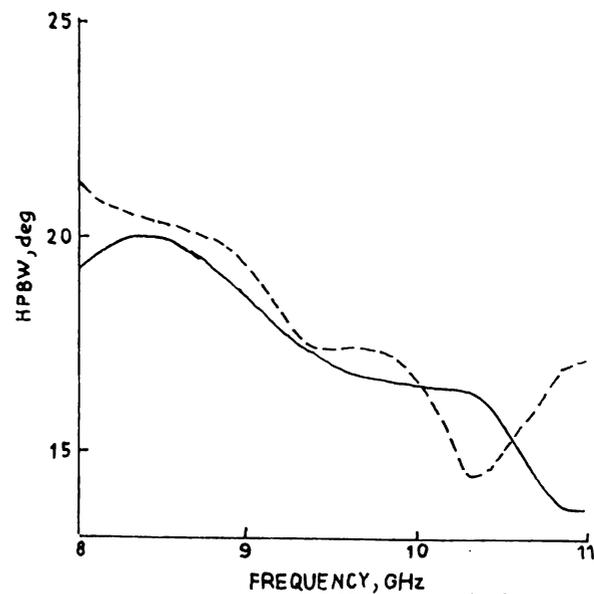
Fif.A.7: Variation of HPBW with frequency.
2$\beta$=60, N= 9,..... H-plane,——E=plane.

Dependence of HPBW in both planes with frequency
is shown in fig.A.7. It is found that the beam-widths in
both planes go together in the X-band frequency.

Antenna gain is calculated from the radiation
patterns by numerical integration method. The variation of
directive gain of the antenna with number of corrugation is
shown in fig.A.8. Natural E-plane gain of the horn is
shown as a straight line at the bottom. Natural H-plane
gain of the horn is also shown as a straight line at the
top of the figure. Variation of antenna gain with frequency
is shown in fig.A.9. It is found that the H-plane and E-plane gain
go together within the X-band.

Modification of the H-plane radiation pattern
can be explained as follows. The tips of the corrugations
act as an array of linear parasitic antennas. At a point in
H-plane the contributions from the aperture of the horn and
this array are considered. This effectively modifies the
H-plane radiation pattern. The variation of on-axis power
density with flange position can also be explained from the
above concept. The distance between the aperture of the horn
and the effective array is varied as we move the flange from
the aperture. Depending upon the distance between the
aperture and the effective array, we can obtain a sharp beam
or split beam.
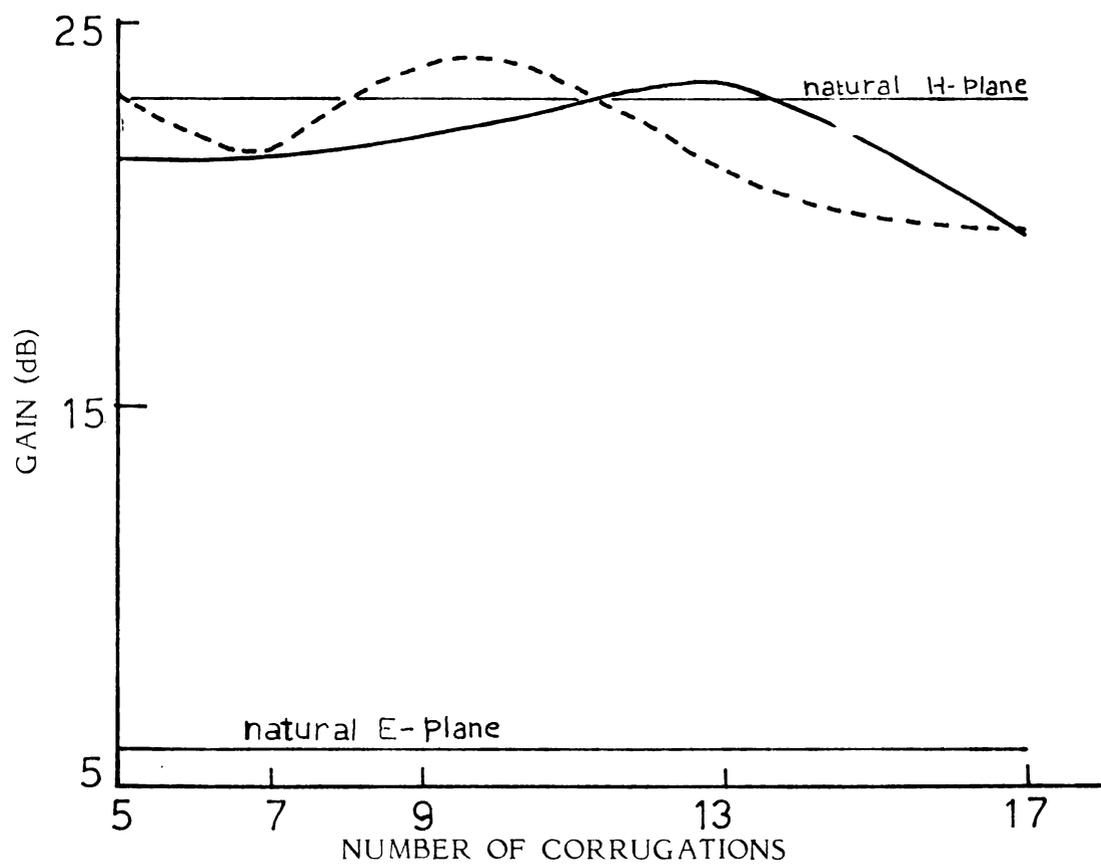
Fig.A.8: Variation of gain with number of corrugatioa.s
Frequency 9.5 GHz,$2\beta$=60,Z= 3·2
-------- H-plane, ———— E-plane.
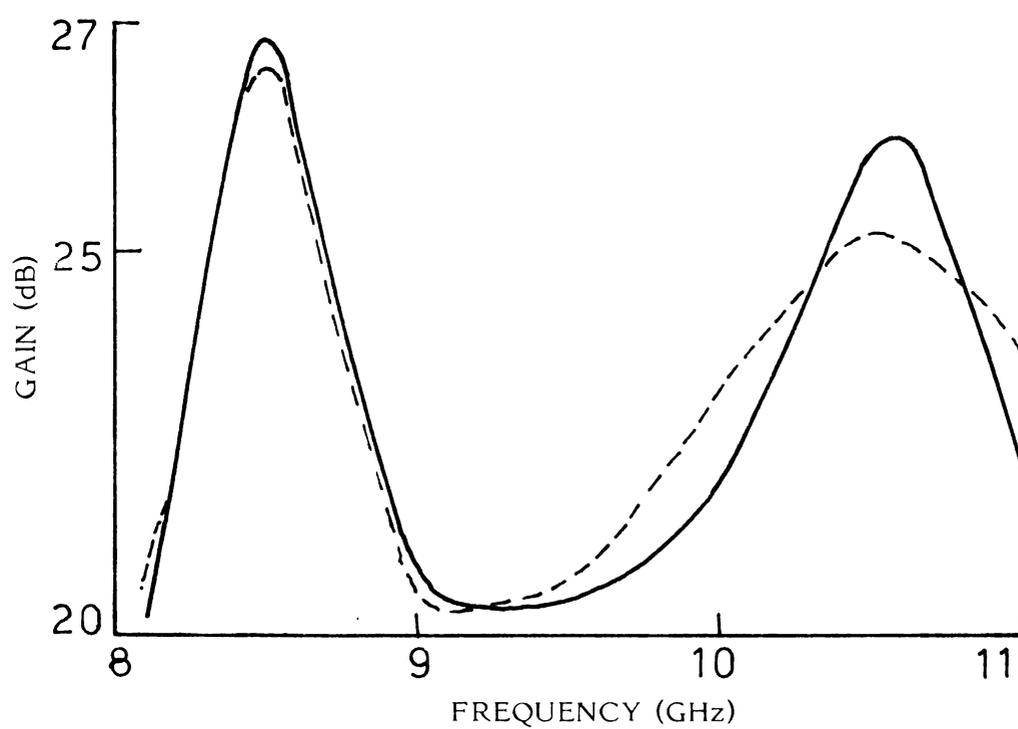


Fig.A.9: Variation of gain with frequency. $2\beta$=60, N= 9, Z= 3·2
------------- H-plane ———— E-plane.

A.3.1  E-plane sectoral horns

A.3.1(a)  On-axis power density and VSWR with the position
of the flange (Z)

The variation of on-axis power density with
position of the flange from the aperture of the horn is
shown in fig.A.10.  As Z is increased gradually the on-axis
power density $P_o$ raises to a maximum value and then falls
steadily.  It is found from the experiments that maximum
on-axis power density is obtained only when the flange is
nearer the aperture of the horn.  The on-axis power density
is increased to 19.22 dB from the natural horn.  From the
VSWR measurements it is found that the position of the
flange is not considerably effecting the matching conditions.

A.3.1(b)  Variation of on-axis power density with the
period of corrugation

For a particular flange angle and position the
on-axis power density varies with the period of corrugation.
It is observed that on-axis power density fluctuates from a
maximum to minimum.  Minimum on-axis power density is obtained
for a particular corrugation period.  This typical variation
is presented in fig.A.11.
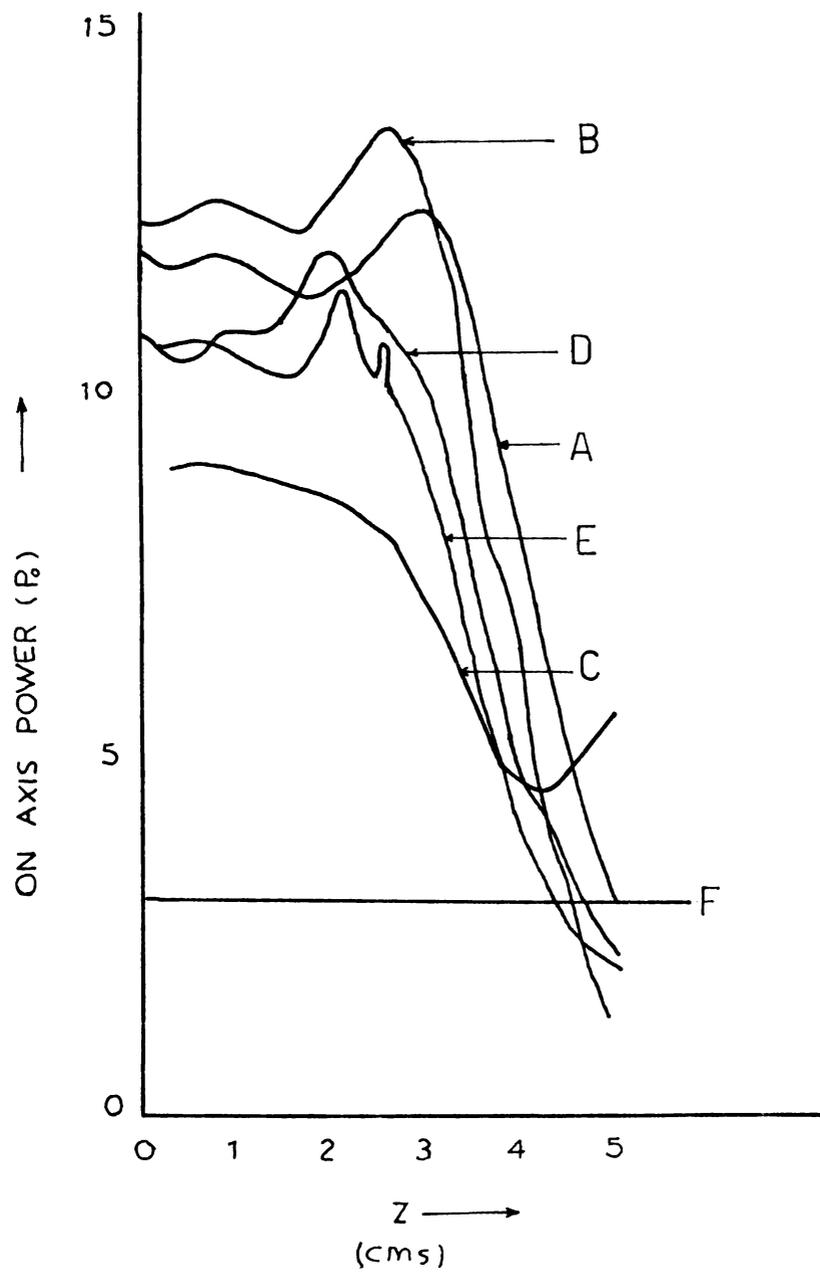
Fig.A.10: Variation of on-axis power density with Z.
Horn E1,2β=60, for corrugation numbers A= 19
B=14, C=11, D=8, E=6 and F=natural.

Fig.a.12: Variation of on-axis power desity with 2β.
Curves a,b,c,d and e are for N=0,6,8,11 and
14 respectively.
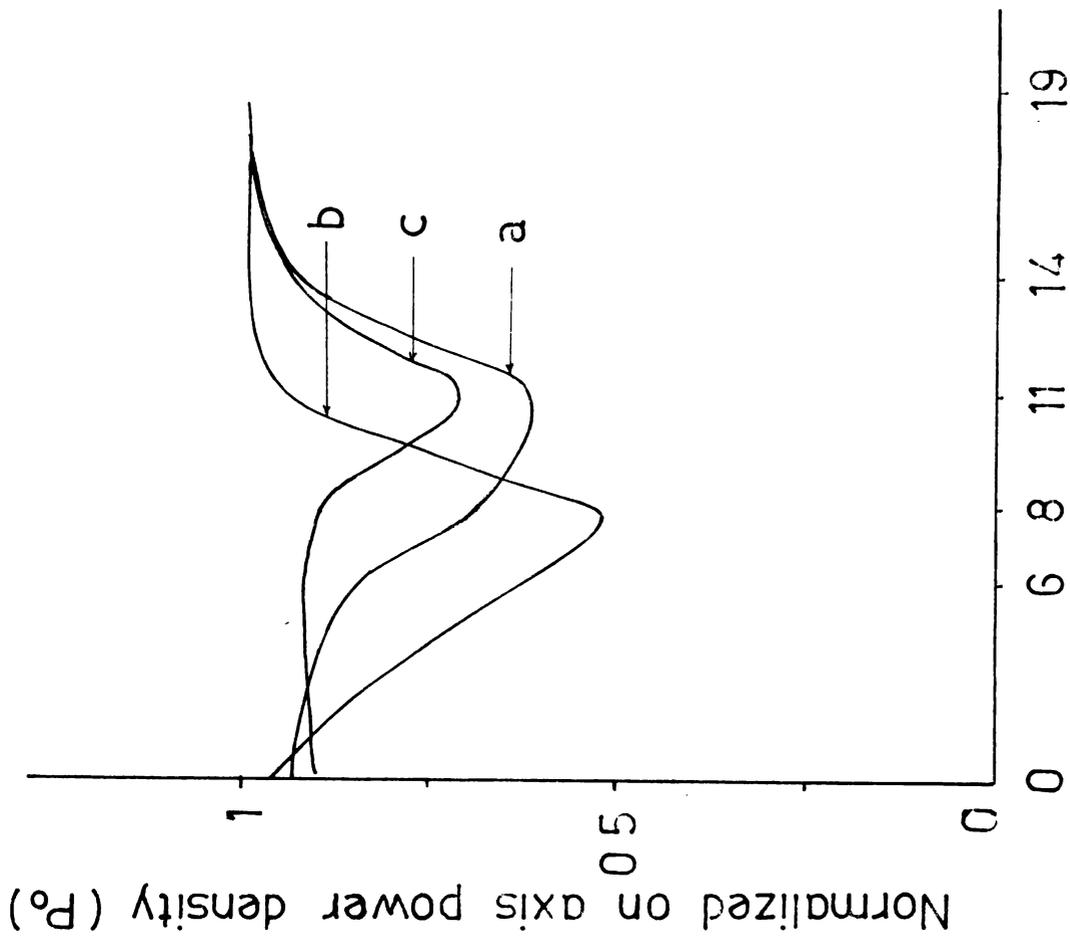


Fig.A.11: Variation of on-axis power density with N.
Curves A,B,C are for 2B=30,45and 60,respectively.

A.3.1(c)  Variation of on-axis power density with flange
          angle

On-axis power density is also found to be strongly
influenced by the flange angle.  A typical such variation is
shown in fig.A.12.  Optimum flange angle is found to be a
constant only for a particular flange and corrugation period.


A.4  Radiation pattern

It is found that at the 'O' position the beam
is found to be sharp.  At the minimum position a broad beam
in the H-plane is obtained.  From the experiments it is clear
that corrugated flanges are effective tool  in controlling
the H-plane radiation pattern of the E-plane sectoral horns.
At the first optimum position the pattern is found to be
axially symmetric.  This is demonstrated in the fig.A.13.
Natural radiation pattern of the horn is also shown for
comparison.  In this typical case the natural HPBWs in H and
E-plane respectively are 74.37° and 21.79°.  But with flanges
at the optimum position it is changed to 22.26°.  Thus we can
produce almost identical pattern  both in E- and H-plane with
increased antenna gain.
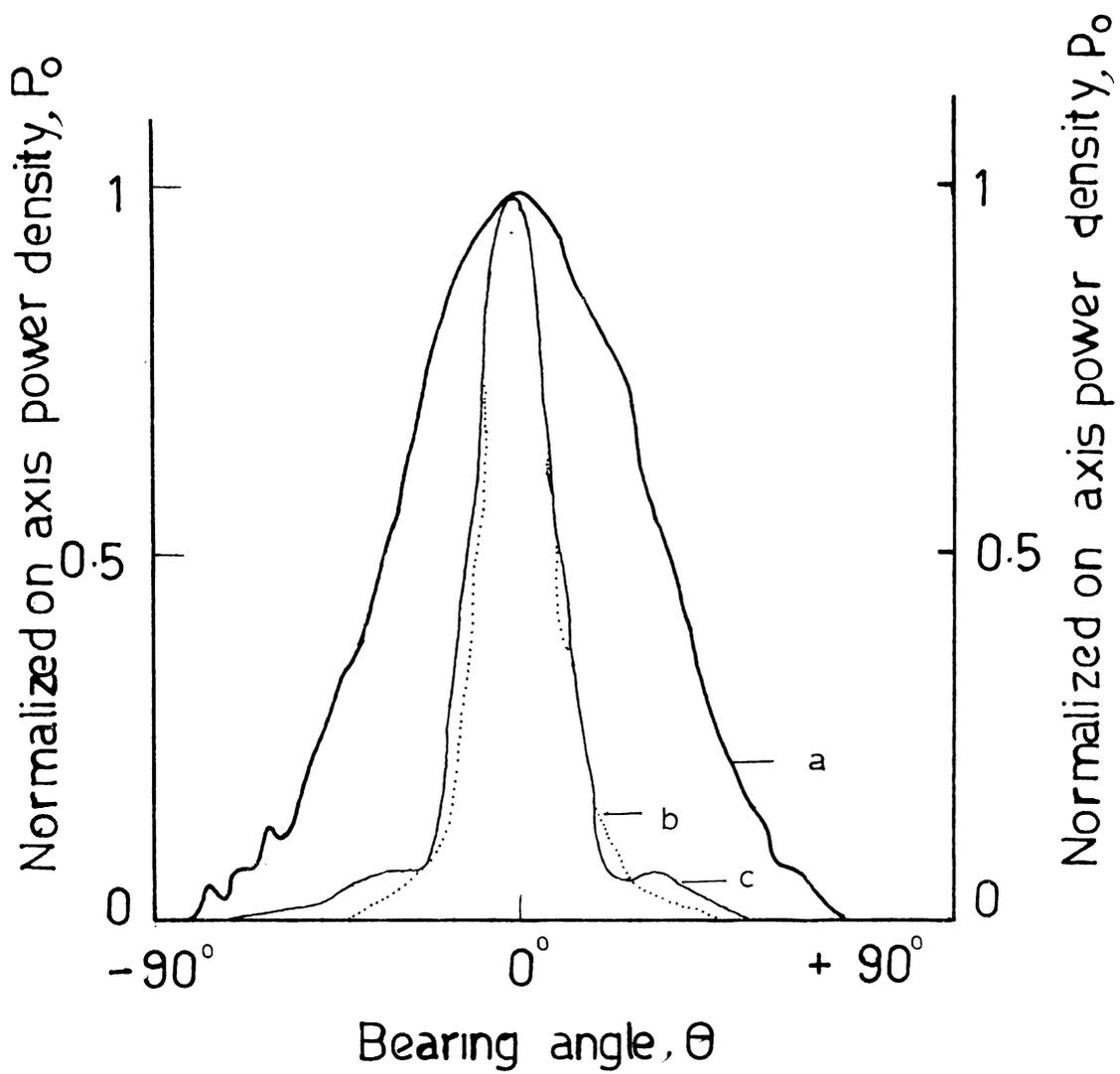
Fig.A.13: Typical radiation patterns.  a) Natural H-plane pattern
b) Modified E-plane pattern, c) Natural E-plane pattern.

## A.5  Conclusion

It is established from the above investigations that conducting corrugated flanges satisfying certain critical conditions will give axially symmetric radiation pattern from H-plane sectoral horns.  Compared to fixed compound horns with grooved walls, the present system offers great convenience in adjusting antenna characteristics by trimming flange parameters.  The present system may find practical application in illuminating symmetric antennas like paraboloids.

# APPENDIX - B

## Feed horn with corrugated flanges for parabolic reflectors

A frequently employed antenna in communication, radar and space application is the paraboloidal reflector. For illuminating this secondary reflector, an electromagnetic horn radiator is generally employed. But these feed systems are far from ideal, because its principal E- and H-plane radiation patterns are quite different. Moreover there will be mismatch due to over-coupling between the primary and the secondary. Many of the papers of great interest in reflector antennas are collectively found in "Reflector antennas" edited by A.W.Love[122]. Nair and Mathew[123] have reported that plane flanged H-plane sectoral horn can effectively modify the radiation pattern of parabolic reflectors. But due to the aperture blocking the gain is not very high. To overcome this difficulty an offset paraboloid is used. This appendix deals with the effect of plane and corrugated flanged H-plane sectoral horn as a primary feed, on the impedance conditions and radiation patterns.

A paraboloidal reflector with a flanged feed horn suffers from the defect of aperture blocking. To eliminate

176

this, an offset paraboloidal reflector is used in this study.
The geometry of the present system is shown in fig.B.1. The
offset paraboloidal has a focal length of 1 m and F/D ratio
0.5 where D is the aperture diameter of the actual paraboloid
of which the offset is a part. The offset angle subtended by
the flanged horn at the centre of the aperture is 60°($\beta$).
The dimensions of the aperture in the horizontal and vertical
planes are nearly 1 m each. A flanged horn is mounted in
front of the reflector so that the aperture of the horn is
in the focal plane of the reflector.

Experimental results

The variation of on-axis power density and reflection
coefficient with the position of the flange from the aperture
of the horn is shown in fig.B.2. On-axis power density and
reflection coefficient are highly influenced by the position
of the flange from the aperture. When the reflection coe-
fficient is minimum the on-axis power density is maximum and
vice-versa. Again VSWR is minimum at the second optimum
position where the primary radiation pattern is found to be
axially symmetric. Variation of reflection coefficient and
on-axis power density from the natural one for different
flange parameters is shown in table B.(1). From the experi-
mental results it is found that corrugated flanges are more
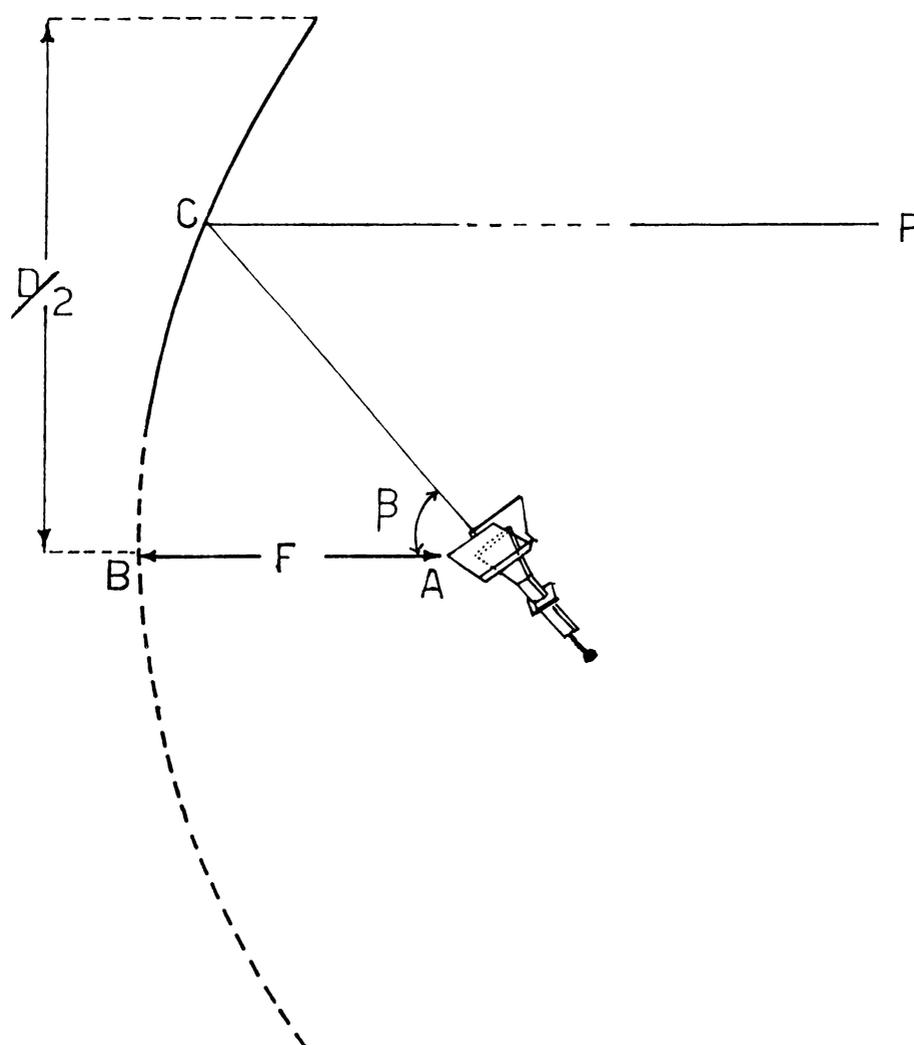
Fig.B.1: Geometry of the offset paraboloid fitted withflanged feed horn.
A is the focus,B is the vertex of the actual paraboloid and c is
the centre of the aperture of the offset paraboloid.
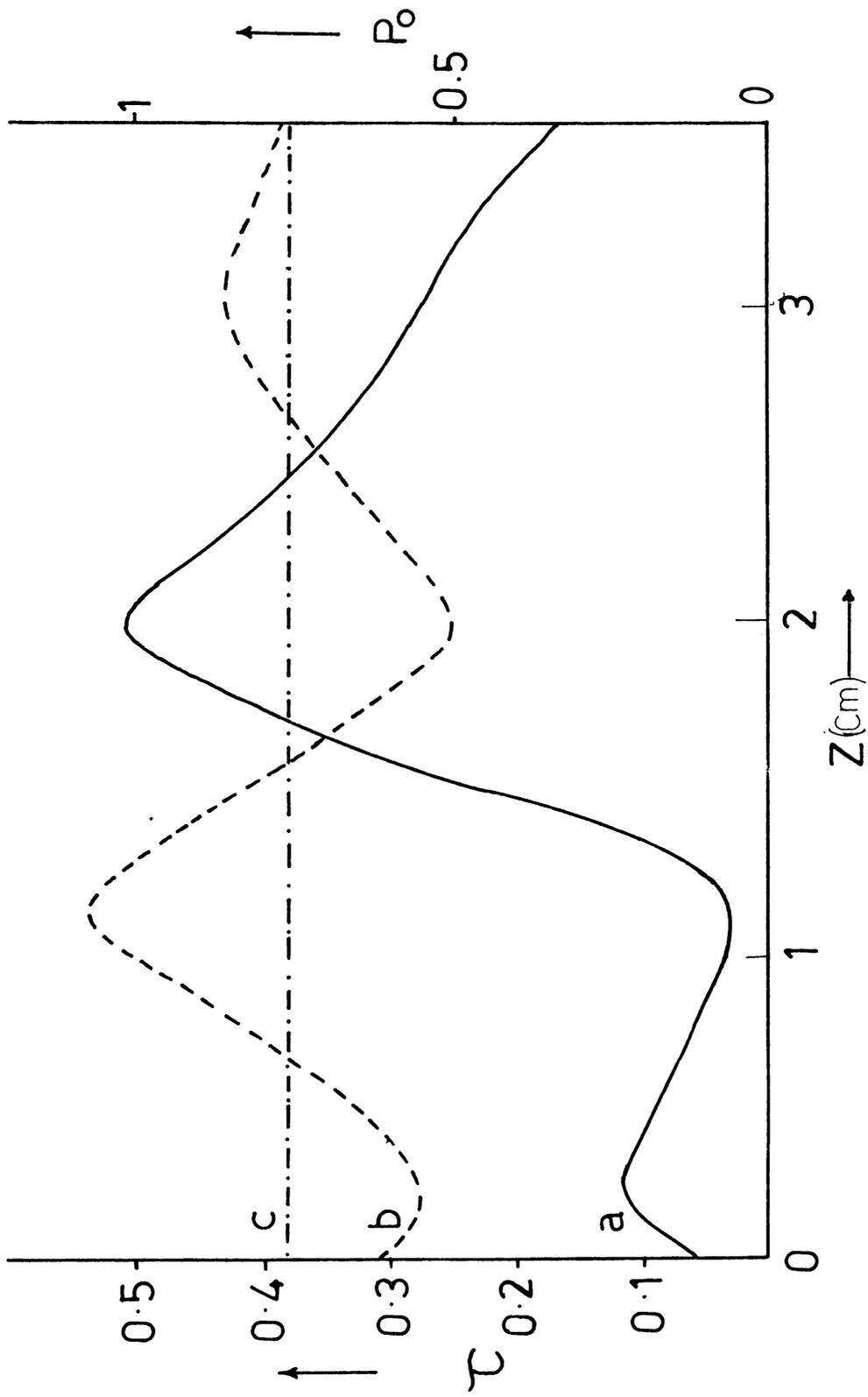
Fig.B.2: Variation of on-axis power density and reflection coefficient with Z; N=6,2$\beta$=45.
— — — — Voltage reflection coeff. –·–·–·– natural ref.coeff. ———— on-axis power density.

Table B(1)  Variation of $\tau$ and $P_o$ from the normal when
the flange is at the optimum position for
different corrugation periods

| No.of corruga-tions | Variation from the normal in dB at 45° position | | Variation from the normal in dB at 60° position | | Variation from the normal in dB at 90° position | |
|---|---|---|---|---|---|---|
| | $\tau$ | $P_o$ | $\tau$ | $P_o$ | $\tau$ | $P_o$ |
| n=0 (plane) | -4.25 | 4.47 | -3.04 | -1.59 | -2.2 | -1.59 |
| 6 | -4.1 | -1.13 | -4.9 | 9.3 | -1.4 | 9.05 |
| 8 | -0.93 | 5.3 | -1.57 | 11.46 | -1.15 | 4.47 |
| 11 | -3.5 | 6.95 | -4.01 | 6.9 | -1.28 | 6.12 |
| 14 | -2.62 | 5.6 | -1.89 | 6.2 | -2.57 | 9.9 |
| 19 | -4.82 | 6.3 | -1.42 | 7.7 | -1.24 | 8.06 |

superior in controlling the on-axis power density and VSWR. Typical
radiation pattern  of the offset paraboloid at the optimum position
is shown in fig.B.3.  Again it is found that the radiation chara-
cteristics are improved by the flange systems.  The sidelobe level
is found to be decreased with increased power gain.  Variation of
gain with number of corrugation is shown in fig.B.4.  The variation
of antenna gain with frequency is shown in fig.B.5.  From these
observations it is found that the antenna characteristics are nearly
independent of frequency in 8.5 to 10.5 GHz band.
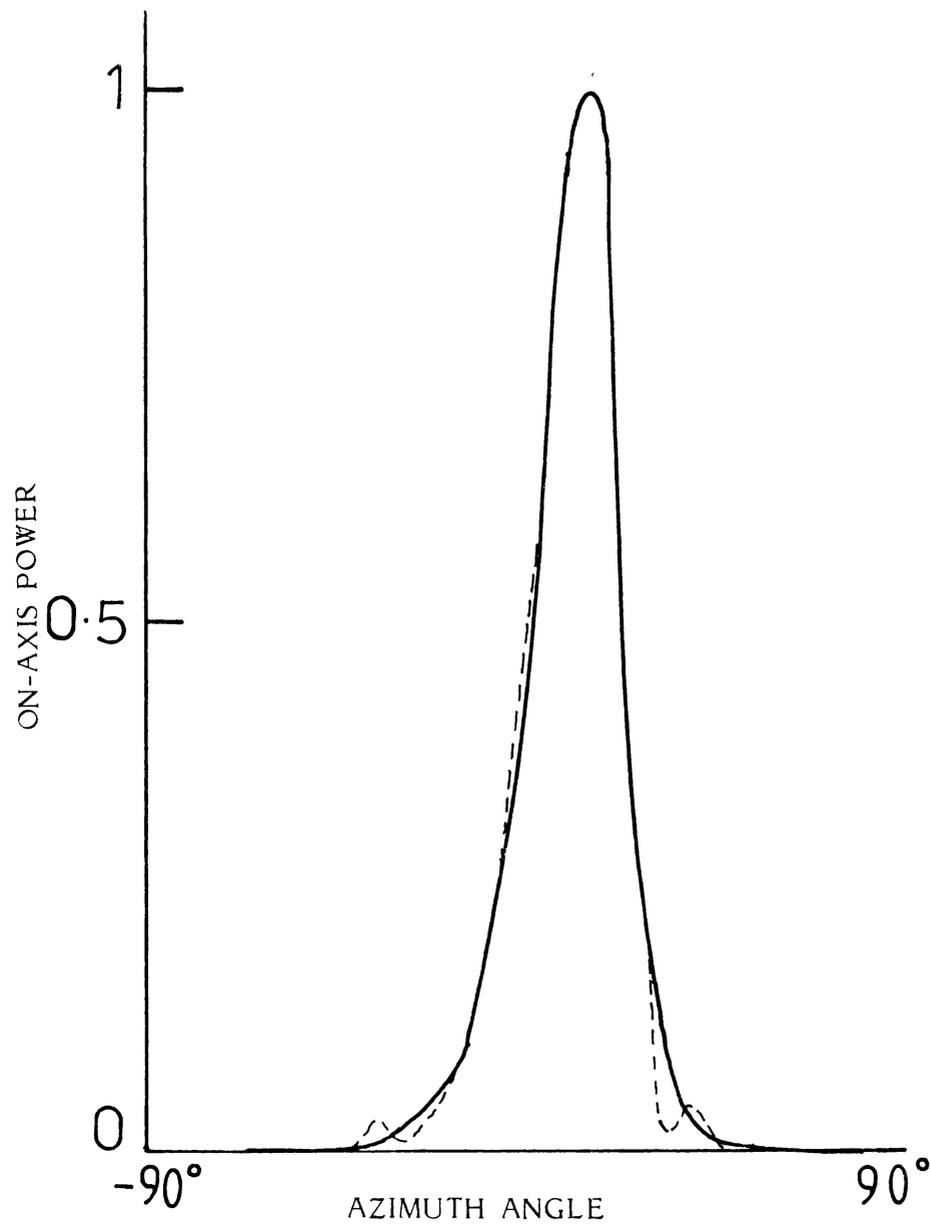
Fig.B.3: Typical radiation patterns of offset paraboloid.
———— H-plane, ·········· E-plane.

Horn H₃ , N = 19 , 2β = 45° , Freq = 10 GHz ·
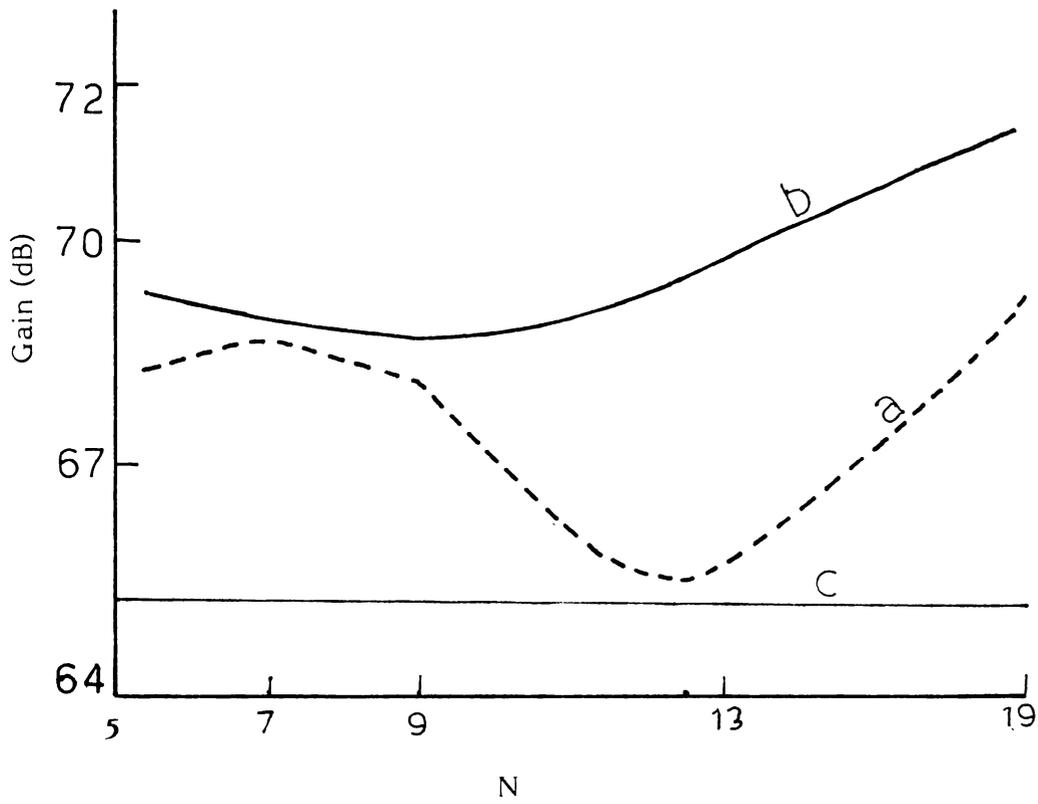
Fig.B.4: Variation of gain with N.Horn H , Freq. GHz,
a) $2\beta=45$ and $Z=3.2$ b) $2\beta=60$ and $Z=4$ c) Natural gain.
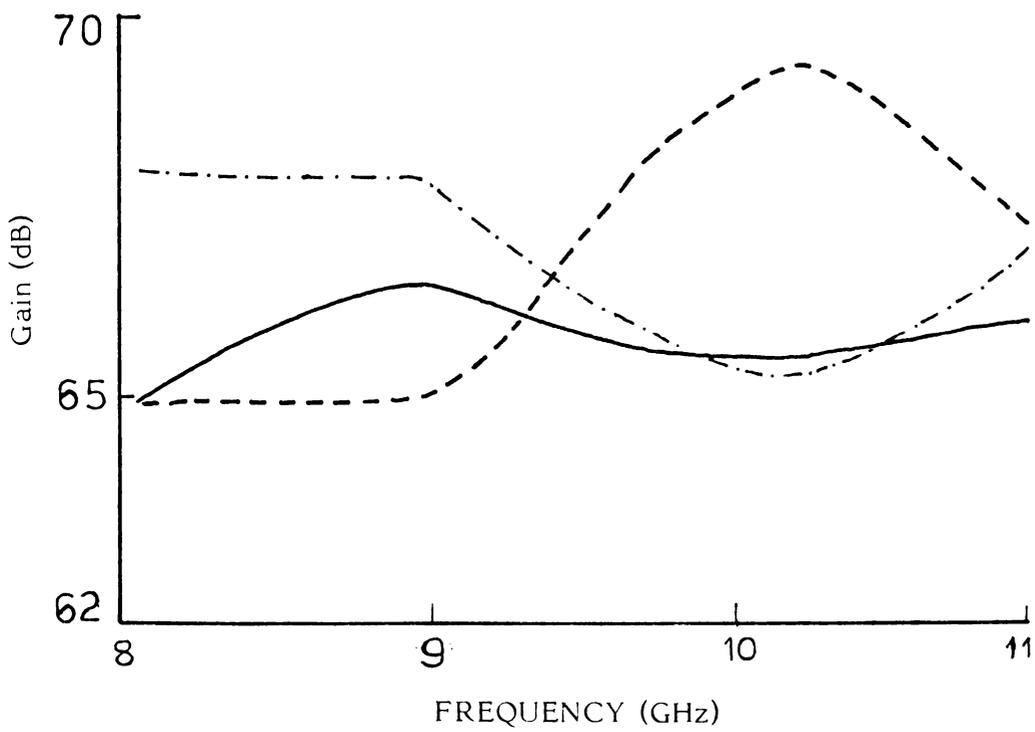


Fig.B.5: Variation of antenna gain with frequency. $2\beta = 30, Z = 2.2$
— — — N = 6 , — · — · — N = 14 , ———— N = 0

## Conclusion

The primary experimental results reveal that flanges having corrugation width of the order $\lambda/2$ are nearly ideal. Thus the corrugated flanges as feed horn may act as "antenna trimmers" for the final adjustment of different parameters. These systems may find great application in radar and satellite communication.

## APPENDIX - C

## Phase modulation of microwave signals using point-contact
## Germanium signal diodes

An electronic microwave phase shifter using a forward biased point-contact germanium signal diode is presented in this appendix. The usefulness of the above arrangement as a phase-modulator for microwave carrier is also demonstrated.

Point contact microwave detector diodes are commonly used as waveguide switches[124,125]. But the action of point-contact small signal diode as phase shifter of microwave signal is not mentioned in literature. This work briefly describes the action of a forward biased point-contact diode as an electronic phase shifter. The diode employed here is a point-contact Germanium signal diode like OA79, OA81 etc. The diode is shunted across the X-band waveguide section along the E-vector. Terminals are given with proper insulation for applying biasing voltage cacross the diode. The phase variation is monitored by a Network Analyser (HP 8410C). The block diagram of the experimental arrangement is shown in fig.C.1.

From the experiment it is found that when a DC voltage is applied across the diode, the phase is changed. This variation

184
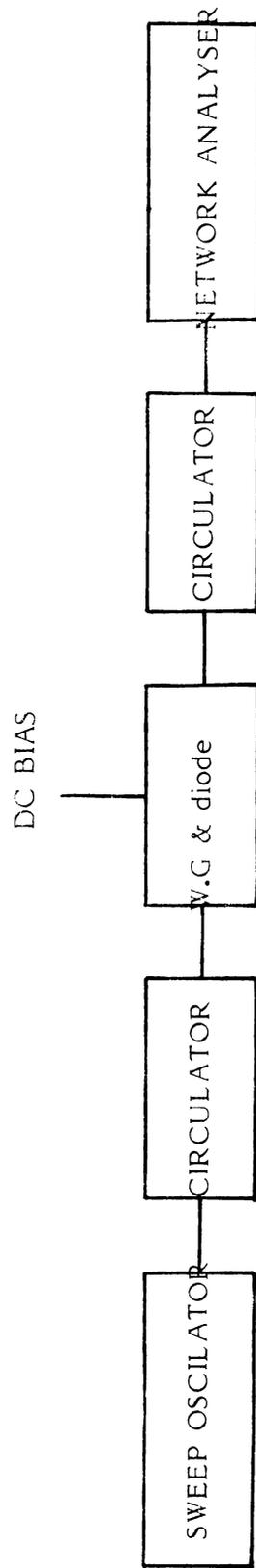
Fig.C.1: Block diagram of the experimental arrangement for measuring the phase change with forward current through the diode.

of phase with forward current is shown in fig.C.2. It is
again noted that the phase shift can be increased by periodi-
cally loading the waveguide with diodes. The maximum phase
shift occurs for anti-resonant spacing and minimum for
resonant spacing.

The maximum insertion loss of the system is found
to be less than 1 dB. With a single diode, the phase shift
is as much as 80° for a current of 12 mA. The arrangement
can be used as a continuously variable electronic phase shifter
in UHF and microwave lines.

Unlike a p-n junction diode[126] point contact diode
is found to produce virtually no phase change in the reverse
bias condition. It is found to be active as a phase shifter
only when a forward voltage is given. Compared to PIN diodes,
point contact diodes are simpler, inexpensive and more readily
available.

The usefulness of this set up as a phase modulator
of microwave is also investigated. Modulating signal is applied
directly across the diode and the modulated microwave signal
is transmitted by a pyramidal horn. It is received by another
horn in the far field and is detected by the network analyser.
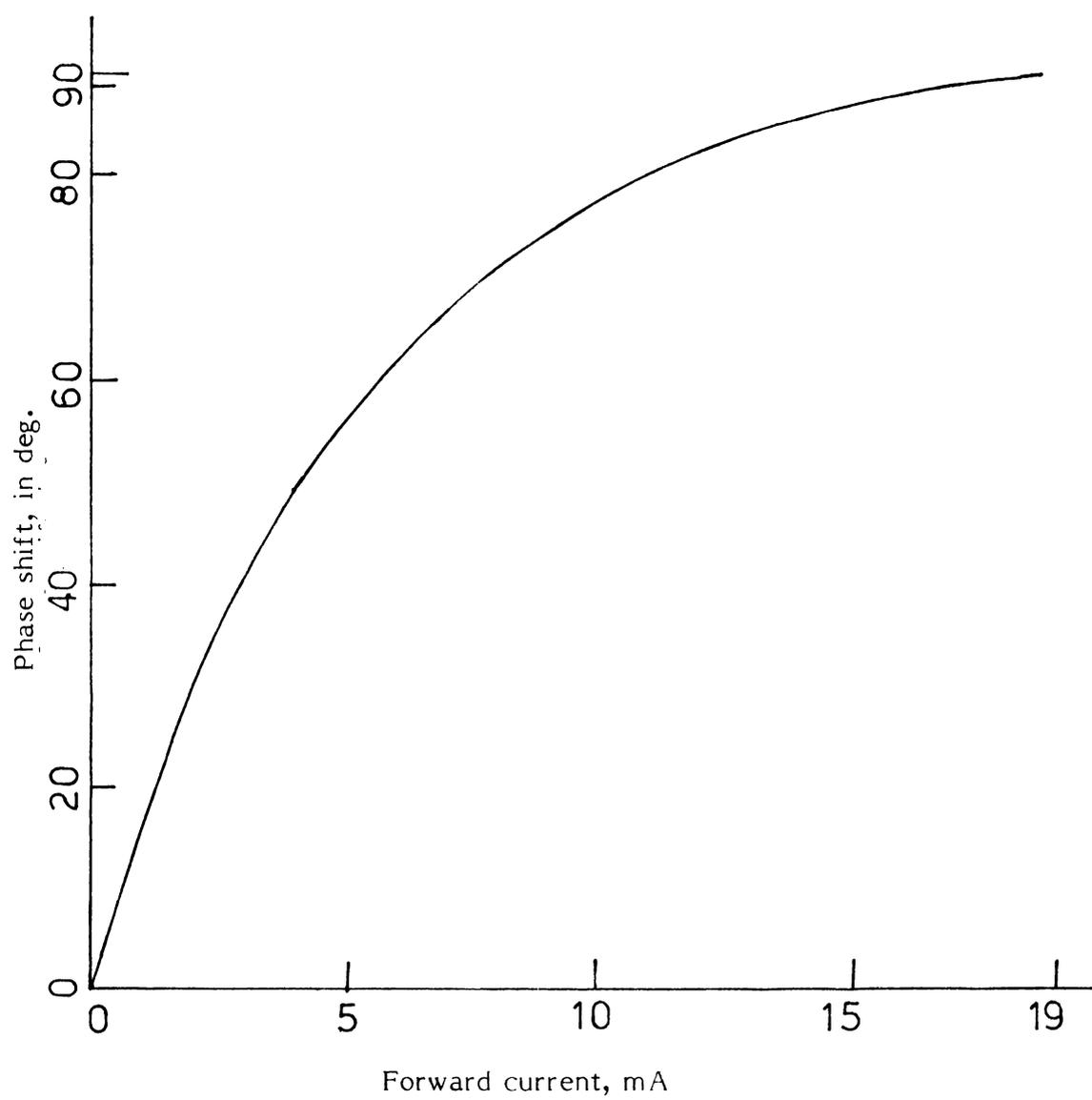
Fig.C.2: Variation of phase with forward current. Diode used is OA-79.

The experimental results are shown in fig.C.3(a) and (b) for

10 KHz sine and square waves. Modulating signals are also

given for comparison in the above figure. It is found from

the photograph that the diode operate well upto 10 KHz. But

due to the limitation  of the band-width of the network analyser,

modulation effects at higher frequencies could not be studied

directly. It is found that phase modulation is accompanied

by small amplitude modulation which is detected by microwave

diode. Since diode is found to be active as an amplitude

modulator even at video ranges it is reasonable to assume

that phase modulation also occurs at these ranges.

The variation of phase with forward bias can be

qualitatively explained as follows. Since the capacitance

of metal semiconductor contact which essentially forms a

Schottky barrier layer, increases with forward bias[127], the

equivalent susceptence also increases with bias current, thus

increasing the resultant phase variation.

In conclusion, a point contact diode can be used as

an effective, simple and low cost phase modulator. However,

its use is not restricted to microwave frequencies alone. The

arrangement described here may find extensive practical uses

in communication, antenna applications like electronic scanning

in phase array radar etc.
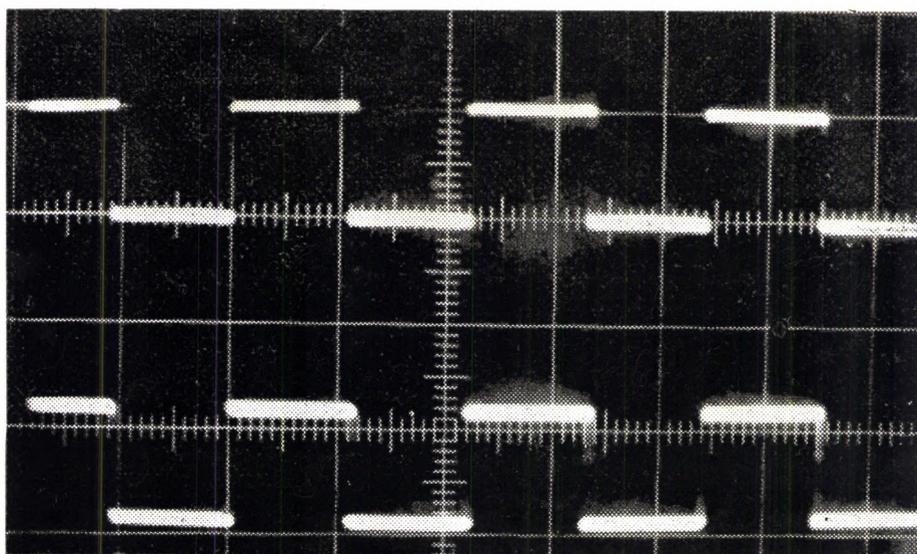
Fig C.3 (a) Upper trace: Phase demodulated 10 KHz square wave.
Lower trace : Corresponding modulating signal.
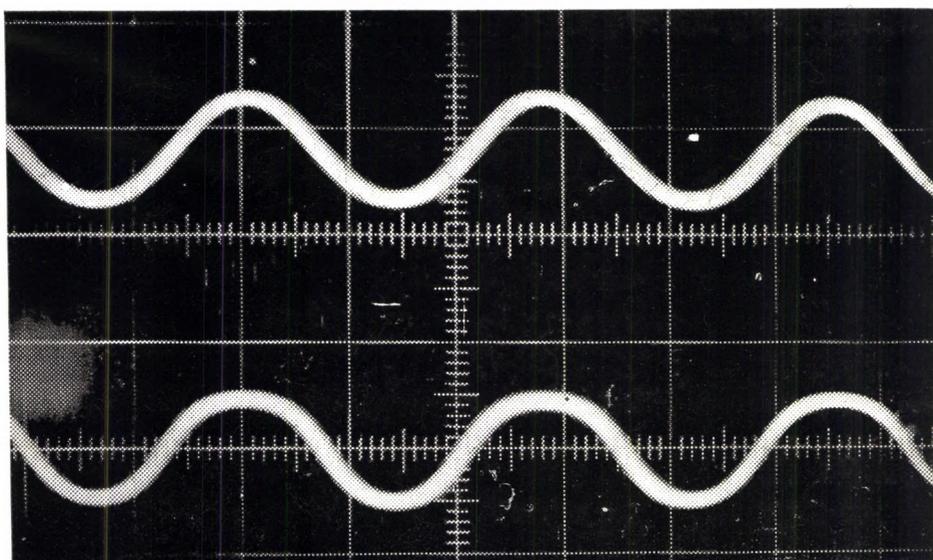


Fig C.3 (b) Upper trace : Phase demodulated 10 KHz sine wave.
Lower trace : Corresponding modulating signal·

REFERENCES

1. J.F.Ramsay, "Microwave antenna and waveguide technique before 1900", Proc.IRE Vol.46, pp.405-415, Feb. 1958.

2. G.C.Southworth, "Hyper-frequency waveguides - General considerations and experimental results", Bell.Syst.Tech. J.Vol.15, pp.284-309, April 1936.

3. W.L.Barrow, "Transmission of electromagnetic waves in hollow tubes of metal", Proc.IRE, Vol.24, pp.1298-1328, Oct. 1936.

4. W.L.Barrow and F.M.Greene, "Rectangular hollow pipe radiators", Proc. IRE, Vol.26, pp.1948-1519, Dec. 1938.

5. W.L.Barrow and L.J.Chu, "Theory of electromagnetic horn", Proc. IRE, Vol.27, pp.51-64, Jan. 1939.

6. G.C.Southworth and A.P.King, "Metal horns as directive receivers of ultra short waves", Proc. IRE Vol.27, pp.95-102, Feb. 1939.

7. L.J.Chu and W.L.Barrow, "Electromagnetic horn design", Trans. AIEE, Vol.58, pp.333-338, July 1939.

8. L.J.Chu, "Calculation of the radiation properties of pipes and horns," J.Appl.Phys., Vol.II, pp.603-610, Sept. 1940.

190

9. C.S.Pao, "Shaping of primary patterns of horn feeds", Radiation laboratory report, No.655, 1945.

10. D.R.Rhodes, "An experimental investigation of the radiation patterns of electromagnetic horn antennas", Proc. IRE, Vol.36, pp.1101-1105, Sept. 1948.

11. R.B.Watson and C.K.Mckinney, "Gains and effective areas of horn antennas", J.Appl.Phys. Vol.19, pp.871-876, July 1948.

12. Woonton, Hay and Vagan, "An experimental investigation of formulas for the prediction of horn radiator patterns", J.App.Phys. Vol.20, pp.71, 1948.

13. C.W.Horton, "On the theory of the radiation patterns of electromagnetic horns of moderate flare angle", Proc. IRE, Vol.37, pp.744-749, July 1949.

14. Herbert S.Bennett, "Transmission-line characteristics of the sectoral horn", Proc. IRE, Vol.37, pp.738-743, July 1949.

15. S.O.Rice, "A set of second order differential equations associated with reflection in rectangular waveguides-- Application to guide connected to a horn", Bell Syst. Tech.J. Vol.XXVIII, pp.136-156, Jan. 1949.

16. G.C.Southworth, "Principle and application of waveguide transmission", Bell Syst.Tech.J. Vol.XXIX, pp.295-342, July 1950.

17. A.P.King, "The radiation characteristics of conical horn antennas", Proc. IRE, Vol.38, pp.249-251, March 1950.

18. Marvin G.Schorr and Fred J.Beck Jr., "Electromagnetic field of conical horn", J.Appl.Phys.Vol.21, pp.795-801, Aug. 1950.

19. W.C.Jakes, "Gain of electromagnetic horns", Proc. IRE, Vol.39, pp.160-162, Feb. 1951.

20. E.H.Braun, "Gain of electromagnetic horns", Proc. IRE, Vol.41, pp.109-115, Jan. 1953.

21. E.H.Braun, "Some data for the design of electromagnetic horns", IEEE Trans.Antennas Propagat., Vol.AP-4, pp.29-31, Jan. 1956.

22. James J.Epis, "Compensated electromagnetic horns", Microwave J, Vol.4, pp.84-89, May 1961.

23. K.L.Walton and V.C.Sundberg, "Broadband rigid horn design", Microwave J, Vol.7, pp.96-101, March 1964.

24. P.M.Russo, R.C.Rudduck and L.Peters Jr., "A method for computing E-plane patterns of horn antennas", IEEE Trans. Antennas Propagat, Vol.AP-13, pp.219-224, March 1965.

25. L.I.Tingye and R.H.Turrin, "Near-zone field of the conical horn", IEEE Trans.Antennas Propagat, Vol.AP-12, pp.800-802, Nov. 1964.

26. Y.S.Yu, R.C.Rudduck and L.Peters Jr., "Comprehensive analysis for E-plane of horn antennas by edge diffraction theory", IEEE Trans.Antennas Propagat, Vol.AP-14, pp.138-149, March 1966.

27. M.A.K.Hamid, "Diffraction by a conical horn", IEEE Trans. Antennas Propagat, Vol.AP-16, pp.520-528, Sept. 1968.

28. T.S.Chu and R.A.Semplak, "Gain of electromagnetic horns", Bell Syst.Tech.J, Vol.44, pp.527-537, March 1965.

29. E.V.Jull, "On the behaviour of electromagnetic horns", Proc.IEEE, Vol.56, pp.106-108, Jan. 1968.

30. E.V.Jull, "Finate-range gain of sectoral and pyramidal horns", Electron.Lett. Vol.6, pp.680-681, Oct. 1970.

31. E.I.Muehldorf, "The phase centre of horn antennas", IEEE Trans.Antennas Propagat. Vol.AP-18, pp.753-760, Nov. 1970.

32. M.S.Narasimhan and B.V.Rao, "Modes in a conical horn : new approach", Proc.Inst.Elect.Eng. Vol.118, pp.287-292, Feb. 1971.

33. M.S.Narasimhan and B.V.Rao, "Radiation from conical horns with large angles", IEEE Trans.Antennas Propagat, Vol.AP-19, pp.678-681, Sept. 1971.

34. M.S.Narasimhan and B.V.Rao, "A correction to the available radiation formula for E-plane sectoral horns", IEEE Trans. Antennas Propagat, Vol.AP-21, pp.878-879, Nov. 1973.

35. John L.Kerr, "Short axial length broad-band horns", IEEE Trans.Antennas Propagat, Vol.AP-21, pp.710-715, Sept.1973.

36. E.V.Jull, "Errors in the predicted gain of pyramidal horns",
    IEEE Trans.Antennas Propagat. Vol.AP-21, pp.25-31, Jan. 1973.

37. P.D.Potter, "A new horn antenna with suppressed sidelobes
    and equal beam-widths", Microwave J. Vol.VI, pp.71-78,
    June 1963.

38. P.D.Potter and A.C.Ludwig, "Beam shaping by use of higher
    order modes in conical horns", North East Electrons.Res. and
    Eng.Meeting, pp.92-93, Nov. 1963.

39. M.F.Iskander and M.A.K.Hamid, "Numerical so ition for the
    nearfield transmission between two H-plane sectoral electro-
    magnetic horns", IEEE Trans.Antennas Propagat, Vol.AP-24,
    pp.87-89, Jan. 1976.

40. E.V.Jull and L.E.Allen, "Gain of an E-plane sectoral horn:
    a failure of Krichhoff's theory and a new proposal", IEEE
    Trans.Antennas Propagat, Vol.AP-22, pp.221-226, March 1974.

41. C.A.Mentzer, L.Peters Jr., and R.C.Rudduck, "Slope diffraction
    and its application to horns", IEEE Trans.Antennas Propagat,
    Vol.AP-24, pp.153-159, March 1976.

42. J.C.Mather, "Broad-band flared horn with low sidelobes",
    IEEE Trans.Antennas Propagat, Vol.AP-29, pp.967-969,
    Nov. 1981.

43. R.C.Menendez and S.W.Lee, "Analysis of rectangular horn
    antennas via uniform asymptotic theory", IEEE Trans.Antennas
    Propagat, Vol.AP-30, pp.241-250, March 1982.

44. A.J.Simmons and A.F.Key, "The scalar feed--A high performance feed for large paraboloidal reflectors", Design and constru- ction of large steerable aerials, IEE Conference Publ. Vol.21, pp.213-217, 1966.

45. R.E.Lawrie and L.Peters, "Modification of horn antennas for low sidelobe levels", IEEE Trans.Antennas Propagat, Vol.AP-14, pp.605-610, Sept. 1966.

46. V.H.Rumsey, "Horn antennas with uniform power patterns around their axis", IEEE Trans.Antennas Propagat, Vol.AP-14, pp.656-658, Sept. 1966.

47. H.C.Minnett and B.Mac A.Thomas, "A method of synthesizing radiation patterns with axial symmetry", IEEE Trans.Antennas Propagat, Vol.AP-14, pp.654-656, Sept. 1966.

48. P.J.B.Clarricoats and P.K.Saha, "Theoretical analysis of cylindrical hybrid modes in a corrugated horn", Electron. Lett, Vol.5, pp.187-189, May 1, 1969.

49. P.J.B.Clarricoats, "Analysis of spherical hybrid modes in a corrugated conical horn", Electron. Lett. Vol.5, pp.189-190, May 1, 1969.

50. P.J.B.Clarricoats and P.K.Saha, "Radiation from a wide-flare angle scalar horns", Electron.Lett. Vol.5, pp.376-378, Aug.7, 1969.

51. B.Mac A.Thomas, "Band width properties of corrugated conical horns", Electron.Lett. Vol.5, pp.561-563, Oct.30, 1969.

52. M.E.J.Jeuken, "Experimental radiation pattern of corrugated conical horn antennas with small flare angle", Electron. Lett. Vol.5, pp.484-485, Oct.2, 1969.

53. M.E.J.Jeuken and C.W.Lambrechtse, "Small corrugated conical-horn antenna with wide flare angle", Electron.Lett. Vol.5, pp.489-490, 1969.

54. B.Mac A.Thomas, "Prime focus one and two hybrid mode feeds", Electron.Lett. Vol.6, pp.460-461, July 23, 1970.

55. M.S.Narasimhan and B.V.Rao, "Hybrid modes in corrugated conical horns", Electron.Lett. Vol.6, pp.32-34, Jan.22, 1970.

56. M.S.Narasimhan and B.V.Rao, "Diffraction by wide flare-angle corrugated conical horns", Electron.Lett. Vol.6, pp.469-471, July 23, 1970.

57. P.J.B.Clarricoats and P.K.Saha, "Propagation and radiation behaviour of corrugated feeds, Part I- Corrugated waveguide feed", Proc.IEEE, Vol.118, pp.1167-1176, Sept. 1971.

58. P.J.B.Clarricoats and P.K.Saha, "Propagation and radiation behaviour of corrugated feeds, Part II- Corrugated donical horn feed", Proc. IEE ,Vol.118, pp.1177-1186, Sept. 1971.

59. R.Baldwin and P.A.Mc Innes, "Surface wave excitation from a corrugated horn", Electron.Lett. Vol.6, pp.259-260, April 1970.

60. B.Mac A.Thomas, "Mode conversion using circumferentially corrugated cylindrical waveguide", Electron.Lett. Vol.8, pp.394-396, July 27, 1972.

61. Jozef, K.M.Jensen, E.J.Martin, Jeuken and Cees Lambrechtse, "The scalar feed", Arch.Elek. Übertragung, Vol.26, pp.22-30, Jan. 1972.

62. Charles M.Knop and Hans J.Wiesenfarth, "On the radiation from an open-ended corrugated pipe carrying the $HE_{11}$ mode", IEEE Trans. Antennas Propagat. Vol.AP-20, pp.644-648, Sept. 1972.

63. M.S.Narasimhan, "Corrugated conical horns with arbitrary corrugation depth", Radio Electron.Eng. Vol.43, pp.188-192, March 1973.

64. M.S.Narasimhan, "Corrugated conical horn as a space feed for phased array illumination", IEEE Trans.Antennas Propagat. Vol.AP-22, pp.720-722, Sept. 1974.

65. C.A.Mentzer and L.Peters Jr., "Properties of cut off corrugated surfaces for corrugated horn design", IEEE Trans. Antennas Propagat. Vol.AP-22, pp.191-196, March 1974.

66. Ross Calde Cott, C.A.Mentzer and Leon Peters Jr., "The corrugated horn as an antenna range standard", IEEE Trans. Antennas Propagat, Vol.AP-21, pp.562-564, July 1973.

67. M.S.Narasimhan and B.V.Rao, "Radiation from wide flare corrugated E-plane sectoral horn", IEEE Trans.Antennas Propagat. Vol.AP-22, pp.603-608, July 1974.

68. R.Baldwin and P.A.McInnes, "Corrugated rectangular horns for use as microwave feeds", Proc. IEE, Vol.122, pp.465-467, May 1975.

69. R.Baldwin and P.A.McInnes, "A rectangular corrugated feed horn", IEEE Trans.Antennas Propagat. Vol.AP-23, pp.814-817, Nov. 1975.

70. P.Bielli, S.De Padova and E.Pagana, "Analysis and synthesis of corrugated conical horns", CSELT Rapporti tecnici- Vol.VI, pp.55-60, March 1978.

71. Geoffrey Morris, "A broad-band constant beam-width corrugated rectangular horn", IEEE Trans.Antennas Propagat. Vol.AP-30, pp.969-974, Sept. 1982.

72. A.R.G.Owen and L.G.Reynolds, "The effect of flanges on the radiation patterns of small horns", J.Inst.Elec.Eng. Vol.93, pp.50-51, March-May, 1946.

73. P.C.Butson and G.T.Thomson, "The effect of flanges on the radiation patterns of waveguides and sectoral horns", J.Inst.Elec.Eng, Vol.106, pp.422-426, 1959.

74. S.Hariharan and K.Gopalakrishnan Nair, "An experimental investigation of the change in radiation patterns in the Fresnels region of sectoral electromagnetic horn antennas due to shorting grills", J.Inst.Telecom.Engrs, Vol.7, pp.189-196, 1961.

75. K.G.Nair and G.P.Srivastava, "Beam shaping of H-plane sectoral horns by metal flanges", J.Inst.Telecom.Engrs, Vol.13, pp.76-82, Feb. 1967.

76. K.G.Nair, V.K.Koshy and G.P.Srivastava, "E-plane sectoral horns yield to flange technique", Int.J.Electronics, Vol.24, pp.93-98, 1968.

77. V.K.Koshy, K.G.Nair and G.P.Srivastava, "An experimental investigation of the effect of conducting flanges on the H-plane radiation pattern of E-plane sectoral horns", J.Inst.Tele.Eng, Vol.14, pp.519-527, 1968.

78. K.G.Nair, G.P.Srivastava and S.B.Singh, "Some effect of metal flanges on radiation patterns of H-plane sectoral horns", J.Inst.Tele.Engrs, Vol.14, pp.352-358, 1968.

79. V.K.Koshy, S.B.Singh, K.G.Nair and G.P.Srivastava, "Effect of asymmetry in amplitude excitation of secondary sources by a primary aperture antenna", Int.J.Electronics, Vol.25, pp.289-291, 1968.

80. S.B.Singh, K.G.Nair and G.P.Srivastava, "Experimental confirmation of the effect of asymmetric flange on radiation patterns of aperture antennas", Int.J.Electronics, Vol.26, pp.173-177, 1969.

81. K.G.Nair, "A modified theory for radiation pattern of an aperture antenna and two secondary sources excited by the primary", Int.J.Elec. Vol.28, pp.459-462, 1970.

82. V.K.Koshy, K.G.Nair and G.P.Srivastava, "Gain improvement of flanged sectoral horn antennas by flange angle variations", Ind.J.Pure Appl.Phys. Vol.9, pp.476-478, July 1971.

83. G.P.Srivastava, K.K.Bhan and R.Baldwin, "Experimental study of a flange mounted waveguide as a device for square radiation pattern", IEEE Trans.Antennas Propagat, Vol.AP-24, pp.242-244, March 1976.

84. K.G.Nair, G.Mohanachandran and K.T.Mathew, "Beam shaping of sectoral horn antennas by dielectric flanges", Ind.J. Radio & Space Phys. Vol.5, pp.254-256, Sept. 1976.

85. Ahmad Safaai-Jazi and E.V.Jull, "A short horn with high E-plane directivity", IEEE Trans.Antennas Propagat, Vol.AP-25, pp.854-859, Nov. 1977.

86. K.T.Mathew and K.G.Nair, "An analysis of the behaviour of flanged sectoral horn antennas and corner reflector system", Ind.J.of Radio & Space Phys. Vol.10, pp.25-30, Feb. 1981.

87. E.J.Zachariah, K.Vasudevan and K.G.Nair, "Metal flanges with more parameters for beam shaping", IEEE Trans.Antennas Propagat, Vol.AP-17, No.9, pp.708-710, Sept. 1979.

88. E.J.Zachariah, K.Vasudevan and K.G.Nair, "Beam shaping and impedance matching of sectoral electromagnetic horn antennas using corrugated flanges", Ind.J.Radio & Space Phys. Vol.8, pp.24-28, Feb. 1979.

89. K.Vasudevan and K.G.Nair, "A corrugated corner reflector system", IEEE Trans.Antennas Propagat, Vol.AP-30, pp.524-526, May 1982.

90. K.Vasudevan and K.G.Nair, "An analysis of radiation patterns of corrugated corner reflector antenna systems", Ind.J.Radio & Space Phys. Vol.11, pp.156-158, Aug. 1982.

91. A.W.Love, "The diagonal horn antenna", Microwave Journal, Vol.V, pp.117-122, March 1962.

92. Ching C.Han and Adam N.Wickert, "A new multimode rectangular horn antenna generating a circularly polarized elliptical beam", IEEE Trans.Antennas Propagat, Vol.AP-22, pp.746-751, Nov. 1974.

93. Robert N.Gruner, "A 4 and 6 GHz prime focus circularly polarized feed with circular pattern symmetry", Int. IEEE/AP-S Symp.Progress & Dig. pp.72-74, June 1974.

94. Takashi Ebisui, Takashi Katagi and Motoo Mizusawa, "A circularly polarized dual mode horn antenna for communication satellite", IEEE/AP-S Int.Symp. Session II, pp.313-316, June 1977.

95. Ebisui, Katagi and Mizusawa, "A circularly polarized flare iris type dual mode horn antenna", Trans.IECE, Japan, Vol.E62, No.12, pp.904-905, Dec. 1979.

96. Yoshihiro Takeichi, Goro Kondo, Motoo Mizusawa, Shunichin Kawabata, Takashi Katazi and Takeshi Shishido, "Intelsat V 4 and 6 GHz earth coverage antennas", Int.Symp.on Antennas & Propagat, Japan, pp.211-214, 1978.

97. R.J.Dewey, "Circularly polarized elliptical beam shape horn antennas", Int.J.Electronics, Vol.53, No.2, pp.101-128, 1982.

98. E.V.Jull, "Reflection circular polarizers", Electron.Lett. Vol.15, pp.423-424, 1979.

99. P.O.Paul and K.G.Nair, "Rotation of plane of polarization of a beam of microwaves by corrugated reflector surfaces", Electron.Lett. Vol.18, No.8, pp.338-339, April 1982.

100. J.F.Ramsey, "Circular polarization for CW radar", Proceedings of a conference on centimetric antennas for marine navigational radar, London, HMSO 1952, June 1950.

101. V.H.Rumsey, "Transmission between elliptically polarized antennas", Proc.IRE, Vol.34, pp.535-540, March 1951.

102. G.A.Deschamps, "Geometrical representation of the polarization of a plane electromagnetic wave", Proc.IEE, Vol.39, pp.540-544, March 1951.

103. M.L.Kales, "Elliptical polarized waves and antennas", Proc.IRE, Vol.39, pp.544-549, March 1951.

104. S.Silver, "Microwave antenna theory and design", McGraw-Hill Book Company, New York, 1949.

105. C.G.Montgomery, "Techniques of microwave measurement", McGraw-Hill Book Company, New York, 1949.

106. J.D.Kraus, "Antennas", McGraw-Hill Book Co.Inc, New York, 1950.

107. H.M.Barlow and A.L.Cullen, "Microwave measurements", Constable and Co., London, 1950.

108. S.A.Schelkunoff and H.T.Friss, "Antennas : Theory and practice", John Wiley & Sons, INC, New York, 1952.

109. L.Thourel, "The antenna", Chapman & Hall, London, 1960.

110. E.A.Jasik, "Antenna engineering hand book", McGraw-Hill Book Co., New York, 1961.

111. "Test Procedure for Antenna", IEEE, New York, 1965.

112. Edward A.Wolff, "Antenna analysis", John Wiley & Sons, New York, 1966.

113. E.C.Jordan, "Electromagnetic waves and radiating systems", Prentice-Hall of India, New Delhi, 1967.

114. R.E.Collin and E.J.Zucher, "Antenna theory - Part I", McGraw -Hill Book Co., New York, 1969.

115. R.E.Collin and E.J.Zucher, "Antenna theory - Part II", McGraw-Hill Book Co., New York, 1969.

116. Harry E.Thomas, "Hand book of microwave technique and equipment", Prentice Hall Inc, New Jersey, 1972.

117. S.Cornbleet, "Microwave optics : the optics of microwave antenna design", Academic Press, New York, 1976.

118. R.S.Elliott, "Antenna theory and design", Prentice-Hall,Inc., New Jersey, 1981.

119. Constantine A.Balaniss, "Antenna theory analysis and design", Harper & Row Publishers, New York, 1982.

120. IEEE Standard definitions of terms for antennas, IEEE Antennas Propagat, Vol.31, Nov. 1983.

121. Claude M.Weil and James B.Kinn, "Advancesiin experimental methods and dosimetric techniques used in radio frequency radian biological effect studies", Proc.IEEE, Vol.71, pp.222-231, Feb. 1983.

122. A.W.Love, "Reflector antennas", IEEE Press, Institute of Electrical and Electronics Engineers, Inc, New York, 1978.

123. K.G.Nair and K.T.Mathew, "Effect of flanged sectoral horn primary feeds on the radiation patterns of secondary reflector antennas", J.Inst.Elec.Telcom.Engrs, Vol.23, pp.148-149, 1977.

124. R.V.Garver, E.G.Spencer and M.A.Harper, "Microwave semi-conductor switching techniques", Proc.IRE Trans.MTT Vol.6, pp.378-383, 1958.

125. R.V.Garver, J.A.Rosado and E.F.Tuner, "Theory of Germanium diode microwave switch", IRE Trans.MTT, Vol.8, pp.108-111, 1960.

126. Merill I.Sholnik, "Radar hand book", McGraw-Hill Book Co.,
     INC, 1970.

127. Edward S.Yang, "Fundamentals of semiconductor devices",
     McGraw-Hill Book Co., 1978.

# LIST OF PUBLICATIONS OF THE AUTHOR

1. "Microwave absorbing material using rubber and carbon", Indian Journal of Pure and Applied Physics, 18, (3), 1980, pp.216-218.

2. "Corrugated flanged horn feed for offset paraboloidal reflectors", Indian Journal of Radio and Space Physics, 10(6), 1981, pp.246-247.

3. "Axially symmetric radiation patterns from flanged E-plane sectoral horn feeds", Indian Journal of Radio and Space Physics II (3), 1982, pp.112-115.

4. "Phase modulation of microwave signal using point contact Germanium signal diodes", Indian Journal of Radio and Space Physics, 13, Feb.84, pp.32-33.

5. "Axially symmetric radiation patterns from corrugated flanged H-plane sectoral horns", Indian Journal of Radio and Space Physics, 13, Feb.84, pp.13-15.

6. "Design, development and performance evaluation of anechoic chamber for microwave antenna studies", Indian Journal of Radio and Space Physics, 13, Feb.84, pp.29-31.

7. "Circularly polarized corrugated flanged feed horn", Indian Journal of Radio and Space Physics, 13, Feb.84, pp.137-138.

8. "Rotation of plane of polarization of a rectangular microstrip antenna with feed position", Communicated to Electronics Letters (GB).

# INDEX